ABSTRACT

Rise of the Givetian (385 Ma) Forests, Northern Appalachian Basin,
Catskill State Park, New York, U.S.A.

Jason S. Mintz, Ph.D.

Committee Chairman: Steven G. Driese, Ph.D.

Forestation on Earth may have profoundly changed fluvial sedimentary patterns, increased the release of bio-limiting nutrients to marine systems and increased the consumption of atmospheric CO_2 through biologic productivity and silicate mineral weathering. Evidence is presented for occurrences of forested ecosystems in swamplands in deltaic coastal settings, across a range of seasonally-drained floodplain overbank environments, and even in what were likely terraced interfluve landscapes during the Givetian in the Appalachian basin. Evidence is also presented that chemical weathering in paleosols on alluvial plains in the Appalachian basin may have increased from the Ordovician through the Middle Devonian.

Temporal correlation of terrestrial and marine strata is essential in order to understand the potential cause and effect relationships between changes in Devonian weathering systems and marine environmental, ecological and geochemical conditions. Over 450 m of nearly continuous outcrop exposure along Plattekill Creek in West Saugerties, New York, was measured in order to develop a sequence-stratigraphic framework, using alluvial stacking-pattern analysis. The analysis reveals several orders of

cyclicity that correspond with Acadian tectophases and previously documented marine depositional sequences. Paleo-precipitation for 37 paleosol profiles was estimated using the CALMAG proxy, a geochemical ratio from bulk soil material in vertic paleosols, which suggests dominantly wet paleoclimates throughout the Middle Devonian, an interpretation also supported by micromorphological data.

The paleosol calcite paleobarometer was used to estimate atmospheric CO_2 decline related to the development of forested ecosystems, as well as determine the initial atmospheric pCO_2 at the onset of forestation. The timing of calcite precipitation in relation to the soil saturation state and soil-atmosphere connectivity was investigated in a modern Vertisol (smectitic, clay-rich soil, seasonally saturated) in Brazoria County, Texas, U.S.A., which is an excellent modern analog to forested paleosols in the Appalachian basin. A luminescent phase of calcite formed during the water-saturated portion of the year, negating its use for pCO_2 estimations. A non-luminescent phase formed during the well-drained portion of the year when atmospheric CO_2 mixed with soil-respired CO_2 and is therefore useful for pCO_2 estimation. From these results a model is presented that independently tests the saturation state of a paleosol at the time of pedogenic carbonate precipitation.

Rise Of The Givetian (385 Ma) Forests, Northern Appalachian Basin,
Catskill State Park, New York, U.S.A.

by

Jason S. Mintz, M.S.

A Dissertation

Approved by the Department of Geology

____
Steven D. Driese, Ph.D., Chairperson

Submitted to the Graduate Faculty of
Baylor University in Partial Fulfillment of the
Requirements for the Degree
of
Doctor of Philosophy

Approved by the Dissertation Committee

____
Steven G. Driese, Ph.D., Chairperson

____
Stacy C. Atchey, Ph.D.

____
Stephen I. Dworkin, Ph.D.

____
Daniel J. Peppe, Ph.D.

____
Joseph D. White, Ph.D.

Accepted by the Graduate School
May 2011

____
J. Larry Lyon, Ph.D., Dean

Page bearing signatures is kept on file in the Graduate School.

TABLE OF CONTENTS

LIST OF FIGURES

LIST OF TABLES

ACKNOWLEDGMENTS

The research I have conducted here at Baylor University has benefited greatly from the financial support from the following: the National Science Foundation (EAR-0643152 and EAR-0921356), Society for Sedimentary Geology (student grant award), The Geological Society of America (student grant award), The Fort Worth Geological Society (FWGS student scholarship) and additional support provided by Husky Energy and Baylor University.

I have watched Dr. Steve Driese lead me and others around me with a quiet and driven determination that has placed the department at the very forefront of terrestrial paleoclimatic and stratigraphic research. The past four years have been an absolute joy working alongside such a kind and deeply-intelligent man. I hope my career as a scientist can live up to the world-class training I have received from Dr. Driese. To my mentor and friend, Steve Driese, I am forever indebted.

I have had the pleasure to gain the expertise and guidance from several faculty at Baylor, whom I count as mentors. My tenure was not spent sheltered in a small laboratory, but rather in amongst a large and vibrant research group. Dr. Stacy Atchley has had a major impact on my career as a stratigrapher, sedimentologist and researcher. Stacy's ability to see big picture problems and ideas for research has made my time at Baylor all the more exciting. Dr. Stephen Dworkin is a scientist that I am proud to have gotten the chance to study under. Steve has a way to latch on to a problem and in one

sentence, if you are listening, change your entire perspective on the matter at hand. It has been great fun tackling problems with him these past years.

One of the greatest and by far most rewarding challenges has been is the ability to help mentor students in their research. I have had the honor in providing guidance to two different undergraduate students, Mr. Colby Wright and Mr. Hunter Harlow, both of which successfully defended a B.S. thesis and presented their research at National Geological Society of America meetings. I have also worked with three different Master's thesis students: Mr. Ryan Dhillon, Mr. Curtis Barclay, and Ms. Kelly Jones, on various research projects. I have no doubt that I have learned more from these experiences than they, I am proud to have worked with each of them and wish them the very best of luck in the future.

I am very grateful of my fellow graduate students for listening to my problems as well as to allowing me to hear yours. It is a great help to be surrounded by such passionate and bright young people to challenge you to work hard and find success. I would particularly like to acknowledge past and present Ph.D. students: Dr. David Cleveland, Dr. Julia Kahmann-Robinson, Ms. Holly Meier, Ms. Lauren Michel, Dr. Aaron Shunk, Mr. Gary Stinchcomb, and Ms. Aislyn Trendell, for their support, which I hope I have been able to reciprocate to some small extent.

Baylor Geology is very fortunate to have an absolutely amazing administrative staff, which keeps the department organized, and sets a warm and positive attitude for the entire department. I would not have survived these four years without Mrs. Paulette Penney, who is not recognized nearly enough for all that she does. Thank you to: Mrs. Janelle Atchley, Mrs. Jamie Ruth and Mrs. Erin Stinchcomb, you are great.

My family has been a huge inspiration and driving motivation in my life. I will represent the third successive generation of Mintz doctors (although my mother is quick to point out, that I will be the type of doctor who cannot actually help anyone) and the second Ph.D. in the DuBois/ Moran family. Hearing whispers of my ancestors that have strived for something has kept me up nights trying to better myself, if only to grab hold of that high bar. The most tangible examples of excellence are from my parents Dr. Richard and Mrs. Maryteresa Mintz. They have provided me with unrelenting support, patience (especially in my early years) and a model for success in work as well as life.

I owe everything good I have in my life to my wife, fellow Ph.D. candidate, Mrs. Hallie Mintz. It is humbling to be married to someone you admire and respect so deeply. I knew nothing of strength, bravery, compassion and love before Hallie. My future looks bright only because you are in it. I am a lucky man.

"It is like a finger pointing away to the moon.

Don't concentrate on the finger or you will miss all that heavenly glory."

–Bruce Lee

For Hallie. [CHOMP]

CHAPTER ONE

Introduction

Earth systems experience a variety of cycles that occur at different time scales, which are preserved in the geologic record. The cycles in Earth processes are disrupted, or punctuated, by anomalous events or periods of time, which commonly are manifested in the rock record as extinction events, volcanic episodes or major reorganizations in Earth surface processes. These anomalous events are critical to our understanding of the chronology of the rock record and the evolution of our planet. One such reorganization of Earth system processes began in the Middle Devonian with the onset of forestation of terrestrial environments (Berner, 1992; Driese et al., 1997; Algeo and Scheckler, 1998; Mintz et al., 2010). As forests began to inhabit different ecological niches, rooting depth and density increased, thereby increasing river channel, overbank and upland landscape stability (Davies and Gibling, 2010), and promoting increases in the depth and degree of physical and chemical weathering (Driese et al., 1997; Algeo and Scheckler, 1998; Mintz et al., 2010; Mintz et al., in review). The increases in physical and chemical weathering associated with forested ecosystems changed the global carbon cycle to include increased carbon consumption from silicate weathering and photosynthetic processes (Berner, 2005). Marine systems were also potentially affected by this reorganization of terrestrial systems because the delivery of clastic sediment (along with vital nutrients for marine organisms) is primarily controlled by fluvial sedimentary processes (Algeo and Scheckler, 1998). Increased weathering and organic productivity created a drawdown in atmospheric CO_2, which is linked to late Devonian/ Carboniferous ice house conditions (Goddéris et al., 2001).

The earliest evidence of forestation on Earth is preserved in Middle Devonian (Givetian) fluvio- deltaic deposits in the northern Appalachian basin (Driese et al., 1997; Mintz et al., 2010). The extent of Middle Devonian forestation in the basin was suggested initially to have been restricted to swampland deposits on delta plains and aquic (water-logged) soil conditions proximal to the strandline (Driese et al., 1997; Algeo and Scheckler, 1998). Chapter two is a reproduction of a manuscript published in *Palaios* that discusses the extent of environmental influence of forestation through paleo-ecological reconstructions of Middle Devonian forested paleosols (ancient soils) (Appendix A) (Mintz et al., 2010). Data presented suggest that forestation was a modifying agent on a wide range of Middle Devonian landscapes forming in the northern Appalachian basin and that it may have been an impetus for many of the changes ascribed to Middle Devonian global conditions (Mintz et al., 2010).

To study potential cause and effect relationships between changes in Devonian weathering systems to marine environmental, ecological and geochemical conditions, coeval terrestrial and marine strata must first be correlated. The Plattekill, Manorkill and Oneonta Formations are terrestrial deposits formed as part of a clastic wedge, derived from the Acadian Mountains adjacent to the Appalachian basin (Ettensohn, 1985a; Ver Straeten, 2010). The Acadian Orogenic belt formed from the collision between the island arc Avalon and Laurentia (proto-North America) as the oceanic plate beneath the Iapetus Ocean subducted under Laurentia (Faill, 1997b). The Acadian orogeny is interpreted as a time-transgressive event that shifted the Appalachian basin depocenter, as the Avalon island arc collided obliquely with Laurentia from northeast to southwest (Ettensohn, 1985b). Chapter three integrates landscape reconstructions and fluvial sedimentary stacking patterns through the Plattekill, Manorkill and Oneonta Formations to present an allostratigraphic correlation of terrestrial and marine stratigraphic successions in the northern Appalachian basin (Mintz et al., in review). A paleoclimate reconstruction of the Middle Devonian in the Appalachian basin is presented, which suggests that early forested conditions occurred in a predominately wet climate (Mintz et al., in review). It is suggested that paleoclimate proxies may also need to be reevaluated from a systems approach of constraining all variables that control pedogenesis rather than just assuming that a climate proxy alone isolates the effects of climate on pedogenesis (Mintz et al., in review).

Soils develop as a combined product of the climatic regime in which they formed, the organisms that live in the soil, their geomorphic position, the composition of the original parent material and the duration of soil formation (Jenny, 1941). Paleosols have the potential to preserve valuable information about these factors of influence in which they formed, however to interpret ancient environmental conditions from soils one needs to understand the influences of soil properties that have good preservation potential (Retallack, 2001). One such product of pedogenesis (soil formation) commonly preserved in the rock record that is sensitive to a variety of soil conditions is pedogenic (soil-formed) carbonate (Cerling, 1999). The precipitation of carbonate in soils records information about past vegetation communities, the carbon isotopic composition of soil gas and ultimately the CO_2 concentration in the atmosphere in which the soil formed (Cerling, 1984; 1991; 1999). Data concerning paleoatmospheres are important in attempting to address the controls of atmospheric CO_2 on paleoclimates. The ability to better understand the timing and degree of atmospheric pCO_2 change during the Devonian is a crucial part of the history of forestation and its impact on the Earth surface and atmospheric systems.

Chapter four is a modern analog study that addresses the influences on the carbon isotopic composition of pedogenic carbonate in a suite of soils interpreted as similar to forested paleosols in the Middle Devonian and is a reproduction of a paper published in the *Journal of Sedimentary Research* (Appendix A) (Mintz et al., in press). Pedogenic carbonates that precipitate in soils incorporate carbon from soil CO_2, a mixture of atmospheric and soil-respired CO_2, so that if one can quantify the other variables in the paleosol barometer equation then one can estimate atmospheric pCO_2 concentrations during the formation of that soil (Cerling, 1999; Ekart et al., 1999). A model was generated to identify carbonates that formed in a soil gas that was a mixture of atmospheric and soil-respired CO_2, and appropriate for determining paleo-pCO_2 concentrations (Mintz et al., in press). By generating estimates of atmospheric CO_2 concentrations at the onset of forestation, through the use of models generated in surface soils, one can better constrain the extent to which early forestation reorganized the Devonian carbon cycle.

CHAPTER TWO

Environmental and Ecological Variability of Middle Devonian (Givetian) Forests in Appalachian Basin Paleosols, New York, USA

Abstract

The inception of terrestrial woody plant ecosystems on the Earth is thought to have caused decreases in atmospheric carbon dioxide and water vapor concentrations in the Middle Devonian. Decreased greenhouse gas concentrations enabled a series of long-term glacial-interglacial cycles from the Late Devonian through the Permian. Here we describe the environmental and ecological variability of the earliest known paleosols with evidence of *in situ* forests (stump casts and attached root systems) from the Appalachian basin. Four examples located in the Manorkill Formation in the Catskill Mountains of New York State, USA, are analyzed using macro- and micromorphological data. Woody plant stump casts and molds on exposed bedding surfaces were mapped at two of the sites and analyzed using nearest-neighbor analysis. This permitted quantification of spatial distribution and ecological conditions of these paleoforests. These fossilized forests exhibit both single and multi-generational growth and formed in both aquic and seasonally well-drained environments, thus indicating established populations and growth adaptations by the represented species. The occurrence of these diverse forested landscapes in the Givetian is concurrent with the onset of the prolonged decrease in atmospheric CO_2 concentrations that have been tied to a series of Paleozoic glaciations.

Introduction

The forestation of Devonian landscapes initiated fundamental changes in terrestrial sedimentation (Driese et al., 1997, 2000; Algeo and Scheckler, 2000; Driese and Mora, 2001; Berner, 2005). Forest development across a diverse range of terrestrial environments is likely to have increased the stability of these landscapes and sedimentologic systems creating more significant periods of time for pedogenic weathering to occur. The advent of forests as a distinct ecological system in the Devonian is associated with the evolution of species with progressively deeper roots initiating deeper pedogenic weathering processes (Gensel and Andrews, 1984; Scheckler, 1986; Driese et al., 1997, 2000; Retallack, 1997; Driese and Mora, 2001). This paper builds on initial investigations begun by Driese et al. (1997) by examining the earliest evidence of *in situ* forests rooted in paleosols contained in the Middle Devonian Manorkill Formation in the Catskill Mountains, New York (NY; Driese et al., 1997) (Fig. 2.1). We examine the pedogenic development in these paleosols associated with forestation in diverse environmental conditions and also assess and compare the community structure of these forests based on mapping and trunk basal diameter.

The rise of large land plants in the Middle Devonian occurred concurrently with the onset of a major decrease in atmospheric CO_2 and global temperatures (Berner 1992, 2005; Berner and Kothavala, 2001; Goddéris et al., 2001; Bergman et al., 2004). The perturbation in atmospheric CO_2 that began in the Givetian has been suggested to be the response to forest development and subsequent associated effects despite what has been thought to be limited geographic extents of forestation (Mora et al., 1991, 1996; Driese et al., 1997; Algeo and Scheckler, 1998). Forests composed of the Givetian cladoxylalean

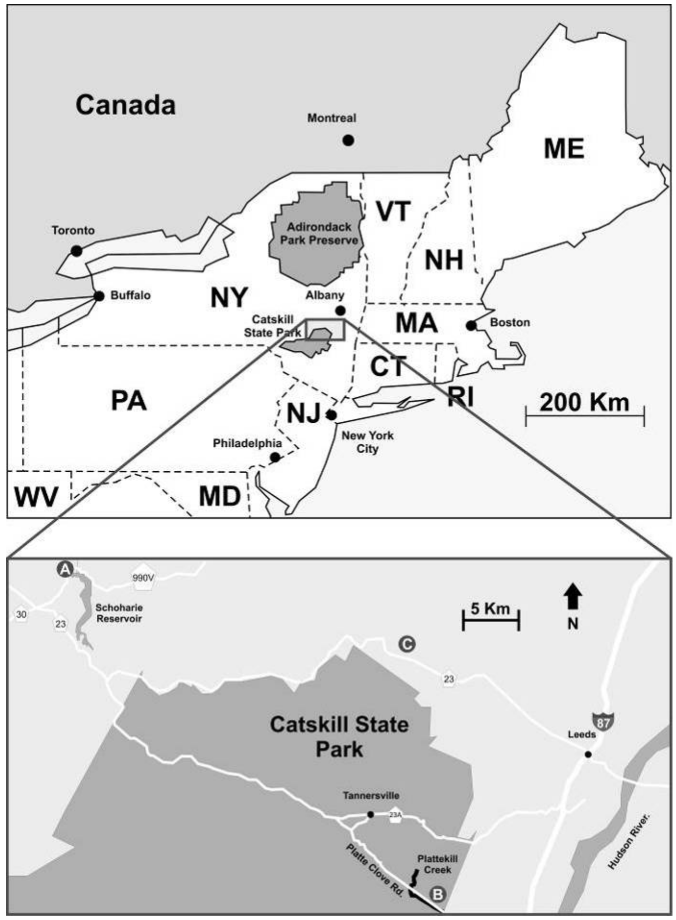

Figure 2.1 Map of study area in New York State, northeastern USA. Site A = Schoharie Creek site north of the Gilboa Dam and the Schoharie reservoir, Gilboa (stop 3 in Johnson, 1987). Site B = outcrops exposed on the bank of Plattekill Creek in West Saugerties. Site C = road-cut section along New York State Route 23 in East Windham. See Appendix B for additional details.

Eospermatopteris have been shown to occupy swampy and boggy environments and are interpreted as limited geographically by the necessity of water for reproduction (Boyer and Matten, 1996; Driese et al., 1997). Retallack (1998) presented evidence that forestation occurred in well-drained paleosols in the Givetian Aztec Siltstone in Victoria Land, Antarctica. These paleosols lacked *in situ* forest remains but had evidence of subsurface weathering conditions that can develop beneath modern forested environments (Retallack, 1998). The purpose of this study is to describe the environmental conditions and ecological framework of a variety of forested communities in the Givetian of New York State.

Background

The continental deposits discussed here formed in the Appalachian foreland basin as a result of a series of orogenic subduction zone, island-arc collision events with Laurentia (Proto-North America) (Woodrow and Sevon, 1985). The Appalachian basin consisted of epicontinental seas with expansive carbonate platforms that experienced terrigenous clastic-sediment progradation into the basin from the east (as it is positioned today) with each subsequent orogenic uplift event. Throughout the Devonian, Laurentia was a landmass straddling the equator with the Appalachian basin in New York positioned ~5–20˚ south latitude (Scotese et al., 1979; Ziegler et al., 1979; Ettensohn and Barron, 1981; Kent, 1985). The Devonian wedge of clastic sediments in the Appalachian basin was derived from the Acadian mountain range formed by a like-named orogenic collision between Laurentia and Avalon (island arc) (Ettensohn, 1985).

Middle Devonian terrigenous strata in New York comprise the Plattekill and Manorkill Formations, a succession of sandstones and mudrock of fluvial-deltaic origin (Fig 2.2). Fine-grained fluvial overbank deposits formed primarily from aggrading, sinuous river systems with developed channel forms on a low-relief alluvial plain (Johnson and Friedman, 1969; Gordon and Bridge, 1988; Willis and Bridge, 1988). Transitional strandline environments are typically estuarine-barrier island complexes and deltaic systems (Johnson, 1987; Bridge and Willis, 1994). Devonian climatic conditions in this region are interpreted as tropical and seasonally wet to semi-arid (Kent, 1985; Woodrow, 1985; Driese and Mora, 1993; Mintz et al., 2005). The maximum height and diameter of vascular land plants, depth and degree of rooting, and the stabilizing nature of plants on the landscape all increased greatly during the Devonian (Algeo and Scheckler, 1998, Driese et al., 2000; Driese and Mora, 2001).

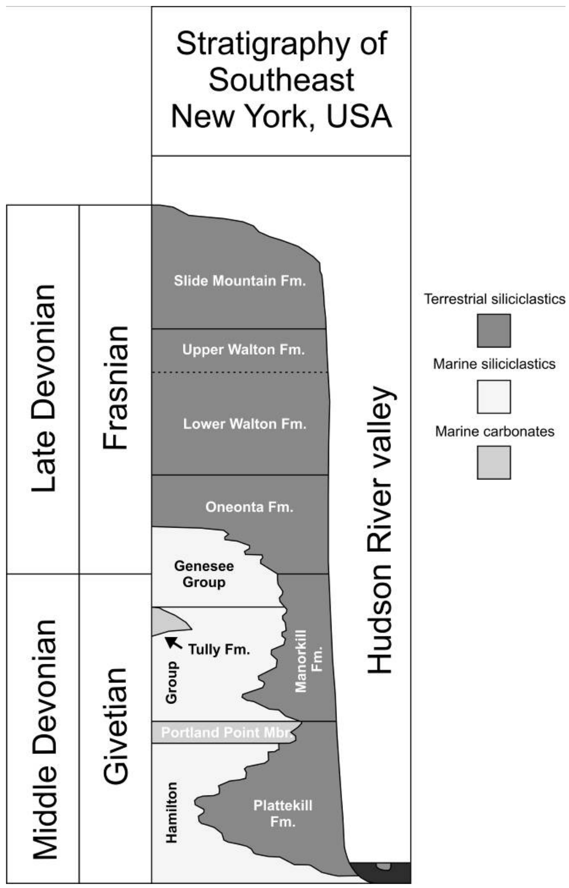

Figure 2.2 Stratigraphic column of Middle–Late Devonian deposits modified from Woodrow and Sevon (1985). Depositional environment interpretations inferred from Rickard (1975). This study focuses on sites within the Manorkill Formation.

Middle Devonian arborescent taxa include the cladoxylalean *Eospermatopteris* and archaeopterids, each of which had a maximum height of 20–25 m (Boyer and Matten, 1996; Algeo and Scheckler, 1998; Berry and Fairon-Demaret 2001; Stein et al., 2007). The root system of *Eospermatopteris* was comprised of dominantly horizontal, 1–2 cm diameter, unbranched to weakly bifurcating roots, which radiating outward from the bulbous base of the plant (Goldring, 1927; Scheckler, 1986; Driese et al., 1997; Algeo and Scheckler, 1998; Meyer-Berthaud and Decombeix, 2007; Stein et al., 2007). Archaeopterid roots, in contrast, consisted of a system of downward tapering and repeatedly bifurcating roots that extended one meter or more downward into the soil (Scheckler, 1986; Driese et al., 1997; Algeo and Scheckler, 1998). Driese et al. (1997) previously described a sandy paleosol with *in situ* stump casts in the Manorkill Formation near Gilboa, New York, which is located at the southernmost end of the Schoharie reservoir (stop 1 in Johnson, 1987) (Fig. 2.1). The deposits at this site were previously interpreted as tidal channel, tidal flat, and shallow bar environments (Johnson, 1987). The paleosol is composed of *in situ Eospermatopteris* stump casts in growth position with short attached, non-branching root traces (Driese et al., 1997). This paleosol is drab colored, contains pyritized organic remains, and lacks pedogenic carbonate, which Driese et al. (1997) interpreted as evidence for paleosol formation in a swamp environment with a permanently high water table. The paleosol described in this paper occurs near Gilboa, NY (stop 3 in Johnson, 1987) and was previously interpreted as distal delta plain or tidal swamp deposits that were buried and preserved during the migration of tidal channels and sand bars; it also contain a series of *in situ Eospermatopteris* stump casts (Johnson, 1987). More recently the near-shore forested deposits along Schoharie creek have been assigned to the Moscow Formation of the Hamilton Group, with the paleoforests occurring below transgressive surfaces of high-order sea-level oscillation cycles (Bartholomew and Brett, 2003; Baird and Brett, 2008). Willis and Bridge (1998) previously described location 1 at Plattekill Creek and interpreted it as consisting of stump casts preserved in floodplain deposits.

Study Sites and Methods

A total of four sites that include paleosols with evidence of forest development are described from three different locations in New York (Fig. 2.1). Location names are referenced to the map in Figure 2.1 and site coordinates are provided in Appendix B. Macroscale field description of paleosols was based on Schoeneberger et al. (2002). Color descriptions were determined in the field from comparison with Munsell rock and soil color charts. Micromorphologic description and terminology are based on Brewer (1976).

Stump casts were mapped using measuring tape and compass, and digitally expressed and analyzed using Surfer 8© (Rockware: Denver, Colorado) 9 (Appendix C). Tree stumps mapped on horizontal bedding planes were identified based on morphologic characteristics, such as the circular stump forms, root scars and radiating root features, relict trunk and bark morphology, and appropriate growth positioning. Stump casts mapped and discussed in this paper are in appropriate original growth positions, commonly with preserved *in situ* root networks, suggesting that these stump features do indeed represent the place in which the trees were growing.

The spatial distributions of stump casts were quantified using nearest-neighbor analysis (Clark and Evans, 1954). The nearest-neighbor statistical value (R) distinguishes clustered distributions from theoretical, purely random, and uniform distributions. The R value is calculated after measuring the distance to the nearest neighbor from each of the data points. This method eliminates the need for the generation of an orthogonal grid, the dimensions of which can influence results independently of the actual distribution of the data. In a completely clustered end member where all data lie at a singular point, R=0, while a random distribution of data is represented by R=1. The R value of a perfectly uniform distribution of spatial features is R=2.1491. The statistical significance of the departure of sampled values from the synthetic random and clustered values can then be tested.

Results

Gilboa Locality

Macromorphology. The *in situ* tree stumps at Gilboa (Fig. 2.1, Site A) are rooted in well-sorted, massive to bioturbated, fine-grained quartz sandstone and are buried by overlying well-sorted, cross-stratified, fine-grained sandstone (Fig. 2.3). These bulbous-based stump casts with shallow non-bifurcating root traces (likely *Eospermatopteris*) are infilled by fine-grained sandstone and range from 8–90 cm in diameter. Past quarrying activities removed a section roughly 19 x 12 meters of the overlying cross-stratified sandstone that encased the tree stump features. What remains within the underlying paleosol are cross sections through the base of the stump casts and more commonly, external molds left by the base of the removed casts. Stump casts have a rounded base that flares outward thereby creating a bowl-like depression in the underlying paleosol (Fig. 2.3). The external molds and stump casts both show linear impressions of relict bark morphology and commonly root scars, which are necessary criteria to identify these features as stump molds and not burrow or root forms. Root traces, stump casts, and molds also commonly have iron-oxide mottling associated with them, likely derived from the surface oxidization of pyritized organic material.

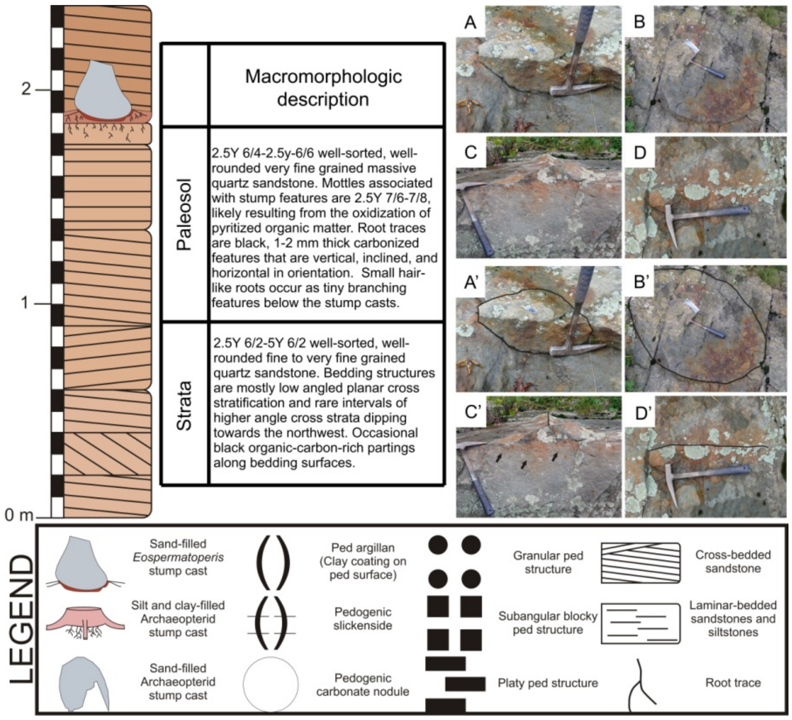

Figure 2.3 Macroscale description and outcrop photographs of site A (see Fig. 2.1). A) Longitudinal cross section of an *Eospermatopteris*? stump cast. B) Plan-view cross-section of an *Eospermatopteris*? stump cast. C) Cross-sectional view of root trace with network of fine branching root forms and iron-oxide staining. D) Plan view of the root trace from Figure 2.3C. Hammer = 35 cm long. Images presented in duplicate as both uninterpreted and interpreted features which are outlined in black. Black arrows = root traces.

Rooting in the paleosol that hosted these stump features does not extend past 20 cm depth in outcrop (Fig. 2.3). The massive, mottled bedding extends to the same depth as the rooting seen in outcrop, thus shallow rooting along with the poorly drained nature of this paleosol likely limited the depth of pedogenesis. Root features observed in split hand samples are 1 cm in diameter, non-branching, carbonized tubular features with millimeter-scale vertical striations oriented longitudinally on the specimen. Neither carbonized root features, nor any other carbonized remains, are visible in outcrop, possibly due to a weathering contrast between carbonized organic matter and the quartz sandstone. Root features on the quarried surfaces are poorly preserved, 1 cm in diameter, and extend out horizontally up to 50 cm. A submillimeter- diameter, weakly branching, root network associated with these features appears to extend 15–20 cm away from the main root cast.

Micromorphology. The paleosol at Gilboa is primarily composed of fine- to very fine-grained, angular-to-subangular quartz sand, with minor amounts of very fine-grained microcline feldspar, mica, and siderite grains. The paleosol has a homogenous bioturbated appearance, with no relict bedding structures or sense of pedality of the matrix (Fig. 2.4). The paleosol matrix is completely devoid of iron oxides, which is anomalous for the highly oxidized Catskill red-bed terrestrial deposits that characterize this region. There are non-bifurcating root fossils ~1 mm in diameter composed of carbonized organic remains with linear striations running the length of the roots, but these are completely opaque under plane-polarized light. Cellular structure is preserved in the carbonized remains in samples viewed under UV fluorescence indicating some preservation of the root organic matter (Fig. 2.4).

West Saugerties Locality

Macromorphology: Location 1. Stump casts at Plattekill Creek Location 1 (Fig. 2.1, Site B) are preserved in laminated, very fine-grained sandstones and siltstones with submillimeter, unidirectional lineations on most bedding-plane surfaces (Fig. 2.5). These lineations do not appear biological and are absent around stump or rooting features. These paleosols are both horizontally and vertically exposed by Plattekill Creek; there appear to be two different forested paleosols exposed on two different horizontally exposed beds (S_1 and S_2) separated by a conspicuous bedding plane and erosional surface (Fig. 2.5). The pedality of the S_2 paleosol is slightly more developed and there is

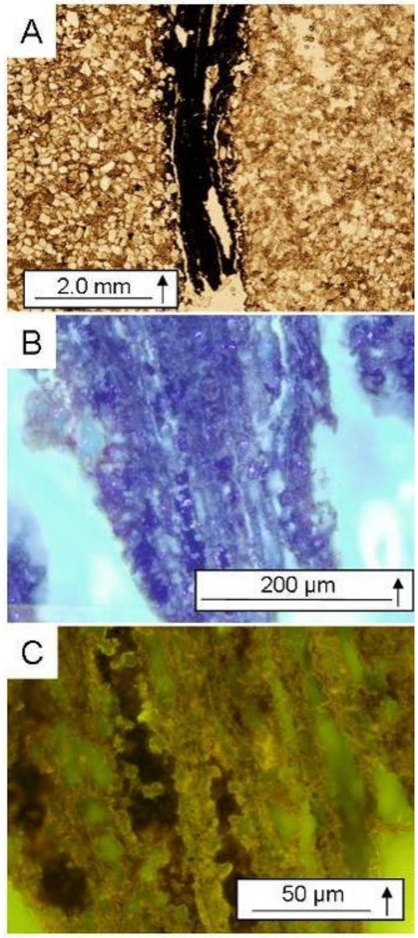

Figure 2.4 Photomicrographs from the Gilboa paleosol (site A). A) Carbonized root in homogenous sandstone in plane-polarized light. B) Cellular structure of carbonized root shown under blue UV fluorescence. C) Cellular structure of carbonized root shown under yellow-green fluorescence.

increased bioturbation, which makes distinguishing stump-cast features in S_2 more difficult. The S_1 paleosol is exposed on the sloping bank of the creek, making the stratigraphic determination of the stump casts relative to each other difficult; however, all stump casts do occur within very close stratigraphic proximity (Fig. 2.5).

The stump features are 15–44 cm in diameter, with 5–10 cm diameter roots that radiate away from the stump subhorizontally. Stump and root casts are most commonly infilled with sediment of similar grain size and color as the surrounding matrix, but lack any primary bedding structure. Below the stumps, networks of 0.1–1 cm-bifurcating-root traces radiate outward in all directions. These are variably colored with some larger roots having 1–5 cm thick gray-green rings surrounding the trace (Fig. 2.5). Branching root systems, 0.5–1 cm in diameter and extending 1.0–1.5 m deep, and typically with a drabbed halo, are associated with root traces in the surrounding paleosol matrix and occur throughout S_1 and S_2 paleosols. These roots were not directly associated with the stumps in outcrop, but are likely part of the tree-root network.

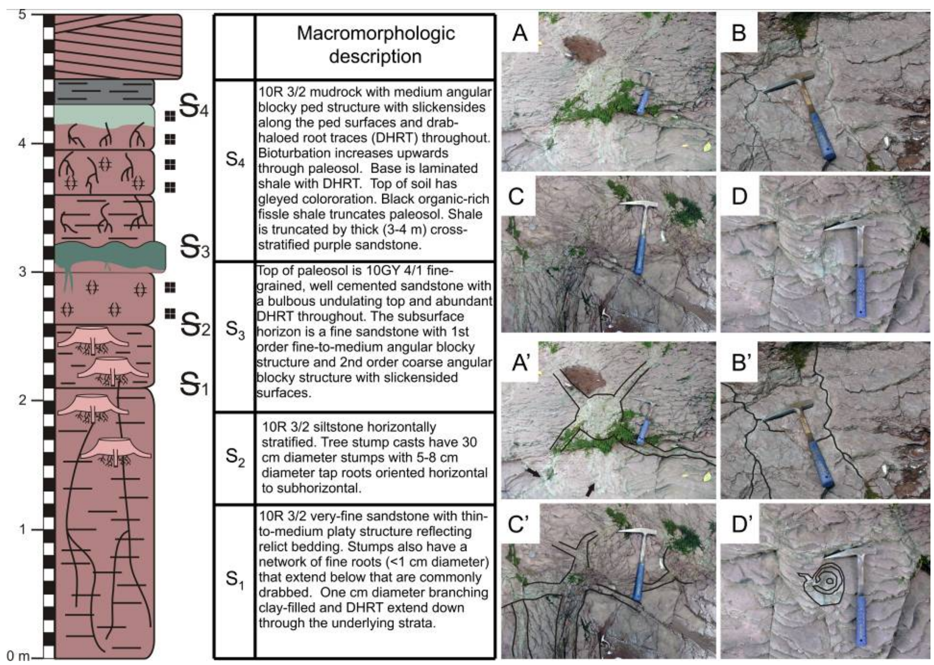

Figure 2.5 Macroscale description and outcrop photographs of location 1, West Saugerties (site B). A) Plan and cross-sectional view of an archaeopterid stump cast and root traces. B) Branching root traces associated with the stump-cast features. C) Plan view of heavily rooted strata in the S_1 paleosol. D) Root trace with ringed drab-halo features. Hammer = 35 cm long. Images presented in duplicate as both uninterpreted and interpreted features which are outlined in black. Black arrows = root traces.

Micromorphology: Location 1. The paleosols contain 20%–35% angular very fine-grained quartz sand grains, as well as 20% detrital mica grains, clay matrix, and iron-oxide staining throughout (Fig. 2.6). The matrix of the S_1 paleosol has well-preserved primary bedding with rare 100 μm diameter root traces bordered by 1–3 mm diameter drab halos. The S_1 paleosol is also devoid of any sepic-plasmic (oriented clay) fabrics. The matrix of the S_2 paleosol has some relict bedding structure, but is commonly bioturbated and homogenized. There are also common drab-haloed root traces throughout the matrix as well as insepic to latticesepic plasmic fabrics in the S_2 paleosol.

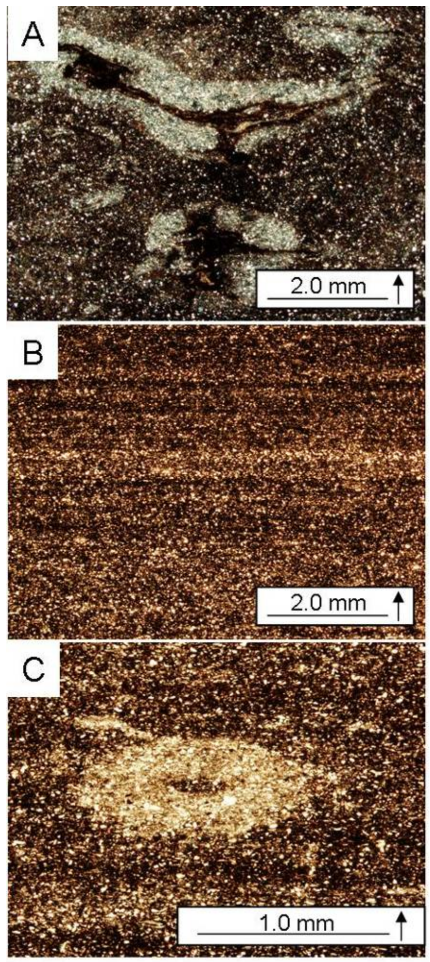

Figure 2.6 Photomicrographs from location 1 paleosol, West Saugerties (site B). A) Drab-haloed root trace from the S_2 paleosol in cross-polarized light. B) Stratified sediment from the S_1 paleosol in plane-polarized light. C) Drab-haloed root trace from the S_1 paleosol in plane-polarized light.

Macromorphology: Location 2. The paleosol at Location 2 in Plattekill Creek (Fig. 2.1, Site B) has multiple, coplanar sandstone-filled stump casts that extend down into the underlying clay-rich paleosol (Fig. 2.7). The A horizon of the paleosol has fine granular ped morphology in which peds increase in size, along with the amount of slickensided ped faces in the Bkss horizon. There are clear expressions of gilgai features preserved as curvilinear, master slickenside planes. Carbonate accumulations occur as nodules that range from 1–3 cm in the Bkss horizon. The pedality decreases in the underlying BC horizon, which has relict primary sedimentary bedding.

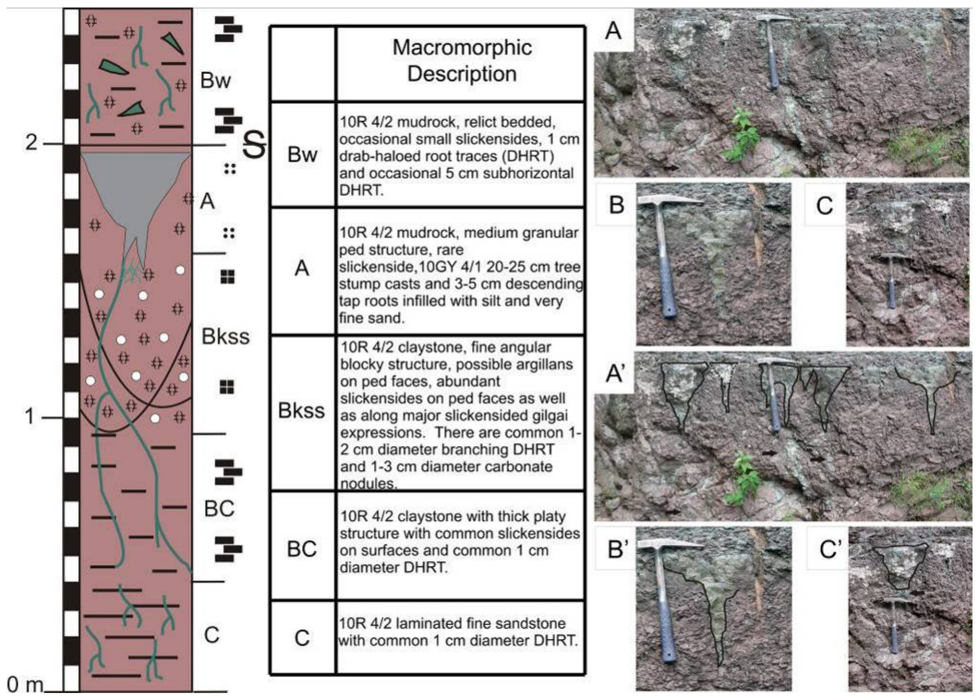

Figure 2.7 Macroscale description and outcrop photographs of location 2, West Saugerties (site B). A) Cross-sectional view of sandstone-filled stump casts in paleo-Vertisol. B) Cross-sectional view of large sandstone-filled root cast oriented vertically downward from the A to the Bkss horizon. C) Large slickensided surface from curvilinear fractures resulting from subsurface gilgai expression. Hammer = 35 cm long. Images presented in duplicate as both uninterpreted and interpreted features which are outlined in black. Black arrows = root traces.

The stump casts filled with fine-grained 10GY 4/1 (dark greenish gray) sandstone contrast markedly against the enclosing 10R 4/2 (weak red) claystone paleosol (Fig. 2.7). Stump and large root features extend 30 cm down into the paleosol profile and are spaced 10–20 cm apart. The tree trunks measured are 20–25 cm in diameter, although determination of the maximum diameter of these stumps was not possible due to the limitations of the vertical 2-D outcrop surface. Large root features are 3–5 cm in diameter and all are oriented vertically downward into the paleosol profile. Smaller branching root traces are 0.5–1.0 cm in diameter and typically have a drab halo which extends over a meter in depth below the sandstone-filled root traces.

Micromorphology: Location 2. The matrix of the Bkss horizon is primarily composed of clay with 5% angular, very fine silt-sized quartz grains (Fig. 2.8). Latticesepic, bimasepic, and unistrial plasmic fabrics are pervasive, as well as stress cutans formed around skeletal grains and hard pedogenic glaebules in the matrix. Banded vug and channel argillans occur throughout the Bkss horizon, as well as ped argillans coating ped surfaces. Argillans also coat pedogenic carbonate nodule surfaces and surfaces of shrinkage cracks within the nodules. Carbonate nodules have irregular, discrete boundaries with a microspar crystalline texture and calcite spar cements infilling some void spaces. Root traces are common; these are 1–2 mm in diameter and have 200–250 μm wide drab haloes with traces of branching root hairs extending off the main root form.

The stump cast is infilled with claystone and 5%–7% angular, coarse silt-sized quartz grains. Lattice-sepic and weak right bimasepic-plasmic fabric development characterizes the matrix. Pedolith fragments occur throughout the matrix, with stress cutan development in the surrounding matrix. Detrital carbonized plant remains that have preserved cellular morphologies are present. The matrix is completely devoid of iron oxide coatings or oxidized mineral assemblages prevalent in most of the terrestrial deposits in this region.

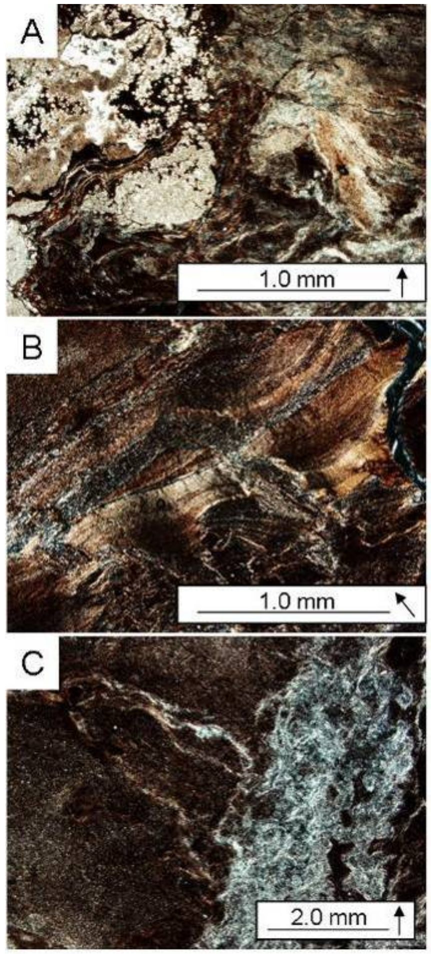

Figure 2.8 Photomicrographs in cross-polarized light from location 2 paleosol, West Saugerties (site B). A) Pedogenic carbonate nodules with argillans coating the outer surface and oriented clay fabrics in matrix from the Bkss horizon. B) Banded argillans infilling channel or vug from the Bkss horizon. C) Drab-haloed root trace with branching morphology from the Bkss horizon.

East Windham Locality

Macromorphology. The sandstone-filled stump casts from this site (Fig. 2.1, Site C) are in original growth position in a clay-rich paleosol (Fig. 2.9). The paleosol is truncated and overlain by laminated sandstone, resulting in varying degrees of stump preservation in the subsurface Btg horizon. The paleosol has well-developed fine-to-medium angular, blocky ped structure with common slickensides and argillan (clay) coatings on ped surfaces. Stump casts are 25–30 cm in diameter and infilled with gray-green laminated fine-grained sandstone. The stump bases commonly flare outward, somewhat resembling the morphology of *Eospermatopteris*; however, there are sandstone-filled tap-root traces 3–5 cm in diameter that extend downward from the stumps, a root morphology that is more consistent with an archaeopterid.

Micromorphology. The Btg horizon matrix is primarily composed of clay with 10% subangular quartz grains that fine upward from coarse to fine silt. Drab-haloed root traces 1mm in diameter are common, some with 100 μm diameter infilled voids with coarser-grained sediment (Fig. 2.10). Argillans occur in the form of vug, channel, and ped argillans. Iron-oxide nodules range from 0.5–1.0 mm in diameter, with common stress cutan development around the perimeter of the nodule. The matrix has lattisepic, bimasepic, and unistrial plasmic fabrics throughout the matrix.

Spatial and Population Distribution Analysis, Gilboa

The sandstone-filled stump casts and molds mapped on the exposed bedding plane at this locality (Fig. 2.1, Site A) are deeply truncated remnants of the tree stump bases (Fig. 2.11). The bedding plane that separates the sandstone paleosol and the cross-stratified sandstone that buried the stump features was apparently a plane of weakness that was exploited during quarrying efforts. Therefore measured diameters of tree molds and stump casts do not necessarily represent maximum trunk diameters, but are treated in the analyses as maxima. Tree stump features were not observed, nor was there any pedogenic modification of sediment below the sandstone paleosol. There was no evidence for stump and tree fossils out of original growth position (i.e., no traces of fallen

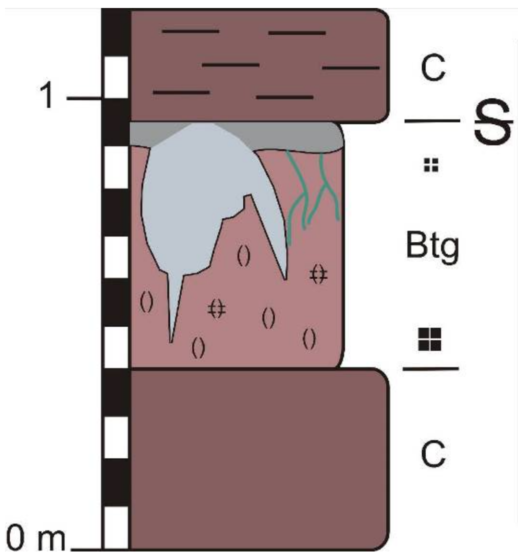

	Macromorphologic description
C	10R 3/1, Horizontally stratified, very fine sandstone.
Btg	10R 3/2 mudrock with very fine sand, Medium-to-fine angular blocky ped structure up through profile, occasional slickensides, drab-haloed root traces in top 30 cm of profile. Drabbed upper 10 cm of profile. Stump casts 25-35 cm diameter and descending tap roots infilled with gray-green laminated very fine sandstone.
C	10R 3/1 very fine sandstone. Massive with medium angular blocky ped structure.

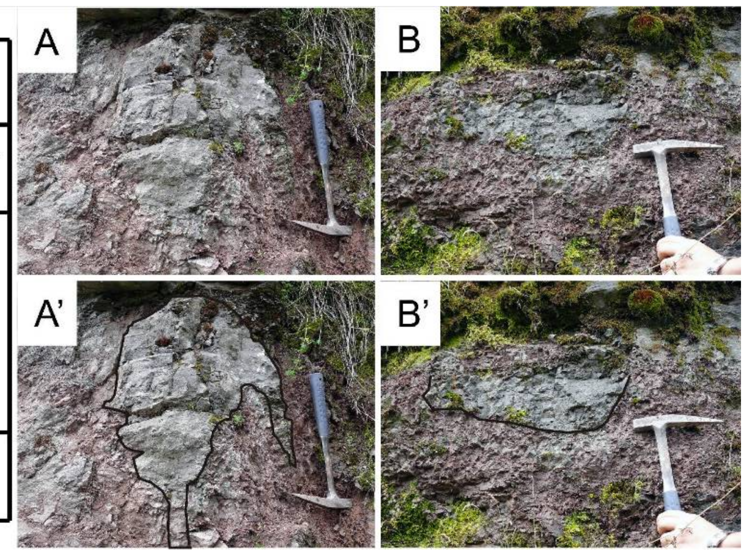

Figure 2.9 Macroscale description and outcrop photographs from East Windham (site C). A) Sandstone-filled stump cast and large branching root trace *in situ* in paleosol. B) Base of stump cast in paleosol. Hammer = 35 cm long. Images presented in duplicate as both uninterpreted and interpreted features which are outlined in black.

trees) in the sandstone paleosol, and none of the stump features were juxtaposed so as to overlap or cross cut one another.

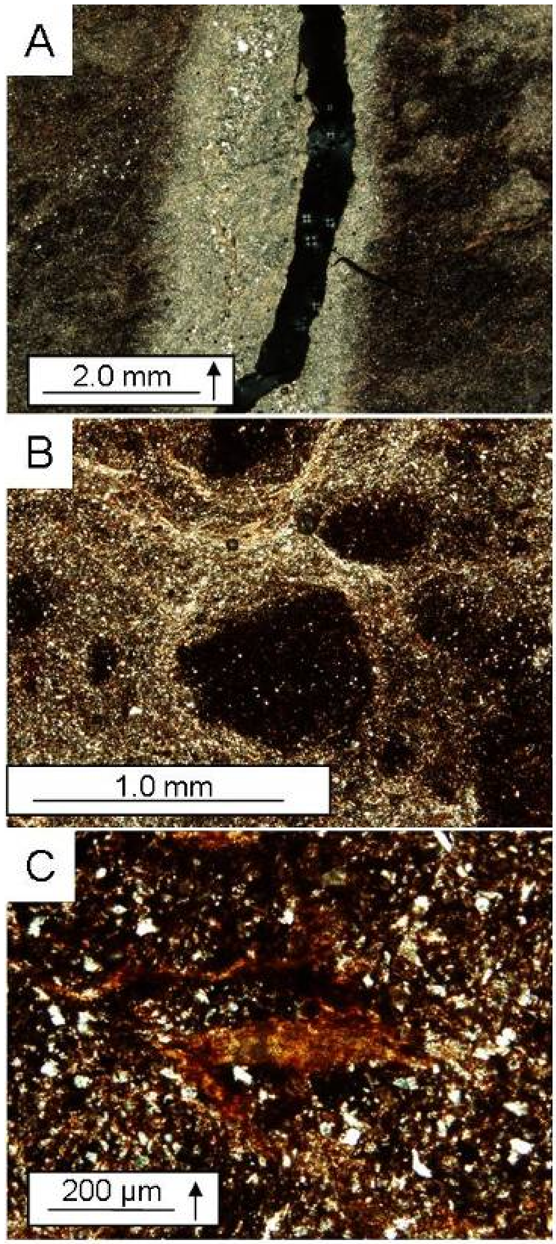

Figure 2.10 Photomicrographs in cross-polarized light from East Windham paleosol (site C). A) Drab-haloed root trace with void infilled with coarser-grained sediment from the Btg horizon. B) Iron-oxide nodules with stress cutans in surrounding matrix from the Btg horizon. C) Banded argillan in channel void from the Btg horizon.

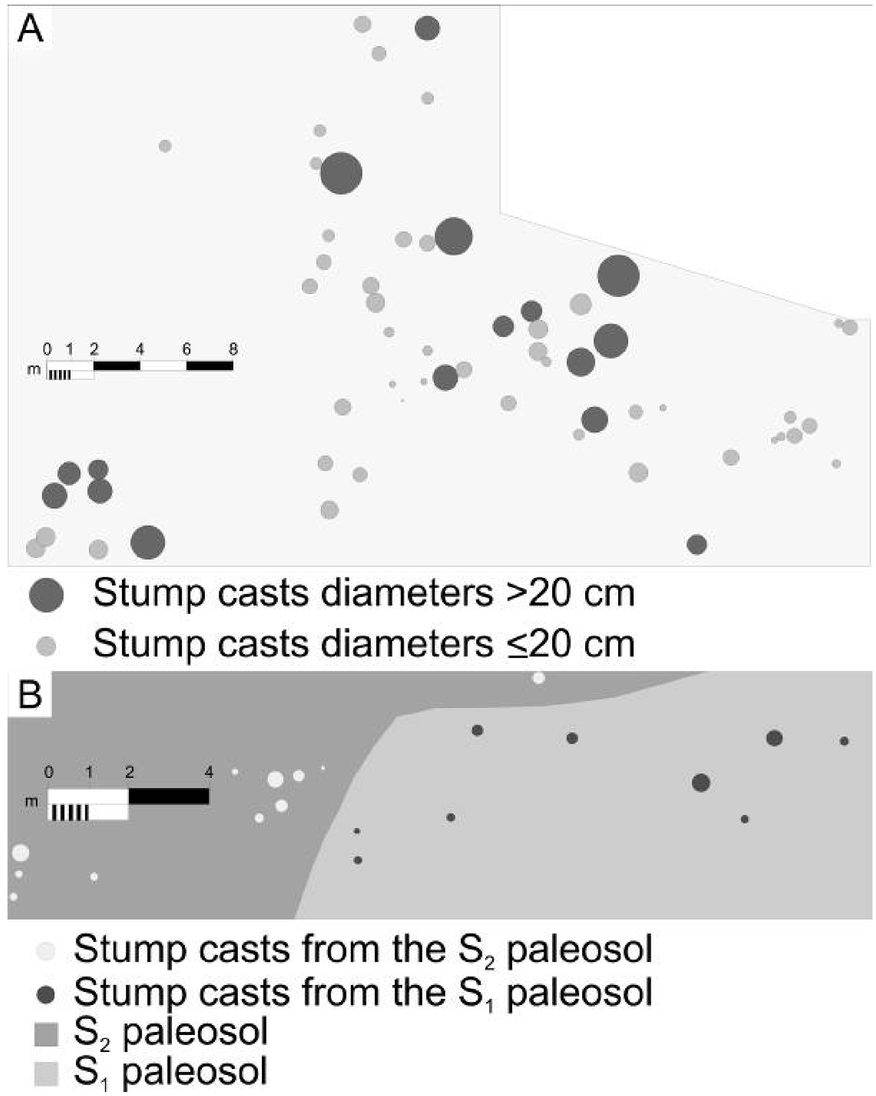

Figure 2.11 Maps of stump casts and molds on horizontally exposed bedding planes. A) Stump casts and molds on the quarried surface from Gilboa locality (site A). B) Stump casts from the S1 and S2 paleosols (Fig. 5) from West Saugerties, location 1 (site B).

The nearest-neighbor R value for the entire population is 0.73, which is a somewhat more clustered value than a random distribution (Fig. 2.13). Based upon the c test of Clark and Evans (1954) the spatial distribution of stump casts has a <1% chance of being the result of random distribution. The mapped subpopulations of ≤20 cm and >20

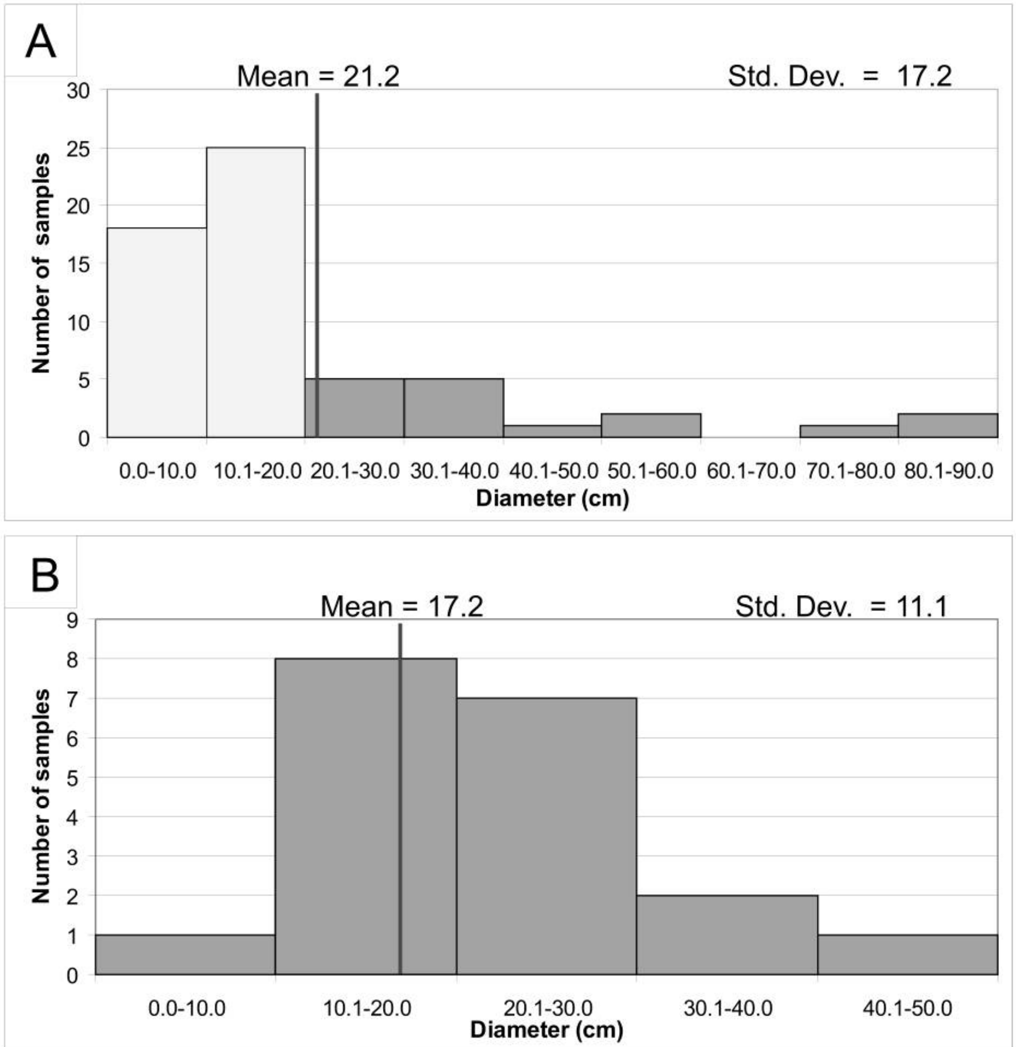

Figure 2.12 Stump and mold-cast diameter distributions. A) Distribution of *in situ* tree stump cast and mold diameters from the quarried bedding plane at the Gilboa locality. Light and dark colors = two subsets in population distribution. B) Distribution of *in situ* stump cast and mold diameters from the outcrop at West Saugerties, location 1.

cm diameter casts have R values of 0.64 and 0.91, respectively. These values suggest that the subpopulation of smaller stumps is more clustered than the subpopulation of larger stump casts. The c test on the smaller stump subpopulation shows that there is a <1% chance that their distribution is random. The large stump diameter subpopulation is indistinguishable from a random distribution based on the c test.

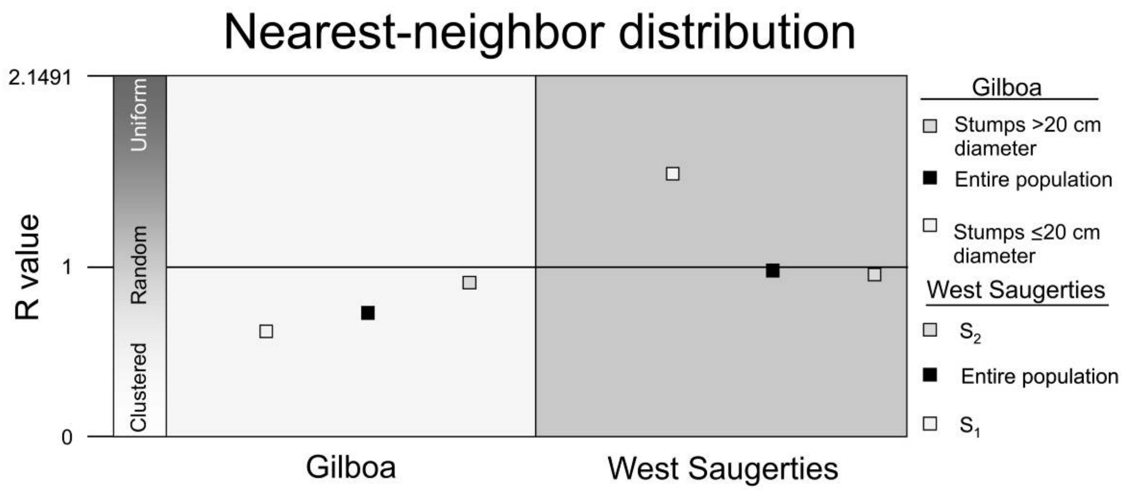

Figure 2.13 Nearest-neighbor distribution values for mapped stump casts in paleosols from Gilboa and West Saugerties (location 1) sites. Method described in Clark and Evans (1954).

Spatial and Population Distribution Analysis, West Saugerties

The stump casts mapped along the bank of Plattekill Creek (Fig. 2.1, Site B) in West Saugerties occur in two distinct bedding planes designating two separate paleosols with forest growth (Fig. 2.11B). The stump casts that occur within each of the two individual paleosols all occupy the same general stratigraphic position, though this is difficult to establish due to slight variances in elevations created by creek erosion. The stump casts did not have bulbous bases, as are common at the Gilboa site, suggesting that the stump fossils exposed in the paleosol represent the diameter maximum (Figs. 2.3, 2.5). There was no juxtaposition of stump casts causing overlap or cross-cutting relationships, nor were there any other stump features noted above or below these two distinct generations of forests (Fig. 2.11B).

The population of 21 stump casts ranges from 15–44 cm in diameter, with an average of 17.23 cm and a standard deviation of 11.12 cm (Appendix C) (Fig. 2.12B).

The stump population from the S_1 paleosol averaged 26.3 cm in diameter (S.D. = 9.8 cm) and that from the S_2 paleosol 24.6 cm (S.D. = 10.3 cm).

The R value for the composite population ($S_1 + S_2$) is 0.998 and R values are 1.56 and 0.95 for the S_1 and S_2 paleosols, respectively (Fig. 2.13). The R values suggest that the composite and S_2 values are very close to random, and that the S_1 paleosol is somewhat on the uniform side of random. All of these values are not statistically distinguishable from a random distribution based on the c test from Clark and Evans (1954).

Discussion

Tree stumps occur in several locations and in several different environments in Middle Devonian strata in the Appalachian Basin of New York. There is variation not only in the environmental settings in which forest development occurred, but also in the arborescent taxa that comprised these forest environments. The fact that all of the stump casts in these various paleosols are in their original growth position, commonly with root traces integrated within the paleosol matrix, leads to the conclusion that the stumps formed within the time frame of paleosol genesis. This conclusion leads to the next natural conclusion that the paleosols in which the stump fossils are preserved directly record the environmental conditions in which the trees grew, although compound genetic processes cannot be ignored. The preservation of these stump casts in the paleosols in which they formed does suggest that little time elapsed between when the forests grew and when they were buried and removed from the zone of active pedogenesis.

Fossil Stump and Root Morphologies

Tree stump-cast morphology alone provides an independent proxy for the environmental conditions during forest formation on these Givetian landscapes. The forest localities were each apparently inhabited by monospecific stands of arborescent plants. The forest at the Gilboa location was entirely composed of *Eospermatopteris,* cladoxylaleans that grew in deltaic and tidal-swamp deposits (Stein et al., 2007). These trees are distinct in their morphological attributes, namely their bulbous flared bases and small diameter, shallow, non-bifurcating root traces. These attributes are successful adaptations for supporting large plant bodies in swampy conditions characterized by persistently high water tables (Driese et al., 1997).

The other sites, including the two along Plattekill Creek and one in East Windham, were likely inhabited by archaeopterids, the principal arborescent progymnosperm species of the oxidized, terrestrial portion of the Catskill succession. Unlike *Eospermatopteris*, which probably had a habit similar to a modern tree fern, the archaeopterids possessed large trunks with dense wood, similar to modern conifers (Meyer-Berthaud and Decombeix, 2007). The stump casts have straight to downward-convergent trunk bases and all have large, 5–10 cm diameter root traces that extend either laterally (those from location 1, Plattekill Creek) or vertically (plunging forms, i.e., those from location 2, Plattekill and East Windham). Networks of smaller, bifurcating root traces 1–10 mm in diameter extend through the paleosol profiles for >1 m in depth. These presumed archaeopterid stump casts occur in more upland positions and well-drained fluvial depositional environments (Driese et al., 1997).

Paleopedology Associated with Givetian Forestation

Evidence for forest development occurring along the shoreline of the epicontinental seaway in the Appalachian basin was within coastal swamps (Driese et al., 1997). The paleosol in Gilboa, New York formed in low-angle cross-stratified, fine- to very-fine-grained quartz-rich sandstone and was completely devoid of oxidized iron or any reductively mobilized mineral assemblages. The likely formation of siderite nodules and the preservation of carbonaceous root remains suggest that this soil was reduced perennially. The presence of organic material with the original cellular structure preserved suggests that forestation occurred in an environment prone to preserve organics but not prone to produce a high volume of organics, as there is little organic matter preserved in the strata. Saturated soil conditions and shallow rooting depth limit the amount of pedogenic weathering that can occur, despite the length of time this soil was exposed to the surface. This limited nature of pedogenic modification would likely support classifying this paleosol as a paleo-Entisol based on the USDA soil taxonomy (Soil Survey Staff, 1990).

The paleosol with forest development at location 1 in Plattekill Creek exhibits weak pedogenic modification, resulting in preservation of the original bedded structure. This paleosol apparently formed in well-drained soil conditions with abundant iron oxide and deeply penetrating, bifurcating root traces. The lack of pedogenic modification, despite the evidence for forest growth in a well-drained environment, suggests that these paleosols were limited in the amount of time in which pedogenesis occurred. These paleosols likely formed proximal to a fluvial channel and would be classified as USDA paleo-Fluvents.

The paleosol at location 2 in Plattekill Creek formed under stable landscape conditions, thereby promoting prolonged periods of pedogenic weathering. The paleosol classifies as a USDA paleo-Vertisol with clear gilgai expression, well-developed wedge and granular pedal structure, sepic-plasmic clay microfabrics, and stress cutans. This paleo-Vertisol formed primarily under well-drained soil conditions, which produced well-developed argillans and pedogenic carbonate nodules. Pedogenic carbonate nodules are coated by illuviated clay, which suggests that this paleosol possibly formed under compound climatic conditions that changed from a drier to wetter climatic regime over time. The degree of clay illuviation, carbonate accumulation, and pedality suggests that this paleosol formed over a prolonged period of time on a distal floodplain or fluvial terrace position.

The paleosol in East Windham along New York State Route 23 is another paleosol that formed under stable landscape conditions. This paleosol classifies as a USDA paleo-Inceptisol with a high degree of pedality, an argillic horizon and hydromorphic properties. This paleosol lacks significant vertic (i.e., shrink-swell) properties beyond minor slickensided ped surfaces, stress cutans, and clay fabrics.

Trunk Diameter Population and Spatial Distribution of Forests

The ecological conditions that influence the spatial distribution and range of stump diameters are an important consideration when addressing the duration of forest development. A Pennsylvanian *Lepidodendron* forest in Illinois was shown to have likely been a short-lived, opportunistic forest that formed along a paleochannel in swamp deposits (DiMichele and DeMaris, 1987). The stumps had a small amount of variation in diameter and a random spatial distribution that trended towards a uniform pattern. This evidence suggests that there was no significant ecological stress influencing clustering or multiple generations of growth and competition for growth and survival.

The forest deposit along the Schoharie Creek in Gilboa, New York has a wide range of stump cast diameters and a large standard deviation. The dichotomy in distribution of stump cast diameters indicates a regenerating forest in which the younger cohort is regenerating within the canopy gaps of the older, mature stand. This intraforest spatial distribution of floral components suggests that there were multiple generations of growth. The larger stump-cast diameter subpopulation was likely a first generation growth of trees that were randomly distributed across an environmentally homogeneous landscape. The smaller diameter subpopulation represents a secondary growth of trees that developed in the remaining environmental niches available for growth, thus creating a clustering effect. The clustered spatial distribution (Clark and Evans 1954) of the casts indicates a resource-limited environment where new individuals grow near resource microsites in the environment (Kroh et al., 2000). These data suggest that this paleosol was stable for a prolonged period of time so as to allow for this type of multi-generational growth, consistent with the pedogenic development at the site, which has removed all relict bedding structures.

The forest deposits along Plattekill Creek in West Saugerties, New York have a much smaller range of stump cast diameters than those mapped at the site in Gilboa. The random spatial distribution of stump casts at this site indicates a non-limiting resource environment. It could also indicate the first stage of stand development of this paleoforest in which competition has yet to affect distribution. The limited size of the data set and the limited surface area of the exposed surface for each paleosol showing forest development, however, can create an artificially high R value, thus making the data appear more random or uniform, e.g., in the S_2 paleosol, than if there were an infinite space in which to sample.

The paleosols with forest development at Plattekill Creek likely development under an opportunistic growth forest that had a single generation of growth for each individual paleosol before burial. The stumps are all of similar diameter, which indicates that growth for all the trees likely began at a similar time. The fact that there is no spatial clustering of stump casts suggests that the trees did not experience environmental stresses, competition for growth, or multigenerational growth. The S_1 and S_2 paleosols are poorly developed; as a consequence original depositional structures are preserved within the parent sediment. The forests at location 1 along Plattekill Creek therefore likely formed during brief periods of subaerial exposure that were long enough to allow for forests to form, but insufficient for pedogenesis to obliterate bedding.

Middle Devonian Forestation

Givetian forests in the Appalachian Basin occurred in a variety of environmental niches varying from deltaic–coastal plain swamps and proximal fluvial environments to distal well-drained so-called upland floodplain conditions. The observations of mature community structure and root evolution in these species suggest that Middle Devonian forest development had a major influence on basinal floodplain and coastal environments through sediment and organic-matter production processes. Forest development in these environments could have had considerable impacts on sediment delivery to the marine system as well as the style of sedimentation and weathering processes that occur on the continents.

Conclusions

Forestation on Deltaic Strandline Swamp Environments

Observed forestation which formed on deltaic, fine-grained quartz sandstones deposited in strandline swamp conditions comprises a flora of arborescent *Eospermatopteris*. The forests had the potential to form multigenerational growth forests on stabilized landscapes over a prolonged period of undetermined time. The forested site at Gilboa, New York includes subsets in the *Eospermatopteris* community of small (≤20 cm diameter), spatially clustered specimens and large (>20 cm) randomly distributed specimens formed over multiple generations of growth.

Forestation on Fluvial Floodplain Environments

Forestation observed proximal to the channel form and sediment source is comprised of what appear to be archaeopterids based on subsurface stump and root-trace morphologies. The forested sites at location 1 in West Saugerties, New York are found in well-drained, weakly developed paleosols. The paleoforests have randomly distributed tree growth of similar-sized specimens, which suggests a limited time of formation before subsequent flooding and burial of the forested landscape.

Forestation observed on distal floodplain to upland settings is comprised of what appear to be archaeopterids based on subsurface stump and root-trace morphologies. The sites on the distal floodplain have evidence of both well-drained and hydromorphic hydrologic conditions. These paleosols are paleo-Vertisols and Inceptisols that formed on stable landscapes and likely had complex floral ecologies; however they are not sufficiently exposed laterally to enable measurement of their spatial ecological distributions.

Impacts from Forestation

Based on this examination of Givetian paleosols, forestation had a significant presence throughout fluvial and deltaic landscapes of the Middle Devonian in the Appalachian Basin. Influences of change brought on by the presence of forestation had potential influences on continental weathering, sediment and nutrient delivery to marine systems and changes in the carbon cycle.

CHAPTER THREE

Middle Devonian Landscapes, Climates and the Correlation of Continental Strata in the Northern Appalachian Basin

Abstract

Middle Devonian terrestrial strata deposited in the Appalachian basin, part of what is known as the Catskill Delta, record dynamic landscapes influenced by rainfall seasonality, tectonically driven changes in sedimentation and the onset of forested ecosystems. The Catskill Delta is a clastic wedge derived from detritus shed from the Acadian orogen that formed during the Devonian as a series of tectophases, as the Avalon island arc accreted obliquely onto the Laurentian continent. These tectophases are a series of orogenic events that generated accommodation and increased sediment yield into the Appalachian basin. Over 450 meters of nearly continuous outcrop exposure along Plattekill Creek in West Saugerties, New York, were measured in order to develop a sequence-stratigraphic framework using alluvial-stacking pattern analysis. The analysis reveals several orders of cyclicity that correspond with Acadian tectophases and previously documented marine depositional sequences. A terrestrial-to-marine stratigraphic correlation in the Appalachian basin is presented here. Paleosols in the Plattekill, Manorkill and Oneonta Formations, along Plattekill Creek, are dominantly hydromorphic in nature and classified as paleo-Vertisols and paleo-Inceptisols. Paleo-precipitation is estimated from 37 paleosol profiles using the CALMAG proxy, an elemental ratio from bulk soil material in vertic paleosols, which suggests humid paleoclimates, an interpretation also supported by micromorphological observations.

Estimates of MAP made using depth to carbonate proxies are significantly lower than CALMAG-based estimates, which suggest semi-arid to arid climates. A series of explanations for the discrepancies in the paleoclimate reconstructions from these different proxy methods are presented. Paleosols in this Middle Devonian succession preserve the earliest examples of forested ecosystems on earth and are preserved in a variety of landscapes. Evidence indicates that increased chemical weathering in paleosols on alluvial plains in the Appalachian basin from the Ordovician through the Middle Devonian, as the result of forestation, had potential impacts on both terrestrial weathering systems as well as on marine organic productivity.

Introduction

Devonian marine deposits in the Appalachian basin demonstrate several cycles of alternating clastic successions with associated deep water, organic-rich shales and marine carbonates (Fig. 3.1) (Heckel, 1973; Brett and Baird, 1985; Johnson et al., 1985; Sevon and Woodrow, 1985). These alternating clastic and carbonate successions in the Appalachian Basin are the result of major changes in sedimentary processes in the basin, which likely had some type of allocyclic driver (Johnson and Friedman, 1969; McCave, 1969; Ettensohn, 1985b; Johnson et al., 1985). The Plattekill, Manorkill and Oneonta Formations have long been recognized as fluvio-deltaic sedimentary successions formed from detritus shed from the Acadian orogen; however interpretations of the controls of long-term trends in sedimentation and how they correlate to the marine cyclo-stratigraphy have been contentious (Fig. 3.1) (McCave, 1969; Brett and Baird, 1985; Willis and Bridge, 1988; Bridge and Willis, 1994; Cotter and Driese, 1998). Anomalously thick fine-grained floodplain successions, which occur several times through the Plattekill and

Manorkill Formations, have been postulated as being genetically related to the marine carbonates in the Appalachian Basin (McCave, 1969; Johnson and Freidman, 1969). These successions have been interpreted to have resulted from either eustatic rise (McCave, 1969; Johnson et al., 1985), paleoclimate change related to tectonically induced monsoonal intensity (Ettensohn, 1985b), or from tectonic forces controlling basin subsidence and sedimentation (Willis and Bridge, 1988; Bridge and Willis, 1994; Ver Straeten, 2010).

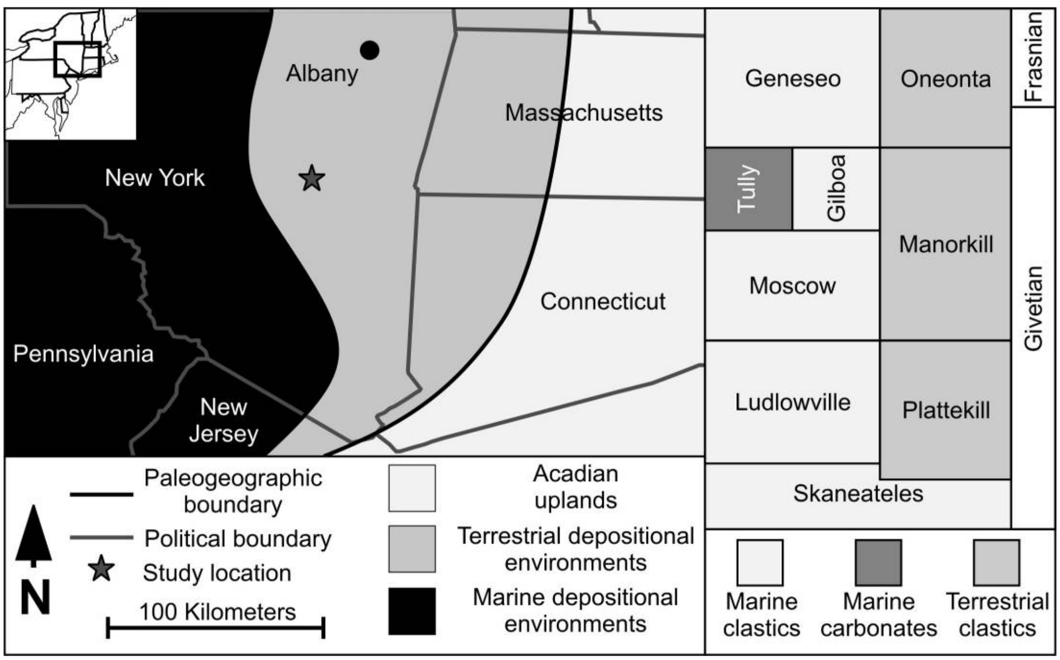

Figure 3.1 Paleogeographic map and regional stratigraphy of the Middle Devonian in the northern Appalachian basin. Paleogeographic reconstruction from Fail (1985), Dennison (1985), and Ettensohn (1985a); stratigraphy from Sevon and Woodrow (1985) and Brett and others (2010).

Records of soil formation on Middle Devonian landscapes, inferred through the physical and chemical state of paleosols (fossilized soils), provide information on the climate in which they formed, organisms that existed in the soil environment, relief on the landscape and the duration of weathering and soil formation. This paper examines paleosols in a measured section through over 450 meters of fluvial strata in order to investigate both the environmental influences on paleosol development as well as to deduce the forcing mechanisms controlling Middle Devonian terrestrial and marine sedimentation (Appendices D and E). Paleosol data, along with fluvial stacking-pattern analysis, are used to develop a sequence-stratigraphic framework within which correlation of fluvial and marine strata in the northern Appalachian Basin is possible. Various paleosol-derived paleoclimate proxies are compared, as well as, paleosol morphologies and trends in base-level through this Middle Devonian section, to determine what factors may have influenced the proxy-based estimations of paleoclimate. Relative elemental losses from paleo-Vertisols formed on alluvial plains in the Appalachian basin suggest that forestation was not only an important influence on terrestrial weathering systems, but also a potential driving influence on marine environmental, ecological and geochemical conditions.

Background

The Appalachian basin experienced several episodes of tectonism beginning in the Ordovician with the Taconic orogeny and ending during the Pennsylvanian-Permian Appalachian-Alleghanian orogeny that formed the Appalachian Mountains (Faill, 1997a, Faill, 1997b). The Acadian orogeny was the second major orogenic event to occur adjacent to the Appalachian Basin, which began in the Early Devonian as the Avalonian island arc collided with Laurentia (Ettensohn, 1985a; Faill, 1997b; Ver Straeten, 2010). The resulting Acadian mountains shed clastic sediments into the basin as fluvio-deltaic deposits, which constructed the classic "Catskill Deltaic wedge" (Johnson and Friedman, 1969; Faill, 1985; Sevon, 1985). The Avalonian island arc chain is inferred to have collided with Laurentia obliquely, creating a diachronous shift in Devonian deltaic depocenters from northeast to southwest (Ettensohn, 1985b; Ver Straeten, 2010). The collision of individual islands along the Avalon arc may have manifested as "tectophases" through the Appalachian basin, resulting in periods of increased subsidence and sedimentation into the basin (Ettensohn, 1985b). Middle Devonian terrestrial strata in southeastern New York consist of the Plattekill, Manorkill and Oneonta Formations, which are successions of fluvial strata that were deposited during the second and third Acadian tectophases (Willis and Bridge, 1988; Bridge and Willis, 1994; Ver Straeten, 2010).

Based on a series of ~30 meter thick outcrops that contain Middle Devonian strandline deposits, the terrestrial sedimentary basin in New York is reconstructed as ~100 km from the Acadian highlands to the paleo-shoreline (Dennison; 1985b; Sevon, 1985; Johnson, 1987) (Fig. 3.1). The position of the shoreline during the Middle Devonian likely fluctuated in response to changes in base-level and sedimentation. The terrestrial strata in southeastern New York have been interpreted as channel sands and overbank fines associated with laterally migrating sinuous river channels (Willis and Bridge, 1988). The paleogeographic position of the Appalachian basin has been positioned astride the paleoequator, placing the northern basin between 5 to 20° south paleolatitude (Woodrow et al., 1973; Kent, 1985; Woodrow, 1985). Other reconstructions suggest that the Appalachian basin may have been at higher latitudes (~30°S) during the Middle Devonian, which could have a significant impact on the type of climates that occurred in the Appalachian basin during the Middle Devonian (Blakey 2003; Blakey, 2010). Retallack and Huang (in press) used depth to carbonate horizon to estimate MAP (Retallack, 1994), and thickness of carbonate horizon (Retallack, 2005), to estimate range of seasonality in paleosols throughout the Middle Devonian in New York, and reconstructed a semi-arid climate with an average of MAP of 484 mm/y ± 147mm, with most mean annual range of precipitation less than 100 mm (Retallack 1994; 2005).

Middle Devonian fluvial and deltaic sedimentary systems were influenced by the entirely new ecological boundary condition of forestation (Algeo et al., 1995; Driese et al., 1997; Elick et al., 1998; Driese et al., 2000; Driese and Mora, 2001; Mintz et al., 2010). Forestation impacted a wide variety of Middle Devonian terrestrial environments in the northern Appalachian basin, from swamplands on delta plains, and both proximal and distal to channel floodplain landscapes in the northern Appalachian basin (Driese et al., 1997; Mintz et al., 2010). Forests formed on Middle Devonian landscapes were composed of either *Eospermatopteris* taxa in swamp lands on delta plains or Archaeopterid species in fluvial overbank depositional environments (Mintz et al., 2010). Middle Devonian Archaeopterids had root systems that extended over 2 meters down into the paleosol profile, which had a significant impact on the depth extent of pedogenic weathering (Mintz et al., 2010). This pervasive presence of deep-rooting vascular plants and forestation as a landscape-modifying agent had major impacts on landscape stability and fluvial sedimentation, transforming fluvial sedimentation patterns from braided- to meandering-dominated fluvial systems (Davies and Gibling, 2010). The onset of forestation was also postulated to have affected marine sedimentary systems through increased flux of biolimiting nutrients into marine systems related to increasing landscape stability and pedogenesis (Algeo and Scheckler, 1998).

Several periods occurred where widespread marine carbonates interrupted otherwise clastic-dominated marine sedimentation in the northern Appalachian basin during the Devonian (Johnson, 1970; Heckel, 1973; Rickard, 1975; Sevon and Woodrow, 1985). Two such anomalous carbonate successions, the Tichenor and Tully Limestones, occur in the otherwise terrigenous-dominated deposits, which are laterally equivalent to the terrestrial redbed clastic successions examined in this study (Sevon and Woodrow, 1985) (Fig. 3.1). A globally correlated extinction event or series of events known as the "Taghanic biocrisis" occurs within the Tully Limestone (Johnson et al., 1985; House, 2001; Baird and Brett, 2008; Zambito et al., in press). One previous hypothesis to explain the occurrence of the Tully Limestone is that it formed as a result of major eustatic rise, trapping terrigenous sediment in coastal and terrestrial systems, and effectively starving the basins of clastic sediment (McCave, 1969; Johnson, 1970; Johnson et al., 1985). Another suggested that the carbonate beds do not reflect deep-water carbonate deposition associated with sediment starvation but rather, that carbonate deposition occurred in shallow-water conditions (Brett and Baird, 1985; Baird and Brett, 2008) when tectonic loading and resulting clastic sedimentation decreased (Ettensohn, 1985a, Ver Straeten, 2010). The formation of these limestone units was, in part, dependent upon a fault-controlled foredeep that acted as a sediment trap, which collected terrigenous sediments, thereby enabling carbonates to form west of the foredeep (Heckel, 1973).

Correlation of Middle Devonian terrestrial stratigraphic sections with marine strata in the northern Appalachian Basin has been proposed in previous studies (Johnson and Friedman, 1969; McCave, 1969; Bridge and Willis, 1994). Thick deposits of overbank fines in the alluvial sections have been inferred as correlative with periods of eustatic rise, which lowered gradients on the alluvial plain and trapped sediment in terrestrial depositional systems (McCave, 1969; Rickard, 1975). Previous sequence-stratigraphic correlation of the Plattekill, Manorkill and Oneonta Formations with coastal-marine sections, using lithologic proportions and grain-size trends, suggests that correlation of the strata throughout the basin is possible (Bridge and Willis, 1994).

Methods

Fluvial systems were the primary method for sediment delivery into the Appalachian Basin during the Middle Devonian (Woodrow, 1985; Willis and Bridge, 1988) and therefore fluvial sedimentation was likely subject to the same factors of influence that act upon marine sedimentation (Catuneanu, 2006). Fluvial sedimentary systems represented in this measured section were relatively close to the strandline in the Middle Devonian (~5-10 km) (Dennison, 1985b; Ettensohn, 1985a) and therefore likely responded in a predictable fashion to changes in coastal and marine deposition (Fig. 3.1). Fluvial stacking-pattern analysis is integrated with changes in landscapes and climates inferred through the analysis of paleosols, in order to interpret changes in fluvial sedimentation in relation to marine sedimentary patterns in the Appalachian Basin.

Stacking-pattern Analysis

Sequences are genetically related strata bound at the base and top by unconformity surfaces, and by their correlative conformities, which provide the potential for allostratigraphic correlation (Mitchum, 1977). Several hierarchical tiers of cyclic stratal units have been shown to occur in paleosol-bearing alluvial successions, from which a sequence-stratigraphic depositional model has been developed in order to subdivide, categorize and ultimately correlate fluvial successions (Wright and Marriott, 1993; McCarthy and Plint, 1998; Kraus, 2002; Atchley et al., 2004). The methodology followed here to develop a terrestrial sequence-stratigraphic framework is based upon defining a hierarchy of cycles defined by thickness and magnitude of change in stacking patterns (Atchley et al., 2004). The highest frequency cycle is defined as fluvial aggradational cycles (FAC), which are successions of fining- or coarsening-upward fluvial deposits, and which may be pedogenically modified, with abrupt basal contacts with underlying strata and capped by another abrupt contact and facies change (Atchley et al., 2004; Cleveland et al., 2007). Individual FAC cycles are interpreted to result from autocyclic processes of stream migration, avulsion and subsequent channel stability and represent the lowest-order cycle and the fundamental building block of the higher order tiers of cyclicity (Bridge, 1984; Kraus, 1987; Kraus and Aslan, 1999; Atchley et al., 2004; Cleveland, 2008). Along with the stratal thickness of FACs we tracked grain-size, sedimentary and biogenic structures and pedogenic features were tracked in order to generate stacked bar charts and cumulative deviation-from-mean plots (CDM) (Fig. 3.2). From these data resolution of both decameter-scale fluvial aggradational cycle sets (FAC-sets) and hectometer-scale fluvial sequences is possible (Atchley et al., 2004; Cleveland et al., 2008).

A FAC-set is a succession of FACs that has an overall decreasing trend in thickness and grainsize and an increase in pedogenic development (Atchley et al., 2004; Cleveland et al., 2008). The formation of FAC-sets has been interpreted as an autocyclic

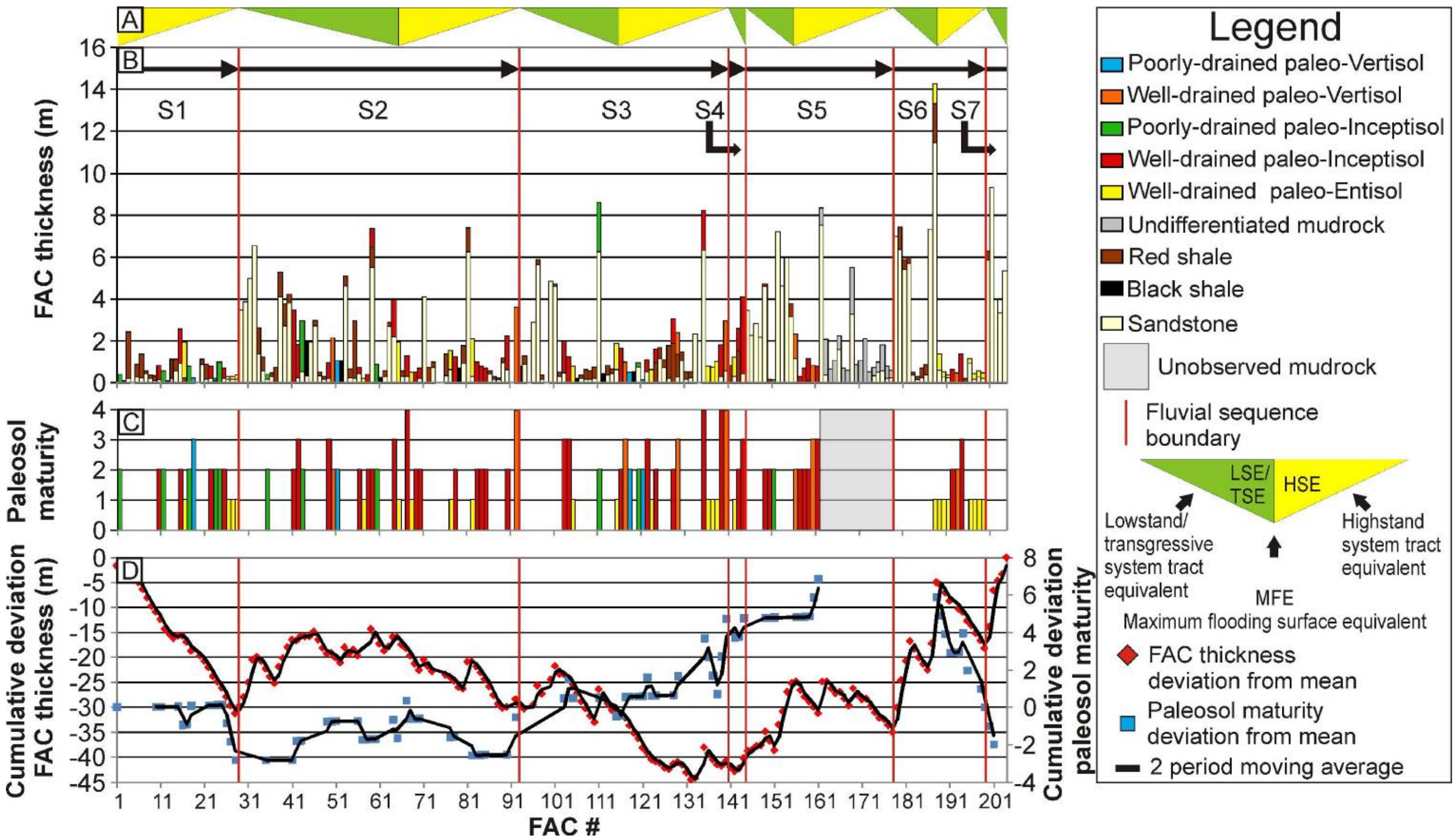

Figure 3.2 Fluvial facies, pedotypes, and paleosol maturity index data of each individual fluvial aggradational cycle (FAC) through the stratigraphic sections along Plattekill Creek. A) System tract equivalents. B) FAC thickness and internal facies and pedotype designation or each individual FAC. C) Paleosol maturity classification for each FAC with evidence of pedogenic modification. D) Cumulative deviation from mean plots of FAC thickness in red and paleosol maturity in blue.

process and was attributed to result from a series of migratory or avulsive episodes relative to a reference point in the basin (Atchley et al., 2004; Cleveland et al., 2008). Fluvial sequences are defined here by trends of decreasing FAC-set thickness succeeded by a trend of increasing thickness and associated increasing paleosol maturity (Atchley et al., 2004; Cleveland et al., 2008). Potential forcing mechanisms attributed to controlling the development of fluvial sequences include tectonism, climate and eustatic changes (Wright and Marriott, 1993; McCarthy and Plint, 1998; Kraus, 2002; Atchley et al., 2004). Fluvial sequences here are subdivided into lowstand and transgressive system-tract equivalents and highstand system-tract equivalents. The lowstand and transgressive system-tract equivalent is defined by FAC-sets with above average thicknesses, poorly-drained and weakly-to-moderately-developed paleosols. The highstand system-tract equivalent is defined by overall below average FAC-sets, relatively well-drained and moderately-to-well-developed paleosols.

Paleosols

The genesis of soil profiles are typically conceptualized through the following equation:

$$s = f(cl, o, r, p, t \ldots) \text{ Equation 1}$$

where soil formation (s) is a function (f) of the independent variables of climate (cl), organisms (o), relief (r), parent material (p) and time or duration of pedogenesis (t) (Jenny, 1941; 1994). These independent variables define the soil system in that for a specific combination of these variables there can exist only one soil profile (Jenny, 1994). This model, when applied to the rock record, enables interpretation of the independent variables of soil formation through the reconstruction of paleosol (ancient soil) profiles

(Retallack, 2001). When interpreting pedogenesis from paleosols by quantitative or qualitative techniques, other variables (in addition to the factors of soil formation) must be considered:

$$ps = f((cl, o, r, p, t) \times (bu, d)) \text{ Equation 2}$$

where paleosol profiles (ps) are a result of the factors of soil formation (Eq. 1) and the mode of burial preservation (bu) and diagenesis (d). Both quantitative and qualitative assessment of each factor of soil formation from paleosols can be modified by the mode of burial preservation, erosional loss of the weathering profile, depth of burial, and what types of physical and chemical changes have occurred through diagenetic alteration.

To aid in interpretation of pedogenesis from paleosols one must rely upon modern soil systems of classification and taxonomy in order to attempt to create analogs of modern pedogenesis. Description of paleosol profiles follows the methodology of Schoenberger et al. (2002), and they are classified, to the extent possible, using USDA Soil Taxonomy (Soil Survey Staff, 2010). Paleosols have been organized into pedotypes, a way of grouping similar paleosol profiles (Retallack, 2001), and named based upon their soil order and interpreted drainage condition (e.g., well-drained paleo-Inceptisol). Drainage classifications are relative terms because most paleosols in this succession, except for some of the paleo-Entisols lacking sufficient pedogenic structure, shows evidence of hydromorphic processes. Drainage designation therefore refers to the apparent dominant hydrologic state evident in both paleosol coloration and horizonation. Microscopic investigation of pedogenic morphologies (micromorphology) in paleosols follows the terminologies and interpretations of Brewer (1964). Colors were determined using a Munsell soil color chart. Assignment of numeric values for degree of paleosol maturity follows the index defined by Retallack (1988; 2001).

To understand how the various soil-forming factors influence weathering profiles, studies of modern soils are performed that isolate single variables of soil formation (e.g., climate for the "climosequence"). Climosequence studies are conducted to understand soil response to differences in climate which can be written as:

$$s = f_{cl}(climate)_{o,r,p,t} \text{ Equation 3}$$

where some soil property (s) is compared to changing climate condition and all the other factors of soil formation are held constant (Jenny, 1994). The application of the climosequence must be constrained to paleosols that are analogous to the soils used in its construction (Sheldon et al., 2002; Sheldon and Tabor, 2009; Nordt and Driese, 2010). The quantification of climate from paleosols, however, is only as good as our ability to constrain all the factors that influence the physical and chemical state (Eq. 2).

Molecular weathering ratios of the bulk soil matrix of subsurface horizons are one such property that has been shown to have a robust correlation to MAP (Sheldon et al., 2002; Sheldon and Tabor, 2009; Nordt and Driese, 2010). From a climosequence that examined a series of Vertisols along a strong precipitation gradient Nordt and Driese (2010) demonstrated a correlation of the chemical ratio CALMAG (Eq. 4) to mean annual precipitation (MAP), with an r^2=0.90. This relationship between the molecular weathering ratio in equation 4 and MAP is

$$CALMAG = \frac{Al_2O_3}{Al_2O_3 + CaO + MgO} \times 100 \text{ Equation 4}$$

derived from a climosequence model as described in equation 3, in which climate is the independent variable. In this study a suite of paleosols that are classified as paleo-

Vertisols or paleo-Inceptisols, and that possess vertic properties that are reasonable analogs to those modern soils used for calculation of CALMAG ratio, were examined. A minimum of two samples for each paleosol were analyzed at ALS chemex laboratories using inductively coupled plasma mass spectrometry, and in many cases entire paleosol profiles were analyzed at a 10 cm sampling interval.

Estimates of MAP from selected paleosols, determined from CALMAG, were compared to MAP estimates from a proxy calibrated to the depth in a paleosol profile to the top of the carbonate horizon (Bk). A positive correlation between the depth to the top of the Bk with MAP in modern soils was first presented by Jenny and Leonard (1934), and this relationship has been iteratively improved upon in subsequent studies and used in paleosols to estimate paleo-MAP in the rock record, as shown in equation 5, where *d* equals depth to top of carbonate horizon (Retallack, 1994). This proxy was constructed from a variety of soil orders, which are freely drained and formed on unconsolidated sediment that was not a clay or limestone parent material, and will be referred to as Depth to carbonate "universal" (DTC(U)) (Jenny and Leonard, 1935; Jenny, 1941; Jenny, 1994;

$$\text{DTC (U): } MAP = -0.013d^2 + 6.45d + 137.24 \text{ Equation 5}$$

Retallack, 1994; 2005). Another depth to Bk proxy for MAP is also compared in these selected paleosols, that was developed from a Vertisol climosequence, referred to as the depth to carbonate "Vertisol" proxy method for 5% pedogenic carbonate nodules (DTC (V)) (Nordt et al., 2006). The DTC (V) curve is distinctly different from that of the

$$\text{DTC (V): } MAP = 4E^{-5}d^2 + 4.251d + 432.27 \text{ Equation 6}$$

DTC (U) proxy due to higher clay content and lower permeability of the Vertisols in the DTC(V) than the majority of the soils used in the DTC(U) proxy, producing a different relationship between depth to carbonate and MAP in Vertisols than in other soil orders (Nordt et al., 2006). Paleosol thicknesses, used in these proxies, are decompacted to their estimated original thickness using equation 7 developed for Vertisols, in which C is the fraction paleosol thickness/original soil thickness and D is the burial depth in km (Sheldon and Retallack, 2001). The maximum burial depth for these strata has been estimated as 6.5 km using vitrinite reflectance from fossil wood

$$C = -0.69[\left(\frac{0.31}{e^{0.12D}}\right) - 1] \text{ Equation 7}$$

and is the same burial depth value used to decompact a succession of paleosols that is laterally equivalent with a portion of the strata described in this paper used to calculate depth to Bk (Friedman and Sanders, 1982; Retallack and Huang, in press).

Results

Stratigraphic Analysis

The 459 m of strata analyzed in this study were exposed along Plattekill Creek in West Saugerties, New York, modifying the stratigraphic analysis of Willis and Bridge (1988) (Appendix D). A total of 204 individual FACs, 26 FAC-sets 5 complete fluvial sequences and 2 more partial sequences at the base and top of the succession, were described (Appendix D). Each individual FAC is displayed in a stacked bar graph representing the proportions of facies and pedotypes that occur (Fig. 3.2B). Where paleosols occur in the section they are assigned a numeric paleosol maturity stage after Retallack (1988) (Fig. 3.2C). Both FAC thickness and paleosol maturity are plotted as CDM plots in which the mean of those data sets (2.03 m; 1.99 respectively) are subtracted from each individual data point and the difference is added to the previous value. Trends in CDM FAC thickness (FAC-CDM) and paleosol maturity (PM-CDM) aided in defining FAC-sets and fluvial sequences.

Paleosols

Eighty-four paleosols were described along Plattekill Creek, all of which occur in fine-grained overbank deposits. Almost all paleosols described here are buried by overlying bedded alluvium separating the next subsequent paleosol, with very few paleosol profiles welded together, thus creating "compound" paleosol profiles. Paleo-Entisols have pedogenic modification in the form of rooting and partial to complete destruction of primary depositional fabric, but no development of a B horizon (Appendix F) (Mintz et al., 2010). Paleo-Inceptisols have developed subangular blocky peds, vertic features such as slickensided ped surfaces and oriented clay fabrics in the paleosol matrix and commonly have illuviated clay and/or pedogenic carbonate in the subsurface horizons (Appendix F) (Fig. 3.3). Paleo-Vertisols have abundant slickensides and stress cutans on ped surfaces, and typically the occurrence of wedge-shaped peds, arcuate master slickenside surfaces and the presence of pedogenic carbonate and illuviated clays evident in thin section (Appendix F) (Fig. 3.3).

From these paleosols, 37 were selected for major and trace element analysis in order to estimate MAP using the paleo-Vertisol proxy CALMAG (Eq. 4; Nordt and Driese, 2010). The average MAP estimate for this Catskill stratigraphic section is 1550 mm/yr, with many of the paleosol CALMAG ratios (Eq. 4) falling outside the range of the calibration, so that much of the curve is extrapolated from the best-fit line (Fig. 3.4). Many of the paleosols had truncated or missing A horizons resulting from erosion prior to burial, which precludes the development of a curve of MAP estimates based on depth to

Bk horizon. Estimation of MAP using DTC(U) and DTC(V) was performed on selected complete paleosols to compare to CALMAG estimations. Measured depths to the Bk horizons in these paleosols are 25 and 40 cm, which are decompacted depths of 32 and 50 cm (Eq. 7). Estimated MAP using DTC(U) (Eq. 5) are 360 and 490 mm/yr for the two paleosols, respectively, and 570 and 645 mm/yr using DTC(V) (Eq. 6) (Fig. 3.5).

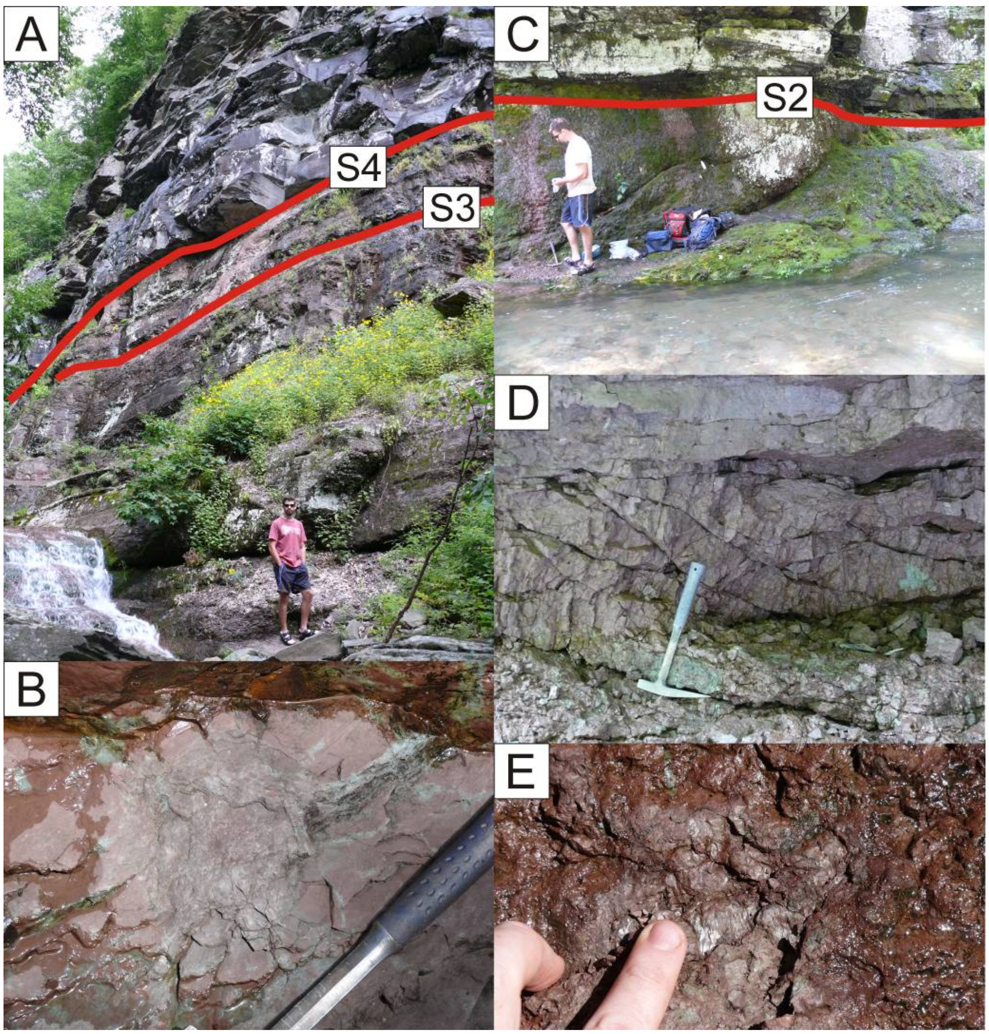

Figure 3.3 Photoplate- A) Stratigraphic section along Plattekill Creek, 3rd and 4th sequence boundary highlighted by red line. B) *Eospermatopteris* stump cast in paleo-Entisol directly above the 4th sequence boundary. C) Paleo-Vertisol in paleo-channel capped by black shale at 2nd sequence boundary highlighted in red. D) Wedge-shaped peds in a paleo-Vertisol. E) Slickensided ped surface at interfluve paleosol near 4th sequence boundary.

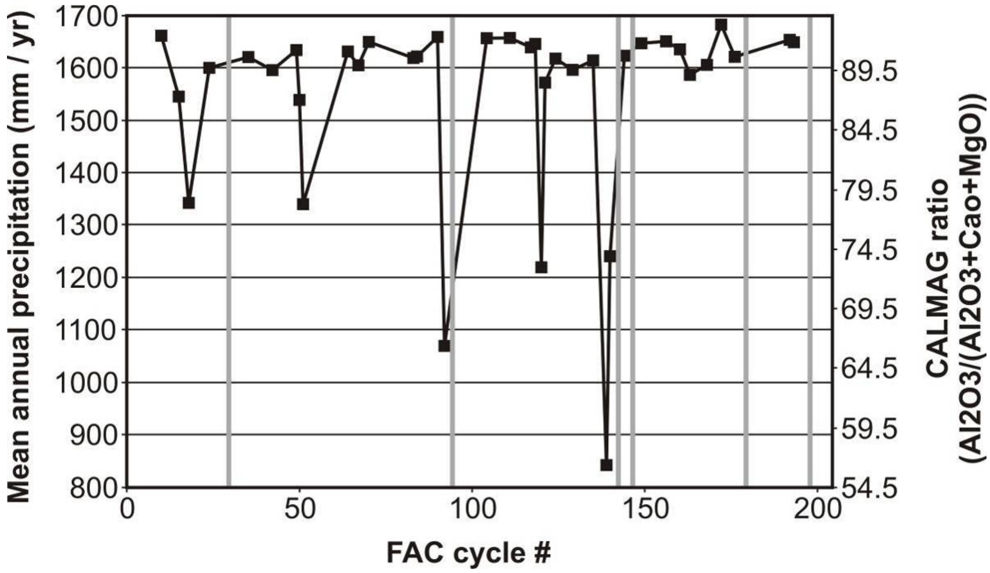

Figure 3.4 CALMAG ratio and calculated mean annual precipitation estimates for selected paleosols in Plattekill creek. Gray bars represent sequence boundaries (See Fig. 3). CALMAG values generated from the undescribed section in Figure 3 comes from laterally adjacent strata on a road cut on Plattekill Road and FAC cycle numbers are inferred from Willis and Bridge (1988).

Discussion

Sequence-stratigraphic Interpretation

Sequence 1 (S1) is incomplete, with only the highstand system-tract equivalent (HSE), exposed above 80 m of covered interval, composed of primarily pedogenically modified mudrock that has a decreasing trend in FAC-CDM (Fig. 3.2). The sequence boundary is defined at the inflection point in FAC-CDM (Fig. 3.2D) from a negative to positive trend, which corresponds with an increase in sandstone deposits and decrease in paleosol occurrence (Fig. 3.2). Sequence 2 (S2) has thick sandstone deposits at the base which formed as the result of high accommodation, stream gradient and sediment yield into the basin (Fig. 3.2). This succession defines the lowstand system-tract equivalent (LSE) and early transgressive system-tract equivalent (TSE), and transitions into dominantly pedogenically modified mudrock and lacustrine black-laminated shale facies

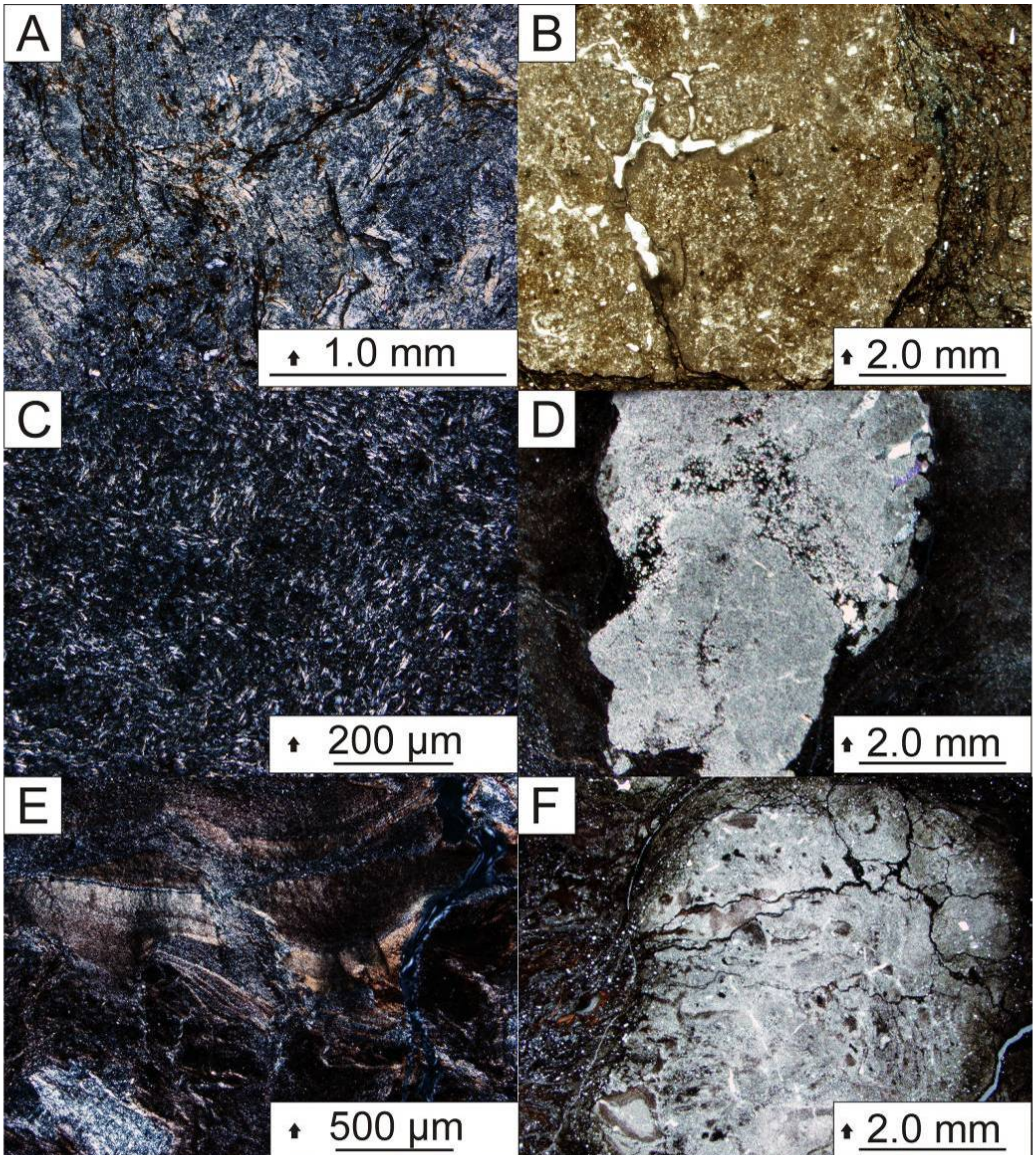

IMAGE: A/B FAC #: 18	IMAGE: C/D FAC #: 139	IMAGE: E/F FAC #: 140
CALMAG = 78.3	CALMAG = 59.0	CALMAG = 78.5
CALMAG MAP = 1340 mm	CALMAG MAP = 800 mm/yr	CALMAG MAP = 1080 mm/yr
Depth to Bk horizon = N/A	Depth to Bk (D) = 32 cm	Depth to Bk (D) = 50 cm
Truncated top of paleosol	•Depth to Bk (U) MAP = 360 mm/yr	•Depth to Bk (U) MAP = 490 mm/yr
Depth to Bk MAP = ? mm/yr	•Depth to Bk (V) MAP = 570 mm/yr	•Depth to Bk (V) MAP = 645 mm/yr

Figure 3.5 Photomicrographs of pedogenic features and paleoclimate estimates from selected paleosols- A) Illuviated clay in a Bkss horizon. Taken in cross-polarized light (xpl). B) Pedogenic carbonate nodule with septarian shrinkage cracks infilled with sparry calcite (xpl). C) Lattice-bimasepic plasmic fabric in Bkss horizon (xpl). D) Pedogenic carbonate in Bkss horizon (xpl). E) Banded illuviated clay and plasmic fabric in a Bkss horizon (xpl). F) Pedogenic carbonate nodule in Bkss horizon (xpl). D= decompacted depth; U = universal depth to Bk proxy (Retallack, 1994); V = Vertisol depth to Bk proxy (Nordt et al., 2006).

in the late TSE (Fig. 3.2). The maximum flooding-surface equivalent (MFE) is at the inflection from increasing FAC-CDM to a decreasing trend that coincides with the last occurrence of the black shale facies in this sequence (Fig. 3.2). The HSE is defined by a decreasing trend in FAC-set thickness and a succession of relatively well-drained paleosols. The sequence boundary occurs at a thick (~3.5 m), well-drained and well-developed paleo-Vertisol that is capped by the black shale facies (Fig. 3.2) indicating a significant rise in base-level.

The LSE and early TSE of sequence 3 (S3) includes a succession of sandstone-dominated FACs that correspond to an increasing FAC-CDM trend that transitions into a succession of mudrock with occasional moderate pedogenesis (Fig. 3.2). The MFE surface is defined at a boundary between a paleo-Entisol below a well-drained paleo-Inceptisol, marking where the succession transitions from few weakly to moderately developed paleosols in the TSE to common moderately to well developed paleosols in the HSE (Fig. 3.2). The succession of well-developed paleosols in the HSE of S3 suggests a period of decreased accommodation and sedimentation on floodplains, which allowed for increased pedogenesis and thin FAC cycles. The sequence boundary of this succession is marked by two thick, very well-developed and well-drained paleosols, the upper of which has preserved Archaeopterid stump casts (Mintz et al., 2010). These paleosols are capped by deltaic deposits of red and gray shales that exhibit soft-sediment deformation, and *Eospermatopteris* stumps in a paleo-Entisol that are commonly associated with delta-plain environments (Fig. 3.3) (Driese et al., 1997; Mintz et al., 2010). The overlying sequence 4 (S4) is a thin TSE succession of deltaic strandline deposits that transitions into well-developed paleosols that are truncated at the erosional S4 sequence boundary, and capped by a thick succession of sandstones (Fig 3.3A).

Sequence 5 (S5) has a LSE and TSE composed of FACs with thick channel sandstones and little mudrock deposition or pedogenesis, with an increasing trend in FAC-CDM (Fig. 3.2). The MFE surface is defined at the top of a thick FAC of sandstone deposits that fines into red shale below a thinner FAC that has sandstone at the base, and fines into a moderately developed well-drained paleo-Vertisol, separating thick sandstone- dominated FACs from thin mudrock-dominated FACs (Fig. 3.2). The sequence boundary defining the termination of the 5th sequence occurs as the inflection point in the FAC-CDM curve, from a decreasing trend to increasing trend at the beginning of the 6th sequence. The base of the sequence 6 (S6) has a TSE that is composed of very thick sandstone deposits, which produces a steep positive slope in the FAC-CDM curve (Fig. 3.2). The MFE occurs at the top of a very thick FAC (~14 m) below a succession of thin FACs that commonly are capped by pedogenically modified mudrock. The PM-CDM decreases through the HSE, suggesting that high sedimentation rates limited landscape stability and pedogenesis. The LSE and TSE of sequence 7 (S7) is a succession of thick sandstone FACs associated with an increasing FAC-CDM and rise in relative base-level that is only partially exposed along Plattekill Creek (Fig. 3.2).

Terrestrial Depositional Cycles

Several hierarchal tiers of cyclicity in the stratal thickness trends can be identified from the FAC-CDM curves based on wavelength and amplitude of change (Fig. 3.2D). The first tier of cyclicity has the maximum amplitude and wavelength in this succession and has roughly one complete cycle in the Plattekill, Manorkill and Oneonta Formations exposed along Plattekill Creek. This trend in FAC-CDM has a descending limb through S1, S2 and S3 and a minimum in the HSE of S3 and S4, and an ascending trend through S5, S6 and S7 (Fig. 3.2). This dominant cycle in FAC thickness has a very similar trend to marine water depths, modeled from deltaic successions, which are interpreted to be controlled by changes in accommodation (Fig. 3.6) (Ettensohn, 1985; Ver Straeten, 2010). Correlation of these two data sets is based on lithostratigraphic mapping and stratigraphic correlation so that some amount of error exists in the association of the terrestrial data with the marine (Fig. 3.6). Despite the inherent uncertainty in correlation, we suggest that, given their similarities, it is most likely that the FAC-CDM and marine water depth curves are genetically related to one another (Fig. 3.6). Tectonic loading not only controlled basin subsidence but also controlled uplift in the highlands and sedimentation rates in the terrestrial basin, which is reflected in the out of phase nature of the PM-CDM relative to the FAC-CDM at this cycle scale (Fig. 3.2).

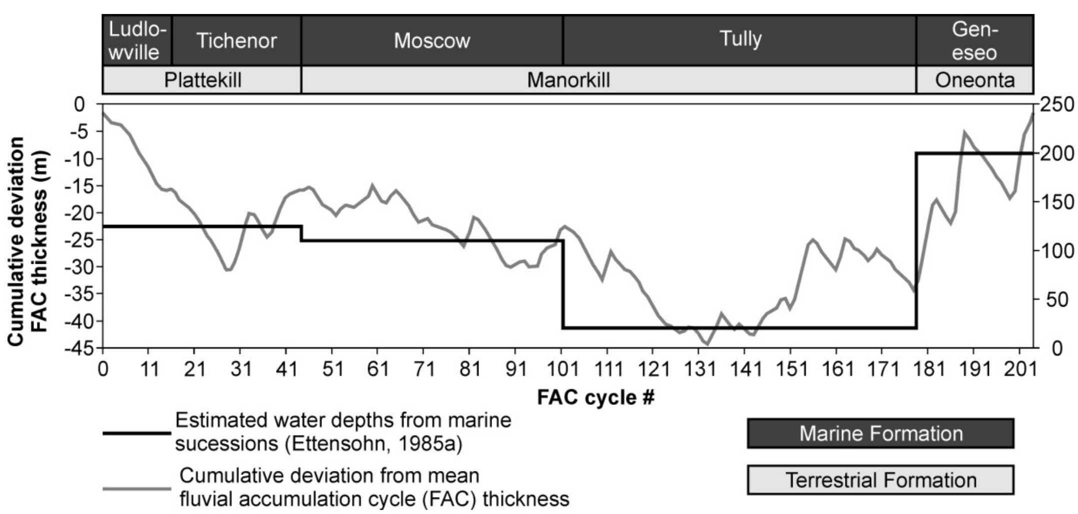

Figure 3.6 Cumulative deviation from mean FAC thickness comparison with modeled estimated water depths from Ettensohn (1985a). Lithostratigraphic correlation based on Sevon and Woodrow (1985).

The second tier of cyclicity is defined as terrestrial sequences, which are typically hectometer-scale cycles controlled by regional changes in either base-level and/or sediment supply related to changes in tectonism, eustacy, climatic or some combination of all three controls (Wright and Marriott, 1993; McCarthy and Plint, 1998; Atchley et al., 2004; Cleveland et al., 2008). The decrease in base-level and relative sea-level, in the Appalachian basin, associated with the formation of the Tully Limestone (Fig. 3.6) occurs during a period of global eustatic sea-level rise (Johnson, 1985; Dennison, 1985a; House, 2002). This suggests that the control of base-level and accommodation trends at the sequence level in the Appalachian Basin was not entirely eustatic (Ettensohn, 1985; Ver Straeten, 2010). Small-scale (parasequence level) deepening events in the marine are hypothesized as eustatic (Brett and Baird 1985; 1996; Brett et al., 2010) leaving the possibility that longer-term trends in accommodation were also controlled, in part, by eustatic changes. The third tier of cyclicity are decameter-scale FAC-set cycles recognized in the FAC-CDM plot as having short relatively small amplitude cycles, which have been suggested in previous studies to represent autocyclic mechanisms of stream meander and avulsion processes (Atchley et al., 2004; Cleveland et al., 2008). These cycles may have potential for correlation in the same fluvial drainage system, however, on a regional basis or from the terrestrial to marine systems correlation is unlikely.

Terrestrial/Marine Correlation

The recognition of sequence-boundary surfaces in the terrestrial strata in the northern Appalachian basin provides the opportunity to construct a detailed terrestrial-to-marine allostratigraphic correlation. Similarities in large-scale trends in terrestrial and marine sedimentation suggest that the two systems were being influenced by the same external controls and were closely interconnected within this basin (Fig. 3.6). The potential to identify genetically related allostratigraphic units in a setting where surfaces cannot be physically traced out across the basin depends upon our ability to understand the changes in terrestrial and marine systems, and how these changes were manifested relative to recognized surfaces. Correlation of marine strata in the northern Appalachian basin through the use of sequence-stratigraphy is the result of careful study of a series of outcrops that extend east-west from Syracuse to Buffalo, New York (Brett and Baird, 1996; Baird and Brett, 2008; Brett et al., 2010; Zambito et al., in press).

The base of the section along Plattekill Creek is the progradational HSE of S1, part of the Plattekill Formation that likely correlates with the Jaycox Member of the Ludlowville Formation, the highstand system-tract (HST) of the Giv-2 sequence (Figs. 3.6, 3.7) (Brett et al., 2010). The sequence boundary defining the end of S1 and the beginning of S2 signifies the onset of a period of sandstone-dominated sedimentation in a high-accommodation basin on Middle Devonian landscapes in response to a relative base-level rise in the Appalachian basin (Fig. 3). The formation of the Tichenor and Menteth Limestones is likely in response to a rise in relative sea-level during the TSE of S2, which would have back-filled valleys created from fluvial incisement and floodplains, during the formation of the S1 sequence boundary (Fig. 3.2). The Tichenor Limestone deposited on top of a regionally extensive, erosional sequence boundary between the Ludlowville and Moscow Formations (Brett et al., 2010). The basal Tichenor Member, followed by the Deep Run Shale Member and the Menteth Limestone Member, comprise the transgressive system-tract (TST) of the Giv-3 sequence (Fig. 3.7)

(Brett et al., 2010). The Tichenor, Deep Run and Menteth Members are roughly equivalent with the Portland Point Limestone, a succession of interbedded limestones and marls, which represents the easternmost limestone deposits (Rickard, 1975; Baird, 1979; Sevon and Woodrow, 1985; Brett et al., 2010). This carbonate succession formed on a broad, westward-dipping ramp that extended into central New York and is thought to represent a condensed succession formed on a sediment starved shelf (Baird, 1979; Brett and Baird, 1996). Marine carbonate deposition in the basin at this time likely occurred during the early formation of the TSE of S2, as clastic sediment was being trapped in terrestrial environments, thus starving the marine system (Figs. 3.2, 3.7). The HSE deposits in S2 that are composed of thin, pedogenically modified FACs formed during a decrease in accommodation gain, which likely correlates with the Lower Windom Member of the Moscow Formation (Fig. 3.7) (Brett et al., 2010).

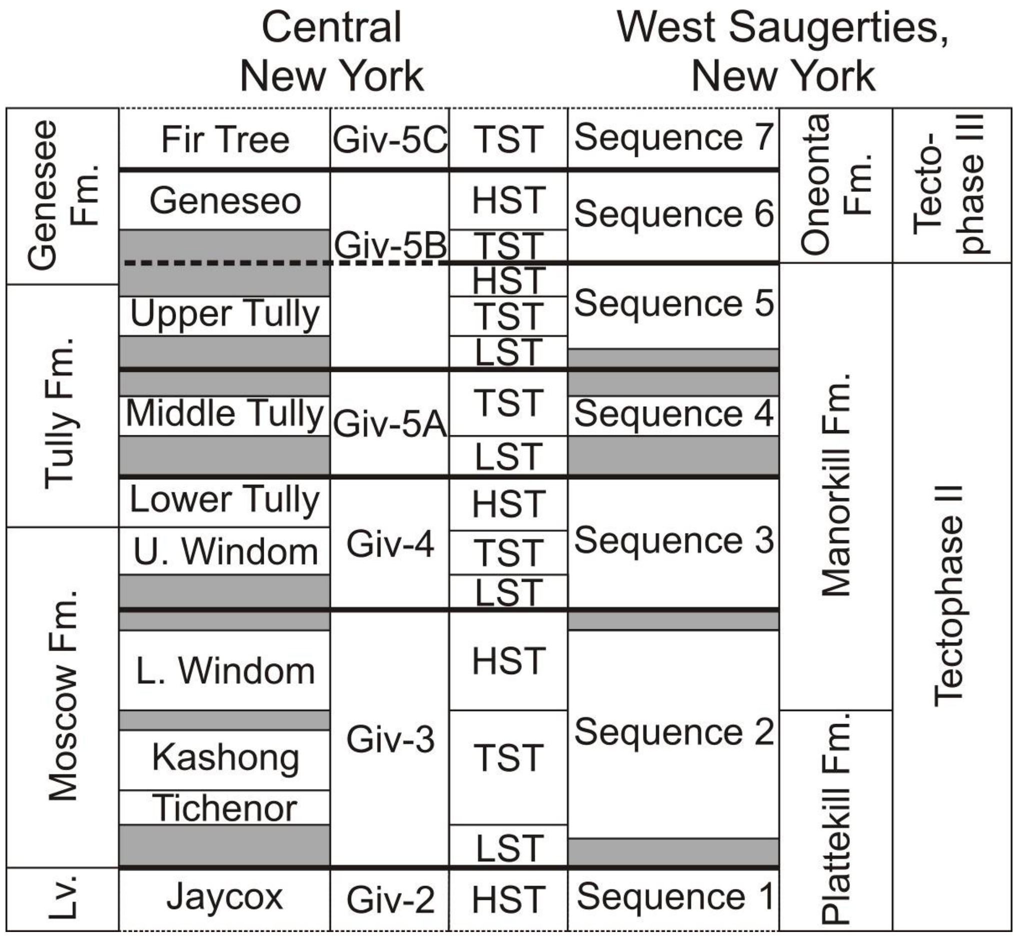

Figure 3.7 Stratigraphic correlation between fluvial and marine strata in the northern Appalachian Basin. Gray areas represent missing time at unconformable surface. Thick black lines represent sequence boundaries. Dashed black line is possible sequence boundary. Lv. = Ludlowville Formation. Marine sequence stratigraphy and nomenclature of the Giv-# sequences based on Brett and Baird (1996) and Brett et al. (2010). Tectophase interpretation from Ettensohn (1985b).

The fluvial strata that comprise the HSE of S3 formed during a period of quiescence in Acadian tectonism (Fig. 3.6), resulting in decreased subsidence and sediment yield in the Appalachian basin. Previous work by Bridge and Willis (1994) interpreted the approximate placement of our MFE as a sequence boundary based on a decreasing trend in grain-size. Based on the appearance of a succession of well developed and well drained paleosols, this succession of fine-grained deposits is more likely related to the aggradation of floodplain sediments in a low accommodation environment (Fig. 3.2). This succession is likely genetically related to the onset of Tully Limestone deposition and deposition of the Lower Tully Formation. Clastic detritus that progradaded into the basin during the period of low subsidence, that would have otherwise prevented carbonate deposition, was trapped by a fault-controlled foredeep that formed in the eastern portion of the marine basin (Heckel, 1973). The Tully Limestone Formation is a carbonate deposit that has three regionally extensive sequence-boundary surfaces: one at the base, another separating the middle Tully from the lower and a third separating the middle from the upper Tully Formation (Brett et al., 2010; Zambino et al., in press). These units are recognized by sharp bedding contacts that separate significant faunal turnovers during the Taghanic biocrisis that occurred during the deposition of the Tully Limestone (Baird and Brett, 1996; Zambito et al., in press).

The two well-developed and well-drained paleosols that occur at the S3 sequence boundary likely correlate with a regional erosional unconformity, termed the Taghanic unconformity within the marine strata (Appendix D) (Fig. 3.2) (Johnson, 1970; Brett and Baird, 1996; Brett et al., 2010). The delta-plain deposits at the base of the S4 TSE transitions into well-drained and highly developed paleosols (Fig. 3.2), a succession that likely formed during a transgressive period in a basin that lacked significant tectonically generated subsidence (Figs. 3.2, 3.6). The TSE of S4 is likely related to the deposition on the Middle Tully Formation, which represents a major transgression after the S3/ Giv-4 sequence boundary to a dysoxic marine carbonate (Fig. 3.7) (Heckel, 1973; Brett and Baird, 2003; Brett et al., 2010). The Middle Tully Formation is the first of three 4^{th}-order sequences of the Giv-5 sequence defined by Brett et al. (2010) (Fig. 3.7).

The S4 sequence boundary is an erosional surface that separates the thin mudrock FACs of S4 and a thick succession of sandstone-dominated FACs in the S5 TSE, that abruptly transitions into thin pedogenically modified FACs (Fig. 3.2). The succession of sandstones in the S5 TSE may represent the onset of renewed Acadian tectonism, however, these FACs abruptly transition back to floodplain overbank deposits with well-developed and well-drained paleosols. This transition suggests that the generation of accommodation had less to do with tectonic-generated subsidence and more with filling space generated from either channel incision during base-level fall or on floodplains during eustatic rise.

The contact between the Tully Limestone and the Geneseo Shale is recognized as a regional unconformity in the marine part of the section, where significant erosion of material resulted in the complete removal of the Tully Formation in western New York (Heckel, 1973; Rickard, 1975; Baird et al., 2010). This boundary has been identified as a maximum flooding surface between of the Giv-5B 4th-order sequence, and a surface of maximum starvation with a layer of reworked pyrite formed during the Geneseo transgression and basin starvation (Baird and Brett, 1991; Ettensohn, 1998; 2008; Baird et al, 2010). The terrestrial system responded to the large increase in accommodation by depositing TSE of S6, a succession of very thick sandstone deposits (Figs. 3.2, 3.6, 3.7) (Baird and Brett, 1991; Ettensohn, 1998; 2008; Brett et al., 2010). This major increase in accommodation has been recognized as sequence boundary by Bridge and Willis (1994) and likely correlates with the surface that divides the Upper Tully Formation and Geneseo Shale (Fig. 3.2). We therefore suggest that the surface of maximum starvation and maximum flooding at the base of the Geneseo may be a condensed section above a sequence boundary (Fig. 3.7). The HSE of S5 may therefore correlate with the condensed section above the Tully limestone or with the erosional surface that stripped the clastic marine sediments down the carbonate Upper Tully succession (Fig. 3.7). The deposition of S6 and the Geneseo Member marks the beginning of the third tectophase during the Acadian orogen (Ettensohn, 1985b; Ver Straeten, 2010). The paleosols in this succession are weak to moderately developed, generating a decreasing trend in PM-CDM (Fig. 3.2). This trend of limited soil formation in floodplain environments suggests that floodplain sedimentation and aggradation rates were elevated, a result of increased sediment supply introduced into the Appalachian Basin from increased uplift and erosion (Fig. 3.2). The incomplete S7 has an exposed TSE that is composed of very thick sandstone FAC cycles, which formed as a result of increased tectonic loading and basin subsidence. This succession correlates with the Fir Tree Member, which is the TST of the Giv-5C 4th-order sequence (Fig. 3.7) (Baird et al., 2010).

Paleoclimate

The majority of the MAP estimates generated using the CALMAG proxy (Eq. 4) are ~1600 mm, except for several anomalous paleosols with lower MAP estimates, lowering the overall average MAP estimate to ~1550 mm/yr for the Middle Devonian (Fig. 3.4). Paleo-precipitation estimates from DTC(U) and from DTC(V), from selected paleosols in this section, as well as those generated from other Middle Devonian paleosol outcrops using the DTC(U) method, are significantly less than CALMAG MAP estimates (Figs. 3.4, 3.5) (Retallack and Huang, in press). Whereas the DTC(V) is a more appropriate proxy because it was developed from analogs to these paleosols, and also gives a higher MAP estimate than the DTC(U) proxy, both proxy estimates are similar at low Bk depths (Nordt et al., 2006). There are several possible explanations for the discrepancy between the CALMAG and the DTC(V) MAP estimations, including: 1) that the chemistry of the paleosol matrix material has been altered through diagenesis, 2) that there are other unconstrained factors of soil formation that influence the CALMAG ratio (Eq. 4), 3) that these paleosols have lost a significant portion of the weathering profile through erosion prior to burial, 4) that there are other unconstrained factors of soil formation that influence the depth to Bk in Vertisols, and 5) that there is a fundamental difference between soil weathering systems that existed in the Middle Devonian versus today.

Each of these are addressed here further: 1) Paleozoic paleosols throughout the Appalachian basin consist of illite, interlayered illite/smectite and chlorite which are products of burial diagenetic recrystallization of the original pedogenic clays (Mora et al., 1998). The Ca^{2+} and Mg^{2+} concentrations may have been affected by the process of burial diagenetic recrystallization of pedogenic clays and fluid interaction with the original clay minerals present in the paleosol. Estimates of MAP, using the CALMAG proxy, suggesting a humid climate, agree with morphological and micromorphological characteristics of these paleosols, which show evidence of seasonal saturation and clay translocation in subsurface horizons, the result of soil water percolation, typical in semi-humid to humid climates (Figs. 3.4, 3.5). Whereas some of the discrepancy may be due to diagenetic alteration of the chemistry, because of the agreement between paleosol morphology and the CALMAG MAP estimates, it does not likely fully explain the discrepancy.

2) There are paleosols with anomalously low CALMAG MAP estimates, which suggests that they formed during short-lived conditions of increased aridity and climatic deterioration. Many of the paleosols with anomalously low CALMAG ratios (Eq. 4) occur at, or near sequence boundaries (Fig. 3.4), or are poorly drained paleosols (Figs. 3.2, 3.4). These anomalous CALMAG ratios may be due, in part, to fluctuations in relative base-level and duration of pedogenesis, thereby creating elevated Ca^{2+} concentrations, through the accumulation of calcium carbonate in that soil matrix and the addition of exchangeable calcium with clay minerals (Fig. 3.4). One of the factors that influenced pedogenesis in this succession is the duration of soil formation, as represented by the PM-CDM graph (Fig. 3.2D) that is, in part, controlled by changes in the rate of sedimentation and stability of floodplain landscapes. The CALMAG values from paleosols that occur at or near sequence boundaries have a pattern that closely resembles the FAC-CDM curve, which suggests that base-level and duration of soil formation influenced the soil chemistry (Figs. 3.2D, 3.4). This is not to imply that climate variation is not influencing these trends, only that it may be difficult to quantify to what extent other factors of soil formation might have influenced the geochemical ratios of soil matrix material. Comparison of micromorphologic features with some of the anomalously low values of calculated MAP from the CALMAG proxy indicates that climate is, indeed, a factor controlling the geochemistry in these paleosols (Fig. 3.5). Paleosols with MAP estimates over 1000 mm/yr contain illuviated clays in the subsurface horizons, whereas paleosols with lower MAP estimates of 800 mm/yr lack illuviated clays (Fig. 3.5). The drop in MAP for the paleosols that occur at the 3rd sequence boundary might then reflect an increase in aridity, from decreased monsoonal

precipitation linked to decreased tectonism at the end of the second Acadian tectophases (Figs. 3.2, 3.4, 3.5) (Ettensohn, 1985b).

3) By rearranging equation 6 in order to solve for depth to the Bk horizon, and using the climate estimates from CALMAG, we can also consider this discrepancy in terms of difference in the measured depth compared to the predicted depth to Bk. For the discrepancy between CALMAG and DTC(V) MAP estimates to be entirely the result of erosion, the selected paleosols would have had to have lost 67 cm of overlying soil material from the paleosol, for the lower MAP estimate, and 89 cm from the paleosol with the higher MAP estimate (Fig. 3.5). Although it is certainly possible that several cm may have been eroded before burial, these paleosols appear to have relatively complete profiles, with at least partial A horizons preserved, making it unlikely that so much of the profile has been removed. It is also not possible that an underestimation in burial depth and thus compaction is responsible for the discrepancy in MAP because the decompaction curve flattens out at ~7 km burial depth making further compaction relatively inconsequential (Sheldon and Retallack, 2001).

4) The depth to carbonate has a robust trend with MAP like CALMAG, however there may be other soil conditions that influence the depth of the Bk in a Vertisol. The MAP estimates using DTC(V) are extrapolated from the best-fit line, because no Vertisols were sampled in a climate drier than 700 mm/yr (Nordt et al., 2006). Thus the possibility may exist that shallow Bk depths may occur in both dry and humid climates, or in Vertisols that are relatively well-drained and poorly drained. Vertisols along the Texas coastal plain at Dance Bayou in Brazoria County, Texas have a wide range in depths to Bk horizon over a very small area. The Pledger and Churnabog soil series there

have Bk horizons that begin between 100 to 130 cm depth in the microlow in a climate that has a MAP of ~1270 mm/yr (Miller and Bragg, 2007). However, the Churnabog series, in some of the most poorly drained and ponded soils, has Bk depths of only 40 cm (Mintz et al., in press), whereas the Pledger series has Bk depths of 190 cm in some of the better drained sites (Miller and Bragg, 2007). This variation in depth to Bk in a single climate regime suggests that the hydrologic condition in Vertisols has the potential to influence the depth to Bk in a manner that is relatively unrelated to climate. Comparison of DTC(V) to CIA-K, another proxy for MAP based on the geochemistry of bulk paleosol material, in a Late Mississippian paleosol shows that the DTC(V) estimate is ~300 mm/yr lower than the CIA-K estimate.

5) The hypothesis that soil-forming conditions were fundamentally different in the Middle Devonian from modern soil systems is difficult to test. This hypothesis would make the relationships between modern soil weathering chemistries and morphologies to climate invalid as analogs for Middle Devonian paleosols. Middle Devonian soil morphologies and weathering products do resemble modern soil profiles and also had the ecological condition of forestation, which might signify the beginning of analogous weathering systems to the modern. At this time there is no reason to suggest that soil weathering systems responded differently to environmental conditions in the Middle Devonian than they do today, however future research may one day challenge this idea.

Climosequence models (Eq. 3) used to calculate paleoclimates from paleosols with varying base-level and duration of pedogenesis can potentially create error without any ability to constrain the other factors of soil formation. Based on the morphology and micromorphology of the paleosols in the Middle Devonian the CALMAG estimates are likely the most accurate for paleoclimate reconstruction (Figs. 3.4, 3.5). More efforts are needed for studies that isolate the other factors of soil formation (e.g. chronosequences, hydrosequences) to quantitatively evaluate their effects on soil morphology and chemistry. The influence of paleoclimate in the Appalachian basin region during the Middle Devonian is important in establishing the environmental conditions influencing sedimentation in the terrestrial system as well as in the marine.

Mixed Siliciclastic and Carbonate Sedimentation in the Appalachian Basin

Formation of marine carbonates, such as the Tully Limestone, seems unlikely in a foreland basin adjacent to a convergent margin and orogenic province in a humid climate with high clastic influx through deltaic sedimentation. The formation of the Tully limestone, however, was facilitated in part by a fore-arc depression that served as a clastic sediment trap (Heckel, 1973). Deposition of the Tully limestone also occurred during a interval of decreased clastic input due to the combined effects of tectonic quiescence, landscape forestation and possibly decreased humidity (Figs. 3.2, 3.4, 3.6, 3.7). Similar conditions of mixed clastic and carbonate deposition exist in southern Belize where Holocene reefs occur < 50 km from a deltaic shoreline. The southern Belize shorelines are < 50 km from the Maya Mountains and occur in a tropical climate regime with a MAP of 1780 mm/yr, a dry winter season for 3-5 months and wet summer season for 7-9 months of the year (Purdy et al., 1975). The carbonate reefs are separated from terrigenous deposits by a lagoon that formed from karstification of a previous buildup, which serves as a clastic sediment trap (Ginsburg et al., 1995). The Belize depositional system is not forming in a foreland basin and likely has different subsidence and sedimentation rates to that of the Appalachian basin. This has consequences on soil development within the terrestrial realm, and accounts for ecological differences in the marine. The nature of Belize coastal deposits, climatic regime, terrestrial forested ecosystems, the distance of fluvial transport and the occurrence of a clastic sediment trap are all similar to conditions within the northern Appalachian basin. As such, the southern Belize depositional system may represent an excellent modern analog for environmental conditions of the Tully Limestone.

Controls on Middle Devonian Landscapes on Marine Environments

Paleozoic atmospheric, climatic and both terrestrial and marine ecosystems were in a period of transition that began in the Middle Devonian (Berner, 1992; Berner, 2005; Driese and Mora, 2001; House, 2002; Driese, 1997; Mintz et al., 2010). Beginning in the Middle Devonian through the late Devonian and into the Carboniferous, atmospheric CO_2 concentrations decreased by as much as 200%, which is likely the cause of Late Devonian through Carboniferous glaciations (Berner, 1992; Berner, 2005; Mora et al., 1991, 1996; Mora and Driese, 1993; Berner and Kothavala, 2001; Goddéris, 2001). Marine ecosystems during the Middle and Late Devonian experienced several periods of anoxia and faunal extinctions (House, 2002, Algeo and Scheckler, 1995; Algeo and Scheckler, 1998; Zambito et al., in press). All of these changes in atmospheric and marine conditions began to occur in the Middle Devonian when arborescent floral taxa evolved and forested ecosystems developed on a variety of landscapes (Driese et al., 1997; Retallack, 1997; Mintz et al., 2010).

A potential mechanism that may explain the near coeval change of all of these systems is the increased delivery of iron and other biologic limiting nutrients, through increased weathering on alluvial plains into the marine sedimentary system (Algeo and

Scheckler, 1998). Comparison of paleo-Vertisols formed in the Appalachian basin shows evidence for a fundamental change in weathering systems through increased depth of root penetration and stripping of iron from the soil profile through iron complexation with organics (Fig.3 8). An Upper Ordovician paleo-Vertisol from the Juniata Formation, interpreted to have formed on subaerially exposed marine strata in a seasonally moist, tropical to subtropical climate in the southern Appalachian basin has a weathering profile that extends ~110 cm depth and has an average loss of Fe in the paleosol compared to the unaltered C horizon of ~10% (Fig. 3.8) (Driese and Foreman, 1992). Compared to the Middle Devonian paleosol in this succession (FAC # 92) one can see evidence for an increase in depth of weathering in this profile, with a depth of ~175 cm to the C horizon, as well as increased average total loss Fe of ~35% (Fig. 3.8). Increased leaching of nutrients from soils, such as iron, on alluvial landscapes, likely increased the amount of biotic production in the marine system. This increase in production helped promote anoxic conditions in the marine and the production of the black shales (Algeo and Scheckler, 1995). The Taghanic biocrisis, as well as the documented onset of faunal cosmopolitanism after the biocrisis (House, 2002) in the Middle Devonian, may also have been influenced by forestation as increased biotic production placed stress on certain fauna while allowing for a more diverse global marine ecosystem. The increase in biotic productivity and storage of carbon in black shales and in terrestrial ecosystems, may have contributed to the global decline in atmospheric CO_2 concentrations and glacial cycles in the Late Devonian. To test the iron-leaching hypothesis, further study of geochemical changes and biotic production in genetically related strata in the terrestrial and marine, both the modern and ancient, is needed.

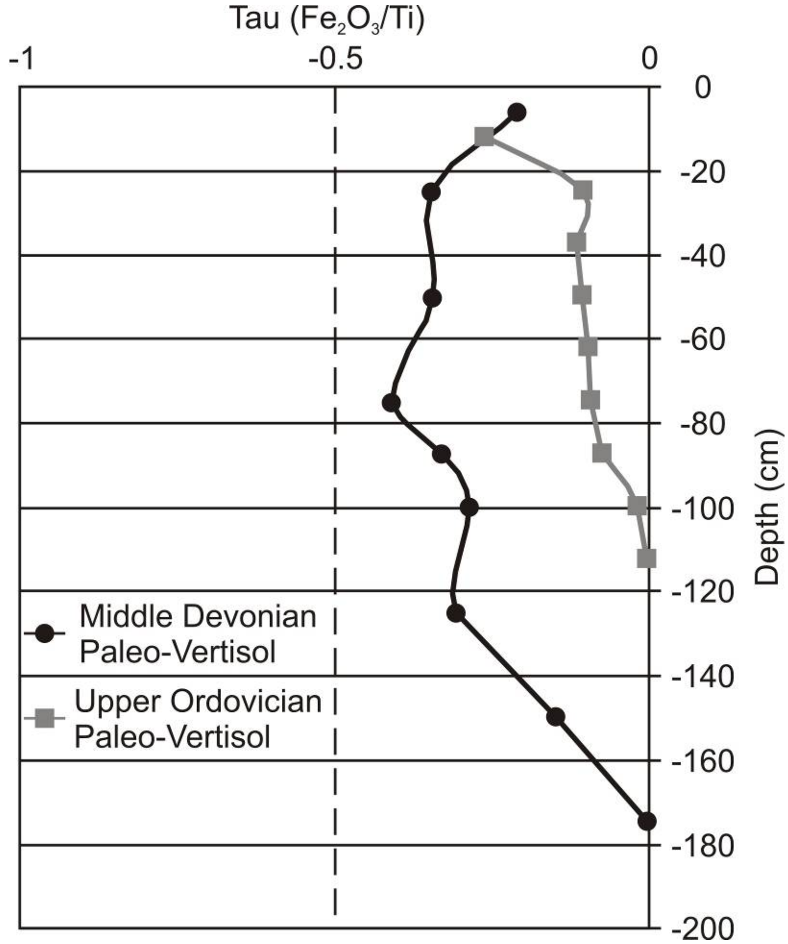

Figure 3.8 Comparison of Vertical mass change of Fe in a paleo-Vertisol profile in the Upper Ordovician and Middle Devonian in the Appalachian basin. Ordovician paleosol data from Driese and Foreman (1992).

Conclusions

1. Middle Devonian fluvial deposits in the northern Appalachian Basin display several tiers of cyclicity in alluvial stacking patterns. Changes in FAC thickness stacking patterns correspond in a predictable way to the facies trends, as well as to paleosol occurrence and maturity. The first hierarchal tier of cyclicity of FAC thickness stacking patterns likely correlates with modeled water depths related to changes in basin subsidence from tectonic loading in coeval marine strata. The second tier of cyclicity is identified as fluvial sequences, which formed as a result

of basin-wide changes in accommodation, the likely result of both tectonism as well as eustacy. A third tier of stacking-pattern cycles are identified as FAC-set cycles, which are autocyclic changes in fluvial sedimentation.

2. The second hierarchal tier of stratal stacking pattern cyclicity are terrestrial sequences, which are bound by sequence boundaries that likely have regional significance in both terrestrial as well as marine stratigraphy. From this sequence-stratigraphic framework we present a terrestrial to marine correlation model for the Middle Devonian strata in New York. The formation of the Tully Limestone, an anomalous marine carbonate, was facilitated in part by a fault-controlled fore-arc depression and likely correlates with a decreasing trend in available accommodation and sediment yield in terrestrial strata. A potential modern analog for conditions in the Appalachian basin during which marine carbonates were deposited is off the coast of southern Belize where reef buildups occur < 50 km from deltaic shorelines. The ability to correlate specific landscapes to marine successions provides a powerful tool to further terrestrial and marine teleconnections research.

3. Paleosols throughout this succession, which formed on fluvial floodplain deposits, are primarily paleo-Inceptisols or paleo-Vertisols that show evidence of hydromorphism throughout the Middle Devonian. Using a geochemical proxy for MAP, developed for paleo-Vertisols, the average MAP was ~1550 mm/yr, which agrees with macro- and micromorphologic characteristics of the paleosols. The DTC(U) model for MAP produces significantly lower MAP estimates than CALMAG proxy. The DTC(V) proxy, developed from soils analogous to these

Middle Devonian paleosols, produces higher MAP estimates than those predicted using the DTC(U), but distinctly lower than the CALMAG estimates. The discrepancy between the CALMAG estimates and those obtained using the DTC(V) may be attributable, in part, to either diagenetic alteration of the soil matrix material and potentially unconstrained factors of influence on both the CALMAG and DTC(V) proxy method.

4. Forestation on Earth had a significant impact on the pedogenic weathering environments increasing depth and intensity of weathering profiles. Stripping of iron from soils through complexation with organic acids on alluvial deposits in the Appalachian basin may have greatly increased from the Ordovician to the Devonian. This increase in stripping of iron and other nutrients from soils, may have caused increased biotic productivity in marine ecosystems. This increase in organic productivity may have been a contributing agent of Devonian extinction and anoxic events, drawdown in atmospheric CO_2, and ultimately late Devonian ice-house conditions.

CHAPTER FOUR

Influence of Changing Hydrology on Pedogenic Calcite Precipitation in Vertisols, Dance Bayou, Brazoria County, TX: Implications for Estimating Paleoatmospheric $_pCO_2$

Abstract

The $\delta^{13}C$ values of pedogenic (soil-formed) calcite preserved in the sedimentary record have been used to estimate atmospheric pCO_2 using the paleosol calcite paleobarometer. A fundamental assumption for applying this paleobarometer is that atmospheric CO_2 concentrations have a direct influence on the measured pedogenic calcite $\delta^{13}C$ values as a result of open-system exchange between atmospheric and soil-respired CO_2. Here we address the timing of calcite precipitation in relation to the soil saturation state and soil-atmosphere connectivity in a modern Vertisol (smectitic, clay-rich soil, seasonally saturated) in Brazoria County, Texas, U.S.A. Luminescent phases of calcite growth, under cathodoluminescence microscopy, have more negative $\delta^{13}C$ values ($\delta^{13}C$ = -11.1 ‰ VPDB $\pm$ 0.78 1σ) than the non-luminescent phases ($\delta^{13}C$ = -2.53‰ VPDB $\pm$1.41 1σ). The luminescent phase of calcite formed during the water-saturated portion of the year, thereby minimizing the incorporation of atmospheric CO_2, and negating its use for pCO_2 estimations. The non-luminescent phase formed during the well-drained portion of the year when atmospheric CO_2 mixed with soil-respired CO_2 and is therefore useful for pCO_2 estimation. From these results we present a model to independently test the saturation state of a paleosol at the time of pedogenic carbonate precipitation. Finally, we calculate soil-respired CO_2 concentrations that are an order of

magnitude lower than those that are typically assumed in the soil-carbonate paleobarometer equation.

Introduction

The precipitation of pedogenic calcite in carbon isotopic equilibrium with soil CO_2 has the potential to record the atmospheric CO_2 concentrations during the formation of the soil (Cerling 1991, 1999; Sheldon and Tabor 2009). Atmospheric CO_2 has a less negative $\delta^{13}C$ value, -8.5‰ VPDB today, than the plant-derived soil-respired CO_2, ranging from -10 to -30‰ VPDB depending on the plant community (Cerling 1991, 1999). The $\delta^{13}C$ value of soil CO_2 depends on the atmospheric to soil-respired CO_2 ratio, which in saturated soil systems can be close to zero (Whelan and Roberts 1973; Sheldon and Tabor 2009). The estimation of atmospheric pCO_2 is appropriate only for calcite that forms in soil systems where the soil CO_2 is a mixture of atmospheric and soil-respired (Cerling 1984, 1999; Sheldon and Tabor 2009). Calcite formed in soils under vadose conditions can be difficult to distinguish from calcite formed in saturated soil conditions or from groundwater precipitates (Wright and Vanstone 1991; Cerling 1999). Confident identification of calcite nodules in buried soils and paleosols that formed during pedogenesis, while atmospheric CO_2 constituted a sustained portion of soil CO_2 diffusion, is a perennial problem. The use of hydromorphic paleosols for atmospheric CO_2 reconstruction has been cautioned against (Cerling 1991, 1999; Ekart et al. 1999); however, avoidance can often prove difficult when dealing with paleosols preserved in sedimentary basins. Here we investigate the isotopic and trace-element geochemistry of pedogenic carbonates in a modern seasonally ponded Vertisol, forming on an alluvial plain, in order to determine the hydrologic controls on carbonate precipitation.

The Diffusion Model and the Paleo-$_p CO_2$ Barometer

The model of soil-CO_2 production and diffusion can be described as

$$[CO_2]_s = S(z) + [CO_2]_{atm} \text{ when } [CO_2]_s = [CO_2]_{atm} \text{ at } z = 0 \ (1)$$

where $[CO_2]_s$ is the concentration of CO_2 in the soil, $[CO_2]_{atm}$ is the concentration of CO_2 in the air, and $S(z)$ is the concentration of soil-respired CO_2 at depth (z) in the soil (Cerling 1999). Determination of $[CO_2]_{atm}$ from the measurement of pedogenic carbonate nodules is determined by the equation

$$[CO_2]_{atm} = S(z) \left[\frac{\delta^{13}C_s - 1.0044\delta^{13}C_r - 4.4}{\delta^{13}C_a - \delta^{13}C_s}\right] (2)$$

where $\delta^{13}C_s$, $\delta^{13}C_r$, and $\delta^{13}C_a$ are the stable carbon isotopic composition of soil CO_2, soil-respired CO_2, and atmospheric CO_2, respectively (Cerling 1999). The carbon-isotope composition of the pedogenic calcite ($\delta^{13}C_{cc}$) can be used to calculate the value of $\delta^{13}C_s$ by using the temperature-dependent carbon-isotope fractionation factor (Romanek et al. 1992). The value of $\delta^{13}C_a$ is either: (1) assumed to be -6.5‰ VPDB (Cerling 1991), (2) calculated from marine carbonates for the given time interval of soil formation (Nordt et al. 2002, 2003), or (3) estimated from either terrestrial organic matter or fossil tooth enamel (Arens and Jahren 2000; Passey et al. 2002). The value of $\delta^{13}C_r$ is either calculated from $\delta^{13}C_a$ (Ekart et al. 1999; Nordt et al. 2003) or assumed to be equivalent to measured $\delta^{13}C$ values of contemporaneous or penecontemporaneous preserved terrestrial organic matter (Nordt et al. 2002; Montañez et al. 2007). The only value that cannot be directly quantified from the pedogenic materials in carbonate-bearing paleosols is $S(z)$, which is typically assumed to be between 5000 and 10,000 ppmV (Cerling 1991). Isotopic equilibrium between pedogenic carbonate and soil CO_2 and water in semiarid soils in New Mexico occurs when soil CO_2 concentrations are very low (< 1000—2000 ppmV), which suggests that researchers may be routinely overestimating *S*(*z*), and thus $[CO_2]_{atm}$ (Equation 2) (Breecker et al. 2009, 2010). The findings presented here are relevant to correctly estimating values of *S*(*z*) for paleosols interpreted as Vertisols in the geologic record and containing pedogenic carbonate sampled for analysis of $\delta^{13}C$ values.

Setting and Methods

Dance Bayou, Brazoria County, Texas, USA

The Vertisols analyzed in this study are mapped as a Churnabog soil series (Fine, smectitic, hyperthermic, Aeric Calciaquerts), formed on the late Quaternary Post-Beaumont alluvium along the San Bernard River on the eastern portion of the Texas coastal plain in a humid climatic regime (Fig. 4.1) (Blum and Price 1998; Miller and Bragg 2007). Sediments are alluvial clays and silt-size quartz grains, likely derived from reworked Colorado River floodplain deposits. The soil matrix ranges from noneffervescent to strongly effervescent at depth with applied HCl and contains no observed detrital carbonate in thin section. A conventional radiocarbon age of 6720 years ± 40 years BP (Beta- 288379) was measured from bulk humate material from a bedded 2C horizon at 265—304 cm depth below a gilgai microlow collected less than 50 meters from the site sampled for pedogenic carbonate. This sample, taken from relatively undisturbed parent material, represents the age of deposition and a maximum age of the onset of pedogenesis.

Vertisols are soils that have ≥ 30% clay in the fine earth fraction between 18 and 50 cm below the mineral surface, a horizon ≥ 25 cm thick containing slickensides and/or wedge-shaped peds and cracks that open and close periodically (Soil Survey Staff 1999). Generally, Vertisols are smectitic soils that experience seasonal wetting and drying that

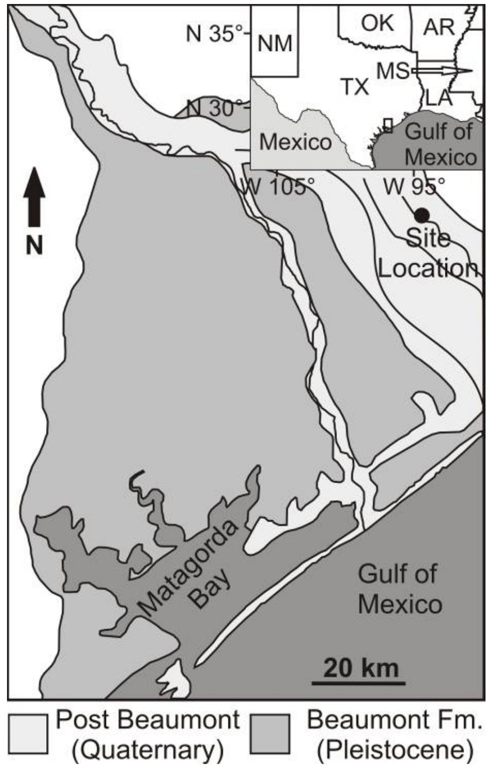

Figure 4.1 Site location along the Colorado River Delta on the Texas Coastal Plain (modified from Blum and Price 1998).

induces shrink-swell shearing and cracking of soil material (Wilding and Puentes 1988; Nordt and Driese 2009). The environmental data (Fig. 4.2) from 2002 show the characteristic pattern of seasonal ponding of this site, which is controlled by changes in evapotranspiration, which alter the water budget (Miller and Bragg 2007). Reducing conditions in the soil (low Eh) are created when the soil is saturated, limiting the transport and availability of oxygen (Fig. 4.2). In this study, six soil core samples were taken to 1.1 meters depth with a U.S. Department of Agriculture, Natural Resources Conservation service (NRCS) probe truck and also removed from two hand-dug pits up to 0.5 m deep. Soil cores typically have A (0—15 cm), Bw/Bg (15—40 cm), $Bkss_1$ (40—

60 cm), Bkss$_2$ (60—100 cm) and B'ss (100—110 cm) horizons. Samples were taken throughout the Bkss horizons, which have stage II pedogenic carbonate accumulation based on the index system from Machette (1985). All of the carbonates sampled were hard nodular masses that are 2 to 3 mm in diameter.

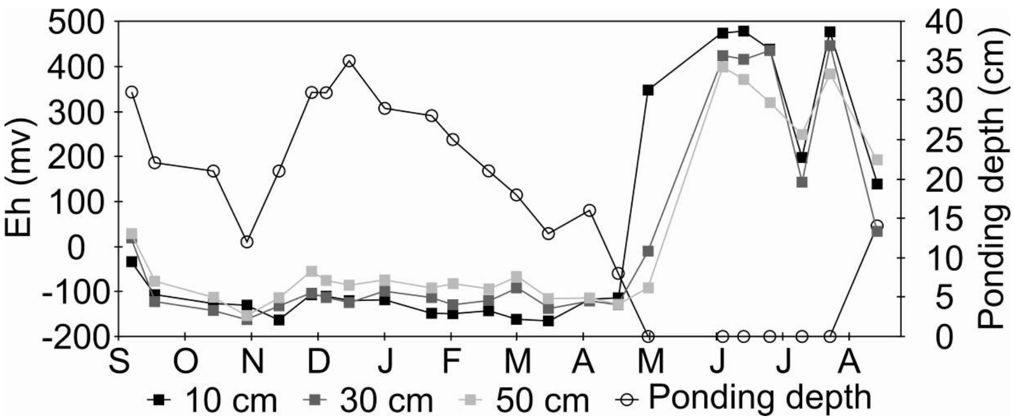

Figure 4.2 Ponding depth and Eh condition of soil at 10, 30, and 50 cm depth from 2001-2002 at site location (Miller and Bragg 2007).

Laboratory Methods

Calcite-nodule luminescence was imaged and mapped at the Kansas Geological Survey Digital Cathodoluminescence Imaging Laboratory, in Lawrence, Kansas. Several ~ 100 μg samples were produced from microdrilling the various phases of luminescence in three to five different nodules of each distinct carbonate nodule morphotype and analyzed on a Thermo Finnigan® Kiel III carbonate reaction device coupled to a MAT 253 Dual-Inlet System at the Keck Paleoenvironmental & Environmental Stable Isotope Laboratory at the University of Kansas. Calcite analyses are reported relative to the Vienna Peedee Belemnite (VPDB) scale, and have a precision of ± 0.03‰ and ± 0.06‰ (1σ) for $\delta^{13}C$ and $\delta^{18}O$ respectively.

The $\delta^{13}C$ of soil organic matter (SOM) samples were measured from each horizon described previously, from one microlow location, starting at a depth of 10 cm in the A horizon. SOM samples were treated with three rounds of a 5% HCl solution and deionized water rinse to remove all inorganic carbon. The $\delta^{13}C$ values of the SOM were measured at the University of Tennessee at Knoxville, using a Finnigan Delta+ XL continuous-flow mass spectrometer with a precision of 0.1‰ (1σ), and reported relative to VPDB.

Monte Carlo Simulation

To model $S(z)$ concentrations needed to calculate accurate modern atmospheric CO2 concentrations, using the $\delta^{13}C$ values of pedogenic carbonate in this soil with the paleobarometer equation, we rearranged Equation 2 to solve for $S(z)$ in a Monte Carlo simulation. Monte Carlo simulations generate solutions to an equation by generating random values between defined ranges for the variables. For the simulation we varied $\delta^{13}C_r$ between -24 and -27‰ VPDB as a range between the measured soil organic matter and an idealized end member for a C3 plant community, $\delta^{13}C_a$ between the preindustrial and modern values of -6.5 to -8.5‰ VPDB, and $[CO_2]_{atm}$ between the preindustrial and modern values of 280 and 380 ppmV. We used the measured $\delta^{13}C_{cc}$ range of the non-luminescent calcite nodules to calculate a range of $\delta^{13}C_s$ using a temperature range 20 to 30°C, the range of monthly temperatures for the non-ponded portion of the year, and solved for $S(z)$ 5001 times.

Cathodoluminescence Variability of Calcite Morphotypes

The luminescence of carbonate found in soils or paleosols observed using cathodoluminescence (CL) microscopy can help indicate the redox condition of the soil water at the time of precipitation. The redox condition in a soil is intrinsically linked to the saturation state controlling the amount of available oxygen for the decay of organic matter. The cations that exert the dominant control on calcite CL intensity are Mn^{2+}, which causes orange luminescence, and Fe^{2+}, which quenches luminescence (Hemming et al. 1989). There is a strong positive relationship between CL intensity and Mn^{2+} concentrations and Mn/Fe ratios in carbonates (Hemming et al. 1989). Elevated concentrations of Mn^{2+} and Fe^{2+} in carbonate minerals are caused by precipitation under low-Eh conditions, prompting the dissolution of iron- and manganese-bearing minerals (Barnaby and Rimstidt 1989).

Several distinctive morphologies of calcite nodules, discernible in reflected-light and CL microscopy, can be divided into morphotypes to describe the morphologies and geochemistry that represents that group. Morphotype 1 (M1) is a light-colored calcite nodule in reflected light with bright orange luminescence under CL (Figs. 4.3A, 4.3A'). Morphotype 2 (M2) is a dark- to red-colored nodule in reflected light and is dull to non-luminescent under CL (Figs. 4.3A, 4.3A'). Morphotype 3 (M3) has concentric, alternating ~ 1 mm bands of light-colored and luminescent phases and dark and weakly luminescent phases (Figs. 4.3B, 4.3B'). Morphotype 4 (M4) is a rhizolith that has a submillimeter-size root tubule in the center with an ~ 1 mm diameter growth of light-colored calcite that is strongly luminescent, followed by a 1-2 mm, darker-colored growth of calcite that is slightly less luminescent than the center (Figs. 4.3C, 4.3C').

Isotopic Compositions

All of the calcite morphotypes have distinct ranges in $\delta^{13}C$ values that fall on a singular meteoric calcite line (Lohmann 1987), defined by similar $\delta^{18}O$ values but variable $\delta^{13}C$ values, which have an average $\delta^{18}O$ value of -3.27‰ VPDB $\pm$ 0.21 (1σ) (Appendix G) (Fig. 4.4). M1 has an average $\delta^{13}C$ value of -11.12‰ VPDB $\pm$ 0.78 (1σ), whereas M2 has an average $\delta^{13}C$ value of -2.53‰ VPDB $\pm$1.41 (1σ) (Appendix G) (Fig. 4.4A). M3 has an average $\delta^{13}C$ value of -7.29‰ VPDB $\pm$ 3.52 (1σ) (Appendix G). The average value and the high variance of M3 $\delta^{13}C$ values is the result of grouping two different phases of calcite growth, similar to M1 and M2, into a single nodule morphotype (Appendix G) (Fig. 4.4B). M4 has an average $\delta^{13}C$ value of -6.18‰ VPDB $\pm$ 2.10 (1σ) (Appendix G) (Fig. 4.4C). There is a decrease in weight % carbon, in SOM, from ~ 1.5% in the A horizon to 0.8% in the $Bkss_2$ horizon (Table 4.1). The $\delta^{13}C$ value of the SOM increases incrementally from -23.7‰ VPDB in the A horizon to -18.0‰ VPDB in the $Bkss_2$ horizon (Table 4.1).

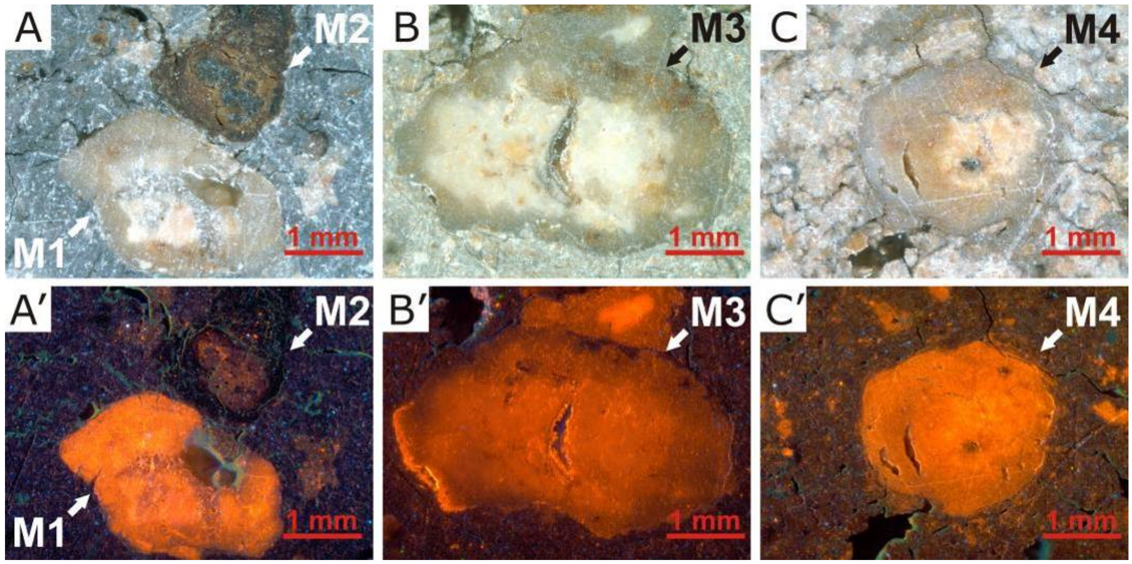

Figure 4.3 A) Reflected-light micrograph of the light colored pedogenic calcite morphotype 1 (M1) and the dark to red colored morphotype 2 (M2). A') Cathodoluminescence (CL) micrograph of bright luminescent M1 and dull to non-luminescent M2. B) Reflected-light micrograph of the concentrically banded morphotype 3 (M3). B') CL micrograph of M3. C) Reflected-light micrograph of the rhizolith morphotype 4 (M4). C') CL micrograph of M4.

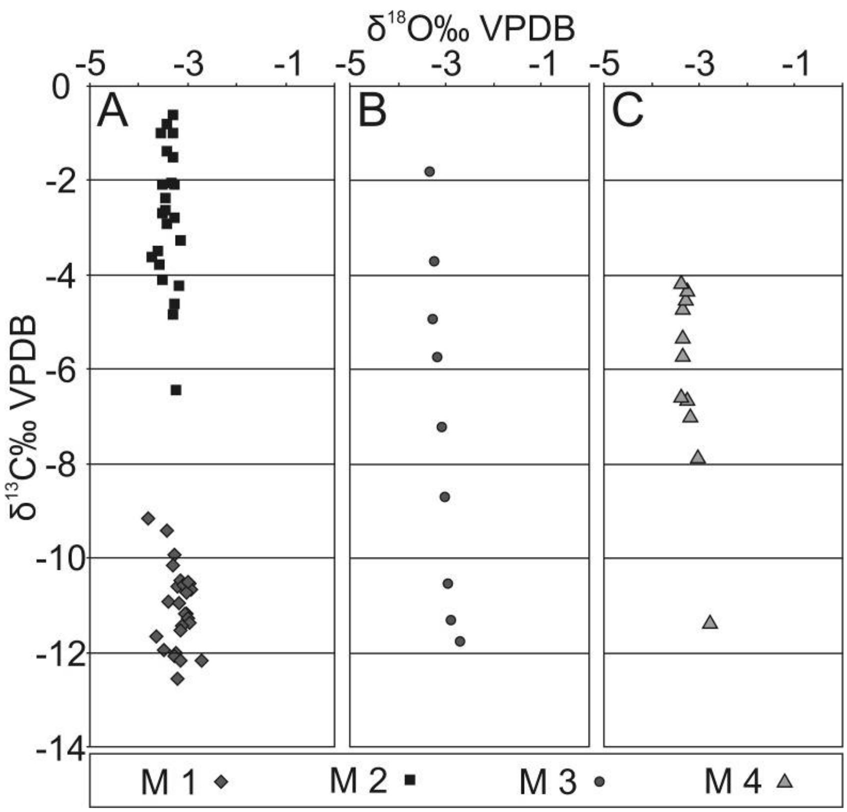

Figure 4.4 A) $\delta^{18}O$ and $\delta^{13}C$ cross-plot of the M1 and M2 morphotypes. B) $\delta^{18}O$ and $\delta^{13}C$ cross-plot of the M3 morphotype. C) $\delta^{18}O$ and $\delta^{13}C$ cross-plot of the M4 morphotype.

Table 4.1 Carbon weight %, $\delta^{13}C$ ‰ (VPDB), $\delta^{15}N$ ‰ (AIR), and C/N ratio of soil organic matter by horizon from microlow in Churnabog Clay soil series.

Horizon	Depth (cm)	Carbon Weight %	$\delta^{13}C$ ‰ (VPDB)	$\delta^{15}N$ ‰ (AIR)	C/N
A	10	1.50	-23.7	4.6	13.5
Bw	25	1.12	-21.2	4.4	15.7
$Bkss_1$	45	0.65	-19.7	5.5	13.8
$Bkss_2$	70	0.86	-18.0	5.0	17.7

Discussion

Controls on the $\delta^{13}C$ Values of Calcite Nodule Morphotypes

M1 (Figs. 4.3A, 4.3A') precipitated during the seasonally ponded, saturated portion of the year when Eh conditions are low (Fig. 4.2), thus liberating Mn^{2+} into solution from dissolution of manganese-oxide minerals. The lowest measured $\delta^{13}C$ values of the luminescent calcite (~ -12‰), are lower than can be explained by the Cerling (1984) steady-state production-diffusion model even if the $\delta^{13}C_r$ is assumed to be equal to the lowest measured $\delta^{13}C$ value of soil organic matter (-23.7‰). The $\delta^{13}C$ value of calcite in carbon isotope equilibrium with soil CO_2 using a soil temperature of 15°C (the measured winter soil temperature) and $\delta^{13}C_r$ = -24‰ is -9.7‰. Using higher values for $\delta^{13}C_r$, equivalent to the measured $\delta^{13}C$ values of SOM in the Bkss horizon of this soil (-18‰) where the carbonate nodules occur (Table 1), makes the discrepancy between modeled and measured values even greater.

There are several potential explanations for the low $\delta^{13}C$ values of luminescent calcite: (1) Soil-respired CO_2 continually accumulates in the soil when ponding occurs because the soil respiration rates are higher than the diffusive CO_2 flux out of the soil, (2) CO_2 transport in ponded soils occurs primarily by diffusion through soil pore water rather than soil pore air, and (3) the $\delta^{13}C$ value of soil-respired CO_2 is substantially lower than the lowest measured $\delta^{13}C$ value of SOM during the time of year when the luminescent calcite precipitates. Explanation 1 would result in lower $\delta^{13}C$ values of carbonate than predicted by the steady-state model because the $\delta^{13}C$ value of soil CO_2 approaches the $\delta^{13}C$ value of soil respired CO_2 under this transient state scenario. Explanation 2 would result in lower $\delta^{13}C$ values of carbonate than predicted by the steady-state model as typically applied because the carbon isotope fractionation resulting from the diffusion of CO_2 through water is ~ 0.7‰ (O'Leary 1984), as opposed to ~ 4.4‰ for diffusion through air, and therefore the $\delta^{13}C$ value of soil CO_2 would be lower and closer to the $\delta^{13}C$ value of respired CO_2 when the soil pore spaces are water-saturated. Explanation 3 does not involve a modification to the treatment of CO_2 transport in the model but instead challenges the assumption that the $\delta^{13}C$ value of respired CO_2 equals the $\delta^{13}C$ value of soil organic matter. In fact, there is no reason to expect that $\delta^{13}C_r$ should equal the $\delta^{13}C$ value of SOM because root respiration is known to commonly contribute approximately 50% of soil-respired CO_2 (Hanson et al. 2000) and the $\delta^{13}C$ value of root-respired CO_2 is inversely proportional to the magnitude of photosynthetic discrimination over the prior several days (e.g., Ekblad and Högberg 2001). Therefore, $\delta^{13}C$ values of soil-respired CO_2 that are lower than the $\delta^{13}C$ value of SOM are likely to occur during the winter when plants are not water stressed and photosynthetic discrimination is large. In this case the

$\delta^{13}C_{cc}$ values generated from M1 may actually represent a more accurate measure of the $\delta^{13}C_r$ than measuring contemporaneous soil organic matter. The magnitude of isotope fractionation associated with diffusion of CO_2 in a gas mixture depends on the average atomic mass of the gas mixture (Jost 1960). Elevated soil CO_2 concentrations result in a small increase in the magnitude of carbon isotope fractionation (to ~ 4.6‰ for a high CO_2 concentration of 21%, compared with 4.4‰ in air) and therefore cannot explain the $\delta^{13}C$ value of luminescent calcite.

The M2 calcite (Figs. 4.3A, 4.3A') precipitated during the well-drained, oxidizing portion of the year when the component of respired CO_2 was low enough that atmospheric CO_2 had a significant influence on $\delta^{13}C_s$. The $\delta^{13}C$ values of the non-luminescent carbonate can be explained by a low relative abundance of soil-derived CO_2 in the soil (i.e., low $S(z)$), due either to low respiration rates or to high porosity and permeability induced by soil cracking during the dry part of the summer. Using the average $\delta^{13}C_{cc}$ of the M2 nodules in a two-end-member mixing model, the soil gas contained between 64 to 70% atmosphere derived carbon during M2 precipitation. This value assumes a $\delta^{13}C_a$ of -6.5‰ VPDB, CO_2-calcite carbon isotope equilibrium at 26.6°C, the average soil temperature at 50 cm depth during oxidized soil conditions (Miller and Bragg 2007), and the same range of $\delta^{13}C_r$ values used in the Monte Carlo simulation. The greater variance in $\delta^{13}C_{cc}$ values for the M2 compared to M1 suggests that M2 formed under varying $S(z)$ concentrations as a function of either depth, soil productivity, or soil moisture, whereas M1 formed in a relatively static system and thus has a lower 1σ of $\delta^{13}C_{cc}$ values.

The M3 calcite consists of concentric growth bands of both luminescent and weakly luminescent calcite phases (Figs. 4.3B, 4.3B'). The $\delta^{13}C_{cc}$ values of these mixed-phase nodules range from -1.81‰ to -11.73‰, which spans the averages of both the M1 and M2 morphotypes, and falls between their ranges, which is likely the result of physical mixing (Fig. 4.4B). The existence of the mixed-phase concentric nodules with alternating M1 and M2 growth phases suggests that both the M1 and M2 calcites likely formed coevally, while this soil was experiencing fluctuations in saturation and aeration through the growth series of this carbonate. Precipitation of M1 and M2 morphotypes likely had depth dependence during their formation, with the M3 morphotype either representing development in a zone of overlap between the two primary morphotype zones, or by entrainment of the nodule by soil mixing processes through the soil profile. Nodules and hard masses in Vertisols are highly mobile due to pedoturbation in the soil column during their formation (Miller et al. 2007); consequently, none of the nodule morphotypes, or the $\delta^{13}C_{cc}$ values, displayed any depth dependence.

The M4 calcite morphotype formed in low-Eh conditions, which is not necessarily reflective of the overall redox state of the soil at the time of calcite formation. Decaying root matter can create micro-reducing environments around root voids, thereby increasing dissolution of manganese-bearing minerals and Mn^{2+} concentrations in solution (Vepraskas 2001). The CL state of these rhizocretions suggests that the reducing conditions decreased away from the root void, but remained sufficiently reducing to produce luminescent calcite (Figs. 4.3C, 4.3C'). The $\delta^{13}C$ values of M4 suggest that rhizocretions may have formed during both well-drained and saturated soil conditions, or in elevated $S(z)$ conditions, thereby making these $\delta^{13}C$ values of rhizolithic calcite difficult to interpret, and possibly invalid for paleoatmospheric pCO_2 estimation. This conclusion contrasts markedly with previous findings of Driese and Mora (1993), who concluded that rhizolith-related pedogenic calcite in Devonian paleo-Vertisols was better than nodules for estimating paleoatmospheric pCO_2 because of its association with root respiration. However, the paleosols described by Driese and Mora (1993) never experienced the fluctuations in saturation state reported here in the Vertisols at Dance Bayou, Texas, thus reinforcing our assertion of the importance of the hydrological state during pedogenic carbonate precipitation.

Utility of Carbonate Nodules from Hydromorphic Paleosols in the Rock Record

Despite this soil being a seasonally ponded hydromorphic soil, M2 and the weakly luminescent phase of M3 formed when $S(z)$ was sufficiently low as to not overwhelm atmospheric CO_2 (Fig. 4.5A). The average calculated value of S(z) is 205 ppmV ± 120 (1σ), using the range of $\delta^{13}C_{cc}$ for M2 in a Monte Carlo simulation, which is equivalent to a $[CO_2]_s$ of ~600 ppmV, a value well below $S(z)$ = 5000-10,000 ppmV, which is used currently in the soil-carbonate paleobarometry equation (Cerling 1991, 1999). From preliminary monitoring at this site we have measured $[CO_2]_{atm}$ of 900 ppm because of a potential canopy effect. Re-running the same Monte Carlo simulation except having the $[CO_2]_{atm}$ range from 280 to 900 ppmV generates an average $S(z)$ of 375 ppmV ± 255 (1σ), which is still remarkably low. These low $S(z)$ values might reflect rapid outgassing of soil CO_2 promoted by cracking in the Vertisol during drained conditions or that the $\delta^{13}C_r$ values we used are too low. Nonetheless, using the assumptions that are typically made when working with paleosols, an $S(z)$ value that equals 200 ppmV would be required to calculate the correct atmospheric pCO_2.

Seasonal ponding of water on this soil influenced both the $\delta^{13}C_{cc}$ and the trace-element geochemistry of the calcite nodules; however, it did not preclude the precipitation of calcite in this soil system (Fig. 4.5B). The wide range in both luminescence state and $\delta^{13}C$ of the pedogenic carbonates is an indicator of the influence of hydromorphic processes. Comparing carbonate luminescent states with their isotopic composition greatly improves the investigators ability to eliminate invalid carbonates (Fig. 4.5). Paleosol carbonates that have a luminescent pattern similar to that of M1

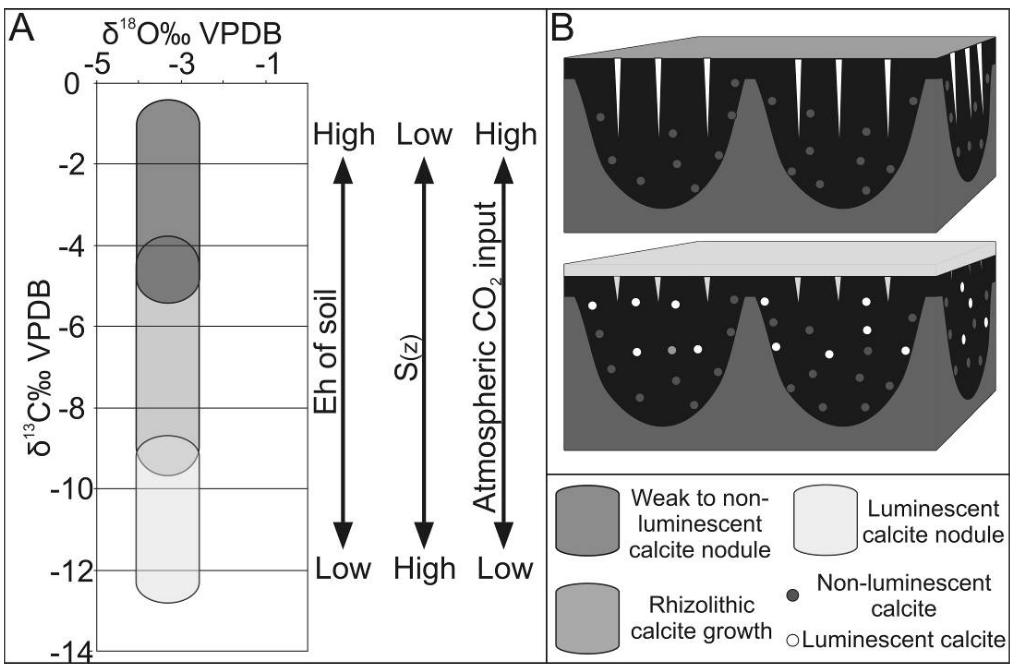

Figure 4.5 A) Comparisons of typical morphotype isotope values with interpreted soil conditions at the time of calcite precipitation. B) Model of carbonate precipitation of non-luminescent calcite nodules (dark circles) in the well-drained portion of the season (top) and luminescent calcite nodules (light circles) in the saturated portion of the season (bottom), in a Vertisol at Dance Bayou, Brazoria Co., Texas.

(uniform bright luminescence) should be avoided, because they likely formed from phreatic soil or ground water precipitation (Fig. 4.3). Rhizolithic carbonates similar in luminescent state to M4 in hydromorphic paleosols may also be unreliable for the calculation of paleo-atmospheric pCO_2 (Fig. 4.3). Carbonates in paleo-Vertisols that have CL patterns similar to M2 or have speckled luminescence in an otherwise predominantly non–luminescent to weakly luminescent, micritic carbonate matrix is more likely appropriate for isotopic analysis to use in the paleosol barometer equation. Diagenetic alteration has the potential to change the original texture, luminescence, and possibly even the $\delta^{13}C$ value of pedogenic calcites preserved in the rock record (Budd et al. 2002; Quast et al. 2006). The small range of $\delta^{18}O$ values for morphotypes that formed at different times and temperatures throughout the season suggests that recrystallization of these calcites is occurring; however, it does not seem to be affecting either the CL or the $\delta^{13}C$ values of the nodules (Fig. 4.4).

The range of $\delta^{13}C_{cc}$ values produced in the modern Vertisol studied here, forming with a presumably narrow range $\delta^{13}C_r$ and $\delta^{13}C_a$ compositions and relatively low $[CO_2]_{atm}$, exceeds the range of average $\delta^{13}C_{cc}$ values and exceeds the 1σ range for all but one data set produced from paleosol carbonate that has been used to estimate $[CO_2]_{atm}$ through the entire Phanerozoic Eon (Fig. 4.6). From this soil, however, we have confidently identified calcite morphotypes that are appropriate for $[CO_2]_{atm}$ calculation and excluded other morphologies that did not form while the soil was at steady state with the atmosphere. Many of the paleosol carbonate data sets (Fig. 4.6) are from paleo-Vertisols, yet none have as wide a 1σ range of $\delta^{13}C_{cc}$ as this modern soil, which suggests that either carbonate heterogeneity was avoided or that some diagenetic alteration affected the range in the $\delta^{13}C$ in the carbonates. The issues of constraining $S(z)$ and the timing of carbonate precipitation are paramount to improving the reliability of paleobarometry as well as paleoecologic data from paleo-Vertisols and other types of paleosols. These issues require continued study of modern soil systems in numerous soil orders (or soil textural classes) and hydrologic regimes.

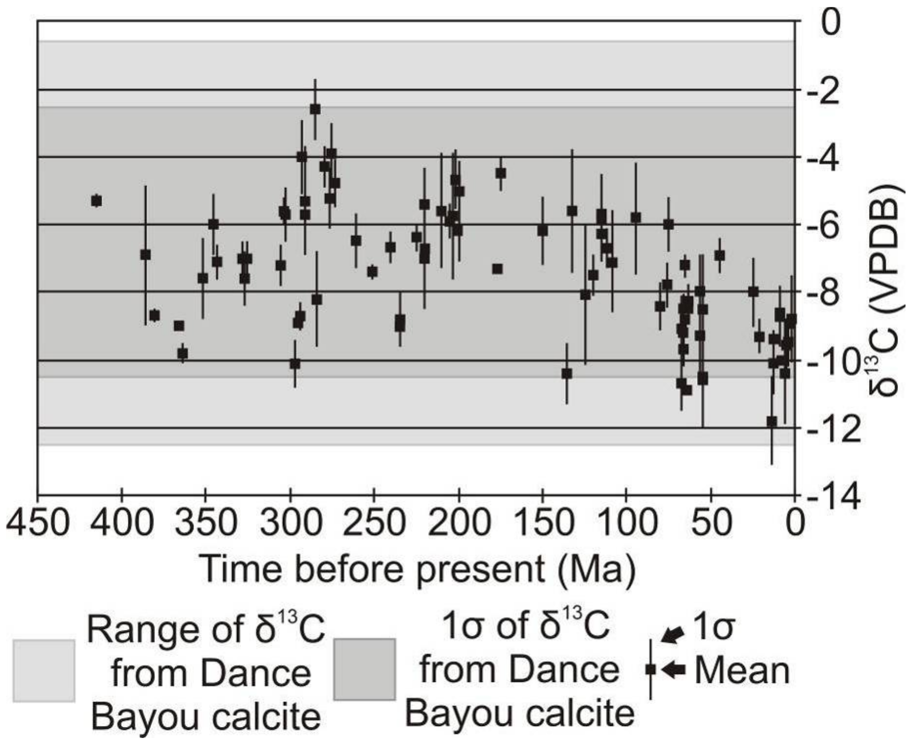

Figure 4.6 Compiled $\delta^{13}C$ values from paleosol carbonates used to calculate atmospheric pCO_2 through the Phanerozoic (Ekart et al. 1999; Lee, 1999; Lee and Hisada 1999; Ghosh et al. 2001; Cox et al. 2001; Robinson et al. 2002; Nordt et al. 2002; Cleveland et al. 2008; Leier et al. 2009) compared to the range of pedogenic carbonate sampled in the Churnabog clay series, a modern Vertisol forming in the Dance Bayou, Texas (from this study).

Conclusions

1. The M1 and M2 morphotypes of pedogenic calcite in Vertisols at Dance Bayou, Brazoria County, Texas, record periods of calcite precipitation in both water-saturated and unsaturated soil conditions. The luminescent calcite (M1), which represents saturated soil-state precipitation, formed in a system where the only significant contribution of carbon is from soil-respired CO_2, and may represent a viable proxy for estimating $\delta^{13}C_r$ values. The non-luminescent calcite (M2), in contrast, formed during well-drained soil conditions in a two-end-member open system described in the Cerling

(1984) CO_2 production-diffusion model, appropriate for estimation of paleoatmospheric pCO_2.

2. A rhizolithic morphotype exists in Dance Bayou Vertisols that is luminescent, which is likely the result of a micro-reducing environment created during the decay of organic material, and has $\delta^{13}C_{cc}$ values that fall between the luminescent and non-luminescent calcites. The $\delta^{13}C_{cc}$ values are the result of either precipitation during both well-drained and poorly drained conditions, or from elevated $S(z)$ concentrations in the rhizosphere from root respiration, making these forms more unpredictable and less reliable calcite for paleobarometry in hydromorphic paleosols.

3. The correspondence of $\delta^{13}C_{cc}$ values with the CL behavior of pedogenic calcites creates the potential to independently test the soil saturation state and atmospheric communicability at the time of calcite precipitation. This type of test can verify the suitability of paleosol calcites for estimation of paleoatmospheric pCO_2 when the CL state of the calcite has not been diagenetically altered.

4. Calculated $S(z)$ values from a rearranged paleoatmospheric pCO_2 equation, using $\delta^{13}C_{cc}$ values of the non-luminescent carbonate, are an order of magnitude lower than currently assumed for $S(z)$ concentrations in the diffusion equation. This suggests that either $S(z)$ in Vertisols can become very low due to deep soil cracking and increased outgassing, or that $S(z)$ values, in general, are overestimated.

5. The range of $\delta^{13}C_{cc}$ values produced from this single soil site in Texas exceeds all of the $\delta^{13}C_{cc}$ values used to estimate $[CO_2]_{atm}$ throughout the entire Phanerozoic Eon (Fig.

6). This observation suggests that our ability to better constrain the concentration of soil-respired CO_2 at the time of carbonate precipitation is crucial to the reliability of estimates of paleoatmospheric pCO_2. In this hydromorphic Vertisol we are able to screen the various calcite morphologies and identify those that formed in an open system with the atmosphere, which as well might be possible with paleosol carbonates allowing for the incorporation of carbonate records from hydromorphic paleosols into paleo- pCO_2 curves.

CHAPTER FIVE

Conclusions

Forestation in Middle Devonian landscapes in the northern Appalachian basin extended from swamplands at the paleo-shoreline to fluvial overbank deposits proximal to channels to distal floodplains and interfluve terraced deposits. The depth and degree of pedogenic weathering produced as a result of forestation was likely heretofore unprecedented on Earth. This increase in pedogenesis had significant consequences to the characteristics of alluvial sedimentary systems, as well as other systems that were directly and indirectly impacted by this change in the terrestrial system. Stripping of iron from soils through complexation with organic acids on alluvial plains in the Appalachian basin may have greatly increased from the Ordovician to the Devonian. This increase in iron loss in soils, as well as for other nutrients, may have caused increased biotic productivity in the marine realm. This increase in organic productivity may have been a contributing agent of Devonian anoxic events, drawdown in atmospheric CO_2 and ultimately late Devonian ice-house conditions.

Middle Devonian fluvial deposits in the northern Appalachian basin display several tiers of cyclicity in alluvial stacking patterns. Changes in FAC thickness stacking patterns correspond in a predictable way to the facies trends, as well as to paleosol occurrence and maturity. The first hierarchal tier of cyclicity of FAC thickness stacking patterns correlates well with modeled water depth in coeval marine strata, which was driven by changes in basin subsidence from tectonic forcing caused by the adjacent Acadian orogen. The second tier of cyclicity is identified as fluvial sequences, which formed as a result of basin-wide changes in accommodation. From this sequence-stratigraphic framework a terrestrial to marine correlation model for the Middle Devonian strata in New York was established. Deposition of the Tully Limestone, which is an anomalous marine carbonate in an overall siliciclastic section, likely correlated with a decreasing trend in available accommodation and sediment yield in terrestrial strata.

Mean annual precipitation (MAP) estimates using CALMAG, a geochemical proxy developed for paleo-Vertisols, suggests that the average MAP was ~1550 mm/yr, which agrees with macro- and micromorphologic characteristics of the paleosols. The depth to carbonate proxies (DTC) for MAP produces significantly lower MAP estimates than the CALMAG proxy. The discrepancy between the CALMAG estimates and those obtained using the DTC proxies may be attributable, in part, to either diagenetic alteration of the soil matrix material and potentially unconstrained factors of influence on both the CALMAG and the DTC proxy methods.

The study of modern analog soil systems is the best possible way to generate new proxies and improve our understanding of ancient soil systems. The different morphotypes of pedogenic calcite in Vertisols at Dance Bayou, Brazoria County, Texas, record periods of calcite precipitation in both water-saturated and unsaturated soil conditions. The luminescent calcite, which represents saturated soil-state precipitation, formed in a system where the only significant contribution of carbon is from soil-respired CO_2. The non-luminescent calcite, in contrast, formed during well-drained soil conditions in a two-end-member open system described in the Cerling (1984) CO_2 production-diffusion model, appropriate for estimation of paleoatmospheric pCO_2. The correspondence of $\delta^{13}C_{cc}$ (calcite) values with the CL behavior of pedogenic calcites creates the potential to independently test the soil saturation state and atmospheric connection at the time of calcite precipitation. This type of test can verify the suitability of paleosol calcites for estimation of paleoatmospheric pCO_2 when the CL state of the calcite has not been diagenetically altered during recrystallization. Calculated soil-respired CO_2 values from a rearranged paleoatmospheric pCO_2 equation, using $\delta^{13}C_{cc}$ values of the non-luminescent calcite (M2), are an order of magnitude lower than currently assumed for *S*(*z*) (soil respired) concentrations in the diffusion equation. The range of $\delta^{13}C_{cc}$ values produced from this single Holocene soil site in Texas exceeds all of the $\delta^{13}C_{cc}$ values used to estimate paleoatmospheric pCO_2 throughout the entire Phanerozoic Era. This observation suggests that our ability to better constrain the concentration of soil-respired CO_2 at the time of carbonate precipitation is crucial to the reliability of estimates of paleoatmospheric pCO_2.

APPENDICES

APPENDIX A

Copyright Permissions

---------- Forwarded message ----------
From: **Mintz, Jason S** <Jason_Mintz@baylor.edu>
Date: Tue, Mar 1, 2011 at 10:21 PM
Subject: FW: Premission to incorporate
To: "solomonthewise@gmail.com" <solomonthewise@gmail.com>

This note should serve as a permission to reproduce for chapter 2 and 4 as she is a representative of SEPM, which has published both of these chapters.

From: Palaios[SMTP:PALAIOS@KU.EDU]
Sent: Tuesday, March 01, 2011 10:20:51 PM
To: Mintz, Jason S
Subject: RE: Premission to incorporate
Auto forwarded by a Rule

Dear Jason,
Thanks for your e-mail asking for permission to reprint your research article as a chapter of your dissertation, which I am happy to grant. We actually allow authors to hold joint copyright to their work, but do let me know if you need a formal letter granting permission, and I'll be glad to send one.

Sincerely yours,
Jill

****
Jill Hardesty
Managing Editor
PALAIOS Editorial Office
Paleontological Institute
Department of Geology
University of Kansas
1475 Jayhawk Blvd., room 119
Lawrence, KS 66045-7613
phone: 785-864-2737

fax: 785-864-3636
e-mail: palaios@ku.edu
www.paleo.ku.edu/palaios<http://www.paleo.ku.edu/palaios>

Online manuscript submission at
http://sepm-palaios.allentrack.net/

From: solomonthewise@gmail.com [solomonthewise@gmail.com] on behalf of Jason Mintz [Jason_Mintz@baylor.edu]
Sent: Thursday, February 24, 2011 5:52 PM
To: Palaios
Cc: Driese, Steven G.
Subject: Premission to incorporate

To whom it may concern:

My name is Jason Mintz, I published a research article in Volume 25, No. 2 (February, 2010) of Palaios, pages 85-96.

This article is a portion of my dissertation work done at Baylor University.

I am writing to request permission that this research article appear as a chapter of my dissertation to be on file at Baylor University and published as part of a dissertation through Proquest UMI.

Thank you, -Jason

--
Jason S. Mintz
PhD candidate
Baylor University
Department of Geology
BSB 4th Floor: Room D409
101 Bagby Ave.
Waco, Tx, 76706
email: Jason_Mintz@baylor.edu<mailto:Jason_Mintz@baylor.edu>
Large Files: solomonthewise@gmail.com<mailto:solomonthewise@gmail.com>
Fax: (254) 710-2673

APPENDIX B

Paleo-forest Site Locations

Location A: N42° 23' 51" W074° 27' 00"

The site is located 0.6 km north of the Schoharie reservoir and the Gilboa dam, along the western edge of the Schoharie Creek. At an abandoned sandstone quarry (listed as stop 3 in Johnson, 1987), this locality contains one sandy paleosol with abundant evidence for forest development, with both vertical and lateral exposures of *in situ* *Eospermatopteris* stump casts. Note: Access to this site is strictly controlled by the New York City Water Intake Authority and a permit must be secured before visiting the site.

Location B: N42° 07' 24" W074° 04' 11"

This location contains 2 different paleosols with evidence for forest development exposed on the flanks of the Plattekill Creek, with both horizontal and vertical exposures of different forest horizons. These sites are referenced by their placement in the detailed stratigraphy of Plattekill Creek in the Appendix of Willis and Bridge (1988). Location 1 is at level 284 m and Location 2 at level 409 m on the Plattekill stratigraphic column of Willis and Bridge (1988). .

Location C: N 42° 20' 13" W074° 06' 59"

A road cut exposed along New York State Route 23 between Cairo and East Windham, this location contains one vertically exposed forest paleosol deposit. The paleosol is the top mudstone unit in a 15 m thick exposure of a fluvial sandstone-mudstone succession. The road-cut exposure is second lowest in elevation in a series of five road-cut exposures increasing in elevation on the southern side of Route 23 and directly across from Hervey Road.

APPENDIX C

Table C.1 Stump Cast Size and Spatial Data from the West Saugerties and Gilboa Localities

Location	diameter (cm)	x (m)	y (m)
West Saugerties	22	-1.67519	2.305698
	40	-3.375	2.38157
	20	-4.09673	0.418979
	44	-5.15581	1.299939
	30	-9.10255	3.845047
	28	-10.5933	2.56799
	20	-11.2361	0.463323
	0	-12.2527	1.928942
	28	-8.29249	2.382111
	15	-13.5165	0.131887
	20	-13.4944	-0.57587
	9	-14.3383	1.661701
	28	-14.9302	1.472411
	40	-15.4972	1.381348
	30	-15.3505	0.747162
	22	-15.8887	0.446336
	15	-16.4795	1.56834
	19	-19.9006	-0.97253
	42	-21.6861	-0.39761
	18	-21.7286	-0.90732
	18	-21.8606	-1.46121
Gilboa	20	-21.3	-21.3
	20	-21.4022	-21.4022
	34	-21	-21
	28	-20.6871	-20.6871
	32	-20.0279	-20.0279
	22	-20.0332	-20.0332
	20	-20.0608	-20.0608
	60	-19	-19
	10	-18.6278	-18.6278

Location	diameter (cm)	x (m)	y (m)
	18	-15.1046	-15.1046
	14	-15.1917	-15.1917
	16	-14.8221	-14.8221
	20	-14.1083	-14.1083
	16	-14.165	-14.165
	14	-15.5229	-15.5229
	72	-12.4348	-12.4348
	14	-15.2268	-15.2268
	15	-13.5117	-13.5117
	10	-15.1185	-15.1185
	10	-15.361	-15.361
	10	-15.3082	-15.3082
	8	-13	-13
	90	-8.90602	-8.90602
	24	-9.70692	-9.70692
	8	-10.5484	-10.5484
	20	-10.6215	-10.6215
	60	-9.06504	-9.06504
	15	-12.4286	-12.4286
	24	-10.7655	-10.7655
	14	-11.2655	-11.2655
	24	-11.3717	-11.3717
	34	-12.6143	-12.6143
	6	-13.0783	-13.0783
	5	-13.5355	-13.5355
	6	-13.7512	-13.7512
	6	-7.95	-7.95
	7	-4.22996	-4.22996
	14	-4.80234	-4.80234
	14	-5.12382	-5.12382
	6	-5.45536	-5.45536
	7	-5.40737	-5.40737
	10	-5.21845	-5.21845
	15	-6.4866	-6.4866
	22	-7.21837	-7.21837
	20	-8.47637	-8.47637
	12	-8.5305	-8.5305
	9	-9.75228	-9.75228
	36	-9.41266	-9.41266

Location	diameter (cm)	x (m)	y (m)
	42	-9.70936	-9.70936
	18	-10.6288	-10.6288
	13	-14.4499	-14.4499
	8	-13.8255	-13.8255
	90	-14.8534	-14.8534
	13	-14.0413	-14.0413
	16	-14.3929	-14.3929
	32	-13	-13
	10	-13	-13
	15	-13	-13
	14	-3.93966	-3.93966
	7	-4.11889	-4.11889

APPENDIX D

Stratigraphic Column of Outcrop Exposed along
Plattekill Creek in West Saugerties, New York. Modified from Bridge and Willis (1988).

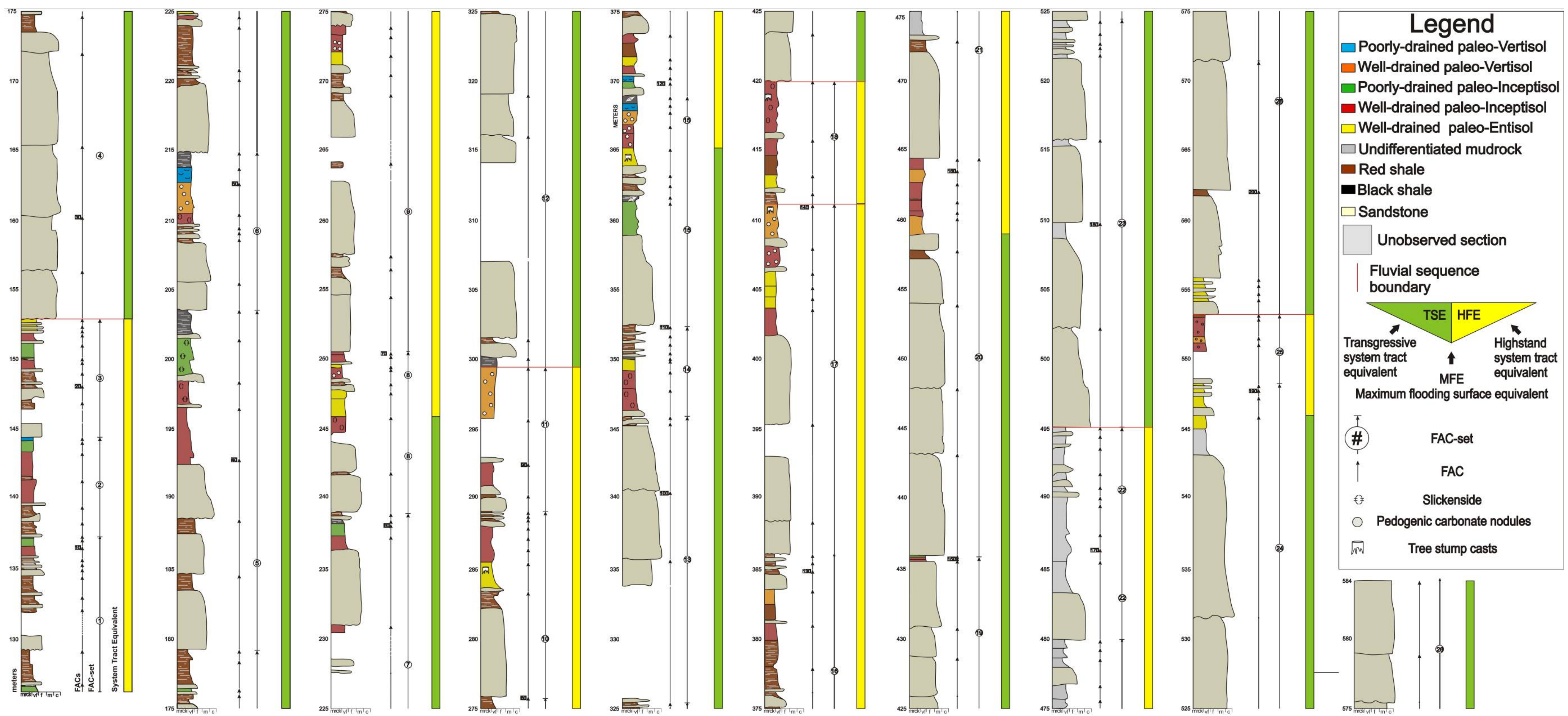

APPENDIX E

Table E.1 Fluvial Aggradational Cycle, Facies and Paleosol Thicknesses and Paleosol Maturity Data from Outcrop Exposed along Plattekill Creek in West Saugerties, New York.

Thickness measurements are in meters.

FAC #	Thickness	FACs w/ Missing Interval	Sand	black shale	red shale	Mudrock	Paleosol	Maturity Scale	W.D. ENT	WD EPT	PD EPT	WD ERT	PD ERT
1	0.389		0	0	0		18	2	0	0	0.389	0	0
2	0.116		0	0.116	0				0	0	0	0	0
3	2.433		0.213	0	2.22				0	0	0	0	0
4		3.03											
5	0.878		0.265	0	0.613				0	0	0	0	0
6	1.397		0.247	0	1.15								
7	0.557		0.434		0.123								
8	0.364		0.21		0.154								
9	0.347		0.12		0.227								
10	0.834		0.15				10	2		0.684			
11	0.55							2			0.55		
12	0.1			0.1									
13	1.112		0.212		0.9								
14	1.11		0.57		0.54								
15	2.56		0.91				116	2		1.65			
16	1.94				0.24		9	1	1.7				
17	0.8						9	2			0.8		
18	0.24						8	3					0.24
19		2.61											
20	1.11		0.85		0.26								
21	0.89		0.18		0.71								
22	0.79		0.21				7	2		0.58			
23	0.22				0.12		7	2			0.1		
24	0.99						7	2			0.99		
25	0.71		0.2				7	2		0.51			
26	0.3		0.18				6	1	0.12				
27	0.3		0.17				6	1	0.13				
28	0.37		0.16				6	1	0.21				
29	3.47		3.47										
30	3.87		3.87										
31	4.99		4.99										
32	6.57		6.57										
33	2.62		1.39		1.23								
34	1.22		0.55		0.67								
35	0.4		0.17				109	2			0.23		
36	0.459		0.29		0.169								
37	0.74				0.74								
38	5.29		4.1		1.19								
39	3.77		2.72		1.05								
40	4.24		3.79		0.45								
41	3.48						110	2		3.48			
42	1.85		0.24				111	3		1.61			
43	2.94		0.54				112	2			2.4		
44	1.98		0.35	1.63									
45	1.95		1.95										
46	2.99		2.72		0.27								
47	0.5		0.32		0.18								
48	0.3		0.17		0.13								

FAC #	Thickness	FACs w/ Missing Interval	Sand	black shale	red shale	Mudrock	Paleosol	Maturity Scale	W.D. ENT	WD EPT	PD EPT	WD ERT	PD ERT
49	0.96		0.22				21	3		0.74			
50	2.14						1	2				2.14	
51	1.04						1	2					1.04
52	1.06			1.06									
53	5.1		4.64		0.46								
54	0.67		0.23		0.44								
55	2.97		0.22		2.75								
56	0.73		0.45				113	2		0.28			
57		1.71					114	1	0.2				
58		3.55					115	2		0.4			
59	7.36		5.52		0.94		29	2		0.9			
60	0.88						29	2			0.88		
61	0.28			0.28									
62	0.57		0.31		0.26								
63	2.89		2.7		0.19								
64	3.98		2.21				28	3		1.77			
65	1.93						27	1	1.93				
66	0.57		0.29		0.28								
67	1.29		0.29				12	4		1			
68	0.5						12	1	0.5				
69	0.5						12	2		0.5			
70	0.7		0.22				13	2		0.48			
71	4.11		4.11										
72	0.72		5.38-4.11		0.72								
73	1		0.72		0.28								
74		6.92											
75		5.07											
76	1.39		0.35		1.04								
77	1.55		0.62				17	1	0.93				
78	1.26						17	2		1.26			
79	0.7			0.7									
80	1.78		0.94		0.84								
81	7.4		6.26		1.14								
82	2.1		0.3				2	1	1.8				
83	1						4	2		1			
84	0.8						4	2		0.8			
85	0.68						4	2		0.68			
86	0.57		0.4		0.17								
87	0.31		0.18		0.13								
88	0.25		0.13		0.12								
89	1.18		0.95		0.23								
90	2.24		0.62				5	2		1.62			
91		3.12											
92	3.62						3	4				3.62	
93	0.78			0.78									
94	1.3		0.9		0.4								
95		15											
96	2.88		2.88										
97	5.91		5.63		0.28								
98	0.37		0.17		0.2								
99		10.42											
100	4.84		4.84										
101	4.73		4.58		0.15								
102	0.5		0.29		0.21								
103	1.99		0.46				20	3		1.53			
104	1.24						20	3		1.24			
105	0.78						20	1	0.78				
106	0.2			0.2									
107	0.36		0.22		0.14								
108	0.62		0.18		0.44								
109	0.56		0.18		0.38								
110	0.77		0.19		0.58								
111	8.61		6.25				19	2			2.36		

FAC #	Thickness	FACs w/ Missing Interval	Sand	black shale	red shale	Mudrock	Paleosol	Maturity Scale	W.D. ENT	WD EPT	PD EPT	WD ERT	PD ERT
112	0.42			0.42									
113	0.82		0.38		0.44								
114	0.65		0.45		0.2								
115	1.89		0.64				32	1	1.25				
116	1.64						16	2		1.64			
117	0.983						16	3				0.98	
118	0.51						16	2					0.51
119	0.53			0.53									
120	0.95		0.75				15	2			0.2		
121	0.15						15	2					0.15
122	1.08		0.52				25	3		0.56			
123	0.64						25	1	0.64				
124	1.62				0.96		25	2		0.66			
125	1.68		1.14		0.54								
126	1.08		0.72		0.36								
127	1.77		0.2		1.57								
128	3.04				1.86		14	2		1.18			
129	2.41		0.27		1.07		24	3				1.07	
130	1.48		1.07		0.41								
131	0.53		0.18		0.35								
132	0.54		0.25		0.29								
133	2.33		2.33										
134		7.16											
135	8.24		6.34				31	4		1.9			
136	0.79						31	1	0.79				
137	0.76						31	1	0.76				
138	1.03						31	1	1.03				
139	1.8		0.3				30	4		1.5			
140	2.94		0.55				26	4				2.39	
141	0.84				0.84								
142	1.22		0.3				23	1	0.92				
143	2.6				1.5		23	2		1.1			
144	4.1		0.43				22	3		3.67			
145	3.43		3.43										
146	2.27		2.27										
147	2.82		2.82										
148	2.18		2.18										
149	4.71		4.58				100	2		0.13			
150	0.17						100	2		0.17			
151	0.13						100	2			0.13		
152	7.21		7.21										
153	4.63		4.63										
154	5.97		5.97										
155	3.772		3.16		0.612								
156	2.33		1.15				102	2				1.18	
157	0.3						102	2		0.3			
158	0.68						102	2		0.68			
159	1.15				0.11		103	2		1.04			
160	0.83						103	3				0.83	
161	0.79						103	3		0.79			
162	8.34		7.53			0.81							
163	2.07		0.36			1.71							
164	0.66					0.66							
165	1.06					1.06							
166	2.25		1.57			0.68							
167	0.71					0.71							
168	0.6					0.6							
169	5.51		3.29			2.22							
170	0.87					0.87							
171	1.06					1.06							
172	2.09					2.09							
173	0.54					0.54							
174	0.72		0.35			0.37							

FAC #	Thickness	FACs w/ Missing Interval	Sand	black shale	red shale	Mudrock	Paleosol	Maturity Scale	W.D. ENT	WD EPT	PD EPT	WD ERT	PD ERT
175	1		0.5			0.5							
176	1.8		0.55			1.25							
177	0.8		0.22			0.58							
178	0.6		0.25			0.35							
179	6.99		6.99										
180	7.44		6.35		1.09								
181	5.89		5.41		0.48								
182	6		5.71		0.29								
183	0.51		0.37		0.14								
184	0.3		0.14		0.16								
185	0.7		0.25		0.45								
186	0.86		0.37		0.49								
187	7.33		7.33										
188	14.29		11.46		1.88			1	0.95				
189	1.39		0.59					1	0.8				
190	0.54		0.27					1	0.27				
191	0.38		0.23					1	0.15				
192		3.04						2		0.63			
193	0.477							2				0.48	
194	1.38							3		1.38			
195	0.22				0.22								
196	1.17		0.94						0.23				
197	0.45		0.17						0.28				
198	0.55		0.28					1	0.27				
199	0.46		0.19					1	0.27				
200	6.31		5.87		0.44			1					
201	9.35		9.35					1					
202	3.96		3.96										
203	3.34		3.34										
204	5.36		5.36										

APPENDIX F

Table F.1 Morphological Characteristics of Pedotypes by Horizon in the Plattekill, Manorkill and Oneonta Formations from Outcrop Exposed along Plattekill Creek, in West Saugerties, New York

Pedotype	Horizons	Color	Structure	Cutans/ slickensides	Nodules/ concretions	Rooting	Sedimentary structures
Well-drained paleo-Entisol	A	10R 3/2 dusky Red	Weak to moderate, medium to thick platy	None	None	8cm sub-horizontal bifurcating roots with downward branching 1 cm bifurcating clay-filled root trace (CFRT) with drab halo extends 1.5—2.0 m below the paleosol surface	0.5—1.0 cm laminar to wavy bedding throughout the profile
	C		None				
Poorly-drained paleo-Inceptisol	A						
	Bg/ Bssg	10GY 3/2 greenish grey	Coarse to fine, angular to subangular blocky	Rare to common stress cutans on ped faces	None	Drab-haloed root trace (DHRT) around millimeter-scale carbonized root fossils	None
	Bkg	10R 3/1 dark reddish grey	Coarse angular blocky	None	Common 1-3 cm carbonate nodules	1-3 cm carbonate rhizoliths	
	C		None	None		None	Thinly-laminated, planar horizontal bedding
Well-drained paleo-Inceptisol	A	10R 3/2 dusky red; 10R 4/2 weak red	Fine to medium angular to subangular blocky	None	Mottling glaebules matrix (5GY 4/1)	Cannot determine	None
	Bt/ Bw/ Btk		2^{nd}- medium prismatic; 1^{st} medium angular blocky	Occasional slickensides and stress cutans on ped faces in Bw horizons; occasional to common argillans in Bt horizons	1-2 cm carbonate nodules in Bk horizons	0.5—1.0 cm DHRT	None
	C		Thin platy; None	None	None	None	Planar laminar bedding
Poorly-drained paleo-Vertisol	A						
	Bssg1	5GY 5/1 greenish grey; 5GY 3/1 very dark greenish grey	Very coarse to medium angular blocky	Occasional to abundant slickensides along ped faces	Soil matrix has strong reaction with dilute HCl	Millimeter-scale carbonized root fossils	None
	Bssg2		Coarse wedge	Well defined master slickensides with subsurface expression of microtopography		Occasional 1-2 cm DHRT	
Well-drained paleo-Vertisol	A	10R 3/3 dusky red; 10R 4/2 weak red	Coarse to medium granular	Rare stress cutans on ped faces	None	Sand filled stump and root casts	None
	Bkss/Bss		2^{nd}- Coarse subangular blocky; 1^{st}- medium subangular blocky	Abundant stress cutans and slickensides on ped faces; defined master slickensides that display subsurface expression of microtopography	Paleosols that lack carbonate nodules have common 3-5 cm Fe nodules	0.5—1.0 cm bifurcating CFRT with drab halos around root void that extends down over 1.0 m into the paleosol	None
	BC		Thick to medium platy	Common stress cutans on ped faces	None	Few to common 1 mm CFRT with 1cm drab halo	Platy structure may follow relict bedding planes
	C		None	None	None	None	Massive upper-fine to lower-medium grained sandstone; wavy laminar mudrock

APPENDIX G

Table G.1 Stable Carbon and Oxygen Isotopic Data from Pedogenic Carbonate Morphotypes from the Churnabog Clay Series at Dance Bayou, Brazoria County, TX

Morphotype	$\delta^{13}C$ (VPDB)	$\delta^{18}O$ (VPDB)
M1	-10.619	-3.218
	-10.494	-2.982
	-10.525	-2.965
	-10.668	-2.919
	-11.446	-3.107
	-10.562	-3.101
	-10.165	-3.315
	-11.194	-3.017
	-10.936	-3.409
	-10.744	-3.019
	-11.268	-3.004
	-9.426	-3.416
	-9.918	-3.262
	-11.53	-3.137
	-10.486	-3.149
	-10.949	-3.174
	-11.377	-2.973
	-11.17	-3.07
	-12.183	-3.154
	-12.175	-2.728
	-11.939	-3.495
	-12.065	-3.268
	-12.544	-3.222
	-11.649	-3.654
	-12.001	-3.249
M2	-3.625	-3.731
	-3.794	-3.587
	-3.505	-3.609
	-2.069	-3.287
	-3.276	-3.162

Morphotype	$\delta^{13}C$ (VPDB)	$\delta^{18}O$ (VPDB)
	-0.614	-3.315
	-0.983	-3.537
	-1.388	-3.42
	-2.075	-3.531
	-4.836	-3.306
	-6.445	-3.226
	-2.704	-3.524
	-4.6	-3.287
	-4.243	-3.184
	-4.111	-3.438
	-2.373	-3.573
	-2.055	-3.504
	-1.516	-3.454
	-2.91	-3.33
	-2.791	-3.294
	-3.227	-3.427
	-1.001	-3.262
	-0.789	-3.26
	-2.643	-3.311
	-2.3	-3.518
	-1.448	-3.42
	-1.342	-3.464
	-1.752	-3.324
	-4.012	-3.656
	-4.399	-3.323
	-3.985	-3.381
	-4.5	-3.366
M3	-4.923	-3.291
	-11.308	-2.919
	-5.731	-3.202
	-10.528	-2.97
	-3.707	-3.259
	-11.732	-2.726
	-1.814	-3.359
	-8.689	-3.045
	-7.209	-3.112
M4	-6.615	-3.267
	-4.509	-3.279
	-4.682	-3.356

Morphotype	$\delta^{13}C$ (VPDB)	$\delta^{18}O$ (VPDB)
	-4.293	-3.271
	-4.139	-3.398
	-6.973	-3.202
	-6.564	-3.375
	-5.676	-3.342
	-7.848	-3.034
	-11.347	-2.788
	-5.305	-3.35

REFERENCES

Algeo, T.J., Berner, R.A., Maynard, J.B., and Steckler, S.E., 1995, Late Devonian oceanic anoxic events and biotic crises: "Rooted" in the evolution of vascular land plants?: GSA Today, v. 5, p. 45, 64-66.

Algeo, T.J., and Scheckler, S.E., 1998, Terrestrial marine teleconnections in the Devonian: links between the evolution of land plants, weathering processes, and marine anoxic events: Philosophical Transactions of the Royal Society of London, v. 353B, p. 113–130.

Arens, N.C., and Jahren, A.H., 2000, Carbon isotope excursion in atmospheric CO_2 at the Cretaceous-Tertiary boundary: Evidence from terrestrial sediments: Palaios, v. 15, p. 314-322.

Atchley, S.C., Nordt, L.C., and Dworkin, S.I., 2004, Eustatic control on alluvial sequence stratigraphy: a possible example from the Cretaceous-Tertiary transition of the Tornillo Basin, Big Bend National Park, west Texas: Journal of Sedimentary Research, v. 74, p. 392-405.

Baird, G.C., 1979, Sedimentary relationships of Portland Point and associated Middle Devonian rocks in central and western New York: New York State Museum Bulletin, v. 433, p. 1-23.

Baird, G.C., Brett, C.E., 1991. Submarine erosion on the anoxic seafloor, paleoenvironmental and temporal significance of reworked pyrite-bone deposits, *in* Tyson, R.V., Pearson, T.H. (Eds.), Modern and Ancient Continental Shelf Anoxia: Geological Society of London, Special Publication 58, p. 223–257.

Baird, G.C. and Brett, C.E., 2003, Taghanic stage shelf and off shelf deposits in New York and Pennsylvania: Faunal incursions, eustacy, and tectonics: Proceedings of 15th Annual International Senckenberg Conference. Courier Forschungsinstitut Senkenberg, v. 242, p. 141-156.

Baird, G.C. and Brett, C.E. 2008, Late Givetian Taghanic bioevents in New York State: New discoveries and questions: Bulletin of Geosciences, v. 83, p. 357–370.

Barnaby, R.J., and Rimstidt, J.D., 1989, Redox conditions of calcite cementation interpreted from Mn and Fe contents of authigenic calcites: Geological Society of America Bulletin, v. 101, p. 795-804.

Bartholomew, A.J., and Brett, C.E., 2003, The Middle Devonian (Givetian) Gilboa forest: sequence stratigraphic determination of the world's oldest fossil forest deposit, Schoharie Co., New York State: Geological Society of America, Abstracts with Programs, Northeastern Section Meeting, v. 35, n. 3, p. 76.

Bergman, N.M., Lenton, T.M., and WATSON, A.J., 2004, COPSE: A new model of biochemical cycling over Phanerozoic time: American Journal of Science, v. 304, p. 397–437.

Berner, R.A., 1992, Weathering, plants, and the long-term carbon cycle: Geochimica et Cosmochimica Acta, v. 56, p. 3225–3231.

Berner, R.A., 2005, GEOCARBSULF: A combined model for Phanerozoic atmospheric O_2 and CO_2: Geochimica et Cosmochimica Acta, v. 70, p. 5633–5664.

Berner, R.A., and Kthavala, Z., 2001, GEOCARB III: a revised model of atmospheric CO_2 over Phanerozoic time: American Journal of Science, v. 301, p. 182–204.

Berry, C.M., and Fairon-Demaret, M., 2001, The Middle Devonian flora revisited, *in* Gensel P.G. and Edwards D., eds., Plants Invade the Land: Evolutionary and Environmental Perspectives: Columbia University Press, New York, p. 120–139.

Blakey, R.C., 2003, Carboniferous-Permian paleogeography of the assembly of Pangea, *in* Wong, T.E., Proceedings of the XVth International Congress on Carboniferous and Permian Stratigraphy, Netherlands, Royal Netherlands Academy of Arts and Sciences, p. 443-456.

Blakey, R.C., 2010, http://jan.ucc.nau.edu/~rcb7/370moll.jpg. Checked January, 15, 2011.

Blum, M.D., and Price, D.M., 1998, Quaternary alluvial plain construction in response to interacting glacio-eustatic and climatic controls, Texas Gulf Coastal Plain, *in* Shanley, K. and McCabe, P., eds., Relative Role of Eustasy, Climate, and Tectonism in Continental Rocks: Society for Sedimentary Geology Special Publication, v. 59, p. 31-48.

Boyer, J.S., Jr., and Matten, L.C., 1996, Anatomy of *Eospermatopteris eriana* from the upper Middle Devonian (= Givetian) of New York: International Organisation of Palaeobotany, Fifth Quadrennial Conference, Santa Barbara, Abstracts Volume, p. 13.

Breecker, D.O., Sharp, Z.D., and McFadden, L.D., 2009, Seasonal bias in the formation and stable isotopic composition of pedogenic carbonate in modern soils from central New Mexico, USA: Geological Society of America Bulletin, v. 121, p. 630–640.

Breecker, D.O., Sharp, Z.D., and McFadden, L.D., 2010, Atmospheric CO_2 concentrations during ancient greenhouse climates were similar to those predicted for A.D. 2100: Proceedings of the National Academy of Sciences, v. 107, p. 576-580.

Brett C.E., and Baird, G.C., 1985, Carbonate-shale cycles in the Middle Devonian of New York: an evaluation of models for the limestones in terrigenous shelf sequences: Geology, v. 13, p. 324-327.

Brett, C.E., Baird, G.C., 1996, Middle Devonian sedimentary cycles and sequences in the northern Appalachian Basin., *in* Witzke, B.J., Day, J. (Eds.), Paleozoic Sequence Stratigraphy; View from the North American Craton: Geological Society of America Special Paper 306, p. 213–241.

Brett, C.E., Baird, G.C., Bartholomew, A.J., DeSantis, M.K., Ver Straeten, C.A., 2010, Sequence stratigraphy and a revised sea-level curve for the Middle Devonian of eastern North America: Palaeogeography, Palaeoclimatology, Palaeoecology, doi: 10.1016/j.palaeo.2010.10.009

Brewer, R., 1964, Fabric and Mineral Analysis of Soils: John Wiley & Sons, New York, 470 p.

Bridge, J.S., 1984, Large-scale facies sequences in alluvial overbank environments: Journal of Sedimentary Petrology, v. 54, p. 583–588.

Bridge, J.S., and Willis, B.J., 1994, Marine transgressions and regressions recorded in Middle Devonian shore deposits of the Catskill clastic wedge: Geological Society of America Bulletin, v. 106, p. 1440–1458.

Budd, D.A., Pack, S.M., and Fogel, M.L., 2002, The destruction of paleoclimatic isotopic signals in Pleistocene carbonate soil nodules of Western Australia: Palaeogeography, Palaeoclimatology, Palaeoecology, v. 188, p. 249-273.

Catuneanu, O., 2006, Principles of Sequence Stratigraphy: Amsterdam, Elsevier, 375 p.

Cerling, T. E., 1984, The stable isotopic composition of modern soil carbonate and its relationship to climate: Earth and Planetary Science Letters, v. 71, p. 229-240.

Cerling, T.E., 1991, Carbon dioxide in the atmosphere; evidence from Cenozoic and Mesozoic paleosols: American Journal of Science, v. 291, p. 377-400.

Cerling, T.E., 1999, Stable carbon isotopes in paleosol carbonates, *in* Thirty, M., Coincon, R., eds., Palaeoweathering, Palaeosurfaces, and Related Continental Deposits: International Association of Sedimentologists Special Publication, v. 27, p. 43–60.

Cleveland, D.M., Atchley, S.C., and Nordt, L.C., 2007, Continental sequence-stratigraphy of the Late Triassic (Norian-Rhaetian) Chinle strata, northern New Mexico: Allo- and Autocyclic origins of paleosol bearing alluvial successions: Journal of Sedimentary Research, v. 77, p. 909-924.

Cleveland, D.M., Nordt, L.C., Dworkin, S.I., and Atchley, S.C., Pedogenic carbonate isotopes as evidence for extreme climatic events preceding the Triassic-Jurassic boundary: Implications for the biotic crisis?: Geological Society of America Bulletin, v. 120, p. 1408-1415.

Cotter, E., Driese, S.G., 1998, Incised-valley fills and other evidence of sea-level fluctuations affecting deposition of the Catskill Formation (Upper Devonian), Appalachian foreland basin, Pennsylvania: Journal of Sedimentary Research, v. 68, p. 347-361.

Cox, J.E., Railsback, L.B., and Gordon, A., 2001, Evidence from Catskill pedogenic carbonates for a rapid Late Devonian decrease in atmospheric carbon dioxide concentrations: Northeastern Geology and Environmental Sciences, v. 23, p. 91-102.

Davies, N.S. and Gibling, M.R., 2010, Cambrian to Devonian evolution of alluvial systems: the sedimentological impact of the earliest land plants: Earth-Science Reviews, v. 98, p. 171-200.

Dennison, J.M., 1985a, Devonian eustatic fluctuations in Euramerica: Discussion: Geological Society of America Bulletin, v. 96, p. 1595-1597.

Dennison, J.M., 1985b, Catskill delta shallow marine strata, *in* Woodrow, D.L., and Sevon, W.D. (eds.), The Catskill Delta: Geological Society of America, Special Paper 201, p. 91-106.

DiMichele and DeMaris, 1987, Structure and dynamics of a Pennsylvanian-age *Lepidodendron* forest: colonizers of a disturbed swamp habitat in the Herrin (No. 6) Coal of Illinois: Palaios, v. 2, p. 146–157.

DiMichele, W.A., Hook, R.W., Beerbower, R., Boy, J.A., Gastaldo, R.A., Hotton, N. III, Phillips, T.L., Scheckler, S.E., Shear, W.A., and Sues, H.-D., 1992, Paleozoic terrestrial ecosystems, *in* Behrensmeyer, A.K., Damuth, J.D., DiMichele, W.A., Potts, R., Sues, H.-D., and Wing, S.L., eds., Terrestrial Ecosystems Through Time: Evolutionary Paleoecology of Terrestrial Plants and Animals: University of Chicago Press, Illinois, p. 205–325.

Driese, S.G., and Foreman, J.L., 1992, Paleopedology and paleoclimatic implications of Late Ordovician vertic paleosols, southern Appalachians: Journal of Sedimentary Petrology, v. 62, p. 71-83.

Driese, S.G., and Mora, C.I., 1993, Physico-chemical environment of pedogenic carbonate formation in Devonian vertic palaeosols, central Appalachians, U.S.A.: Sedimentology, v. 40, p. 199-216.

Driese, S.G., Mora, C.I., and Elick, J.M., 1997, Morphology and taphonomy of root and stump casts of the earliest trees (Middle to Late Devonian), Pennsylvania and New York, U.S.A.: Palaios, v. 12, p. 524-537.

Driese, S.G., and Mora, C.I., 2001, Diversification of Siluro-Devonian plant traces in paleosols and influence on estimates of paleoatmospheric CO_2 levels, Plants Invade the Land, Columbia University Press, p. 237-253.

Driese, S.G., and Mora, C.I., 2001, Diversification of Siluro-Devonian plant traces in paleosols and influence on estimates of paleoatmospheric CO_2 levels, *in* Gensel, P.G., and Edwards, D., eds., Plants Invade the Land: Evolutionary and Environmental Perspectives: Columbia University Press, New York, p. 237–253.

Driese, S.G., Mora, C.L., and Elick, J.M., 2000, The paleosol record of increasing plant diversity and depth of rooting and changes in atmospheric pCO_2 in the Siluro-Devonian, *in* Gastaldo, R.A., and DiMichele, W.A., eds., The Paleontological Society Papers: Phanerozoic Terrestrial Ecosystems: v. 6, p. 47–61.

Ekart, D.D., Cerling, T.E., Montañez, I.P., and Tabor, N.J., 1999, A 400 million year carbon isotope record of pedogenic carbonate: implications for paleoatmospheric carbon dioxide: American Journal of Science, v. 299, p. 805–827.

Ekblad, A, and Högberg, P, 2001, Natural abundance of ^{13}C in CO_2 respired from forest soils reveals speed of link between tree photosynthesis and root respiration: Oecologia, v. 127, p. 305-308.

Elick, J.M., Driese, S.G., and Mora, C.I., 1998, Very large plant and root traces from the Early to Middle Devonian: Implications for early terrestrial ecosystems and pCO_2 estimations: Geology, v. 26, p. 143-146.

Ettensohn, F.R., 1985a, The Catskill delta complex and the Acadian orogeny: A model: *in* Woodrow, D.L., and Sevon, W.D. (eds.), The Catskill Delta: Geological Society of America, Special Paper 201, p. 39-51.

Ettensohn, F.R., 1985b, Controls on development of Catskill delta complex basin-facies: *in* Woodrow, D.L., and Sevon, W.D., eds., The Catskill Delta: Geological Society of America Special Paper 201, p. 39–51.

Ettensohn, F.R., 1998. Compressional tectonic controls on epicontinental black shale deposition: Devonian–Mississippian examples from North America. In: Schieber, J., Zimmerle, W., Sethi, P. S. (Eds.), Shales and Mudstones, vol., 1 (Basin Studies, Sedimentology, and Paleontology). E. Schweizerbart' sche Verlagsbuchhandlung (Nägele u. Obermiler); Stuttgart, 109–128.

Ettensohn, F.R., 2008. Chapter 4: The Appalachian foreland basin in eastern United States. In: Hsu, K.V. (Ed.) Sedimentary Basins of the World. Vol. 5. The Sedimentary Basins of the United States and Canada. Miall, A.B. (Ed.) Elsevier, The Netherlands, p. 105–179.

Ettensohn, F.R., and Barron, L.S., 1981, Depositional model for the Devonian–Mississippian black shales of North America: a paleoclimatic-paleogeographic approach, *in* Roberts, T.G., ed., Geological Society of America Cincinnati, '81 Field Trip Guidebooks, Volume 2: Economic Geology, Structure: American Geological Institute, Falls Church, Virginia, p. 344–361.

Faill, R.T., 1985, The Acadian orogeny and the Catskill Delta, *in* Woodrow, D.L., and Sevon, W.D., eds., The Catskill Delta: Geological Society of America Special Paper 201, p. 15–38.

Faill, R.T, 1997a, A geologic history of the North-Central Appalachians, Part 1, Orogenesis from the Mesoproterozoic through the Taconic orogeny: American Journal of Science, v. 297, p. 551-619.

Faill, R.T., 1997b, A geologic history of the North-Central Appalachians, Part 2: The Appalachian Basin from the Silurian through the Carboniferous: American Journal of Science, v. 297, p. 729-761.

Gensel, P.G. and Andrews, H.N., 1984, Plant Life in the Devonian: Praeger, New York, 380 p.

Ghosh, P., Ghosh P., and Bhattacharya, S.K., 2001, CO_2 levels in the Late Paleozoic and Mesozoic atmosphere from soil carbonate and organic matter, Satpura basin, Central India: Palaeogeography, Palaeoclimatology, Palaeoecology, v. 170, p. 219-236.

Ginsburg, R.N., Eberli, G.P, McNeill, D.F., and Grammar, G.M., 1995, Comparative sedimentology of a mixed carbonate/siliciclastic system, Belize, Central America, Guide Book, University of Miami.

Goddéris, Y., François, L.M., and Veizer, J., 2001, The early Paleozoic carbon cycle: Earth and Planetary Science Letters, v. 190, p. 181–196.

Goldring, W., 1927, The oldest known petrified forest: The Scientific Monthly, v. 24, p. 514–529.

Gordon, E.A., and Bridge, J.S., 1988, Evolution of Catskill (Upper Devonian) river systems; intra- and extrabasinal controls: Journal of Sedimentary Petrology, v. 57, p. 234–249.

Hanson, P. J., Edwards, N.T., Garten, C.T., and Andrews, J.A., 2000, Separating root and soil microbial contribution to soil respiration: A review of methods and observations: Biogeochemistry, v. 48, p. 115-146.

Heckel, P.H., 1973, Nature, origin, and significance of the Tully Limestone: The Geological Society of America Special Paper 138, 244 p.

Hemming, N.G., Meyers, W.J., and Grams, J.C., 1989, Cathodoluminescence in diagenetic calcites: The roles of Fe and Mn as deduced from electron probe and spectrophotometric measurements: Journal of Sedimentary Petrology, v. 59, p. 404-411.

Jenny, H.J., 1941, Factors of soil formation: New York, McGraw-Hill, p. 281

Jenny, H.J., 1994, Factors of Soil Formation; A System of Quantitative Pedology: New York, Dover Publications, U.S., 281 p.

Jenny, H.J. and Leonard, C.D., 1935, Functional relationships between soil properties and rainfall: Soil Science, v. 38, p. 363-381.

Johnson, J.G., 1970, Taghanic onlap and the end of North American Devonian provinciality: Geological Society of America Bulletin, v. 81, p. 2077-2106.

Johnson, K.G., 1987, Strand-line facies of the Catskill Tectonic delta complex (Middle and Upper Devonian) in eastern New York State, *in* Roy, D.C., ed., Northeastern Section of the Geological Society of America, Centennial Field Guide, v. 5, p. 129–132.

Johnson, K.G., and Friedman, G.M., 1969. The Tully clastic correlatives (Upper Devonian) of New York State; a model for recognition of alluvial, dune (?), tidal, nearshore (bar and lagoon), and offshore sedimentary environments in a tectonic delta complex: Journal of Sedimentary Petrology, v. 39, p. 451–485.

Johnson, J.G., Klapper, G., Sandberg, C.A., 1985, Devonian eustatic fluctuations in Euramerica: Geological Society of America Bulletin, v. 96, p. 567-587.

Jost, W., 1960, Diffusion in Solids, Liquids, Gases: Academic Press, New York, NY, 558 p.

Kent, D.V., 1985, Paleocontinental setting for the Catskill Delta, *in* Woodrow, D.L., and Sevon, W.D., eds., The Catskill Delta: Geological Society of America Special Paper 201, p. 9–13.

Kraus, M.J., 1987, Integration of channel and floodplain suites, II. Vertical relations of alluvial paleosols: Journal of Sedimentary Petrology, v. 57, p. 602–612.

Kraus, M.J, 2002, Basin-scale changes in floodplain paleosols: Implications for interpreting alluvial architecture: Journal of Sedimentary Research, v. 72, p. 500-509.

Kraus, M.J., AND Aslan, A., 1999, Palaeosol sequences in floodplain environments: a hierarchical approach, in Thiry, M., and Simon-Coincon, R., eds., Palaeoweathering, Palaeosurfaces and Related Continental Deposits: International Association of Sedimentologists, Special Publication 27, p. 303–321.

Kroh, G.C., White, J.D., Heath, S.K., and Pinder, J.E., 2000, Colonization of a volcanic mudflow by an upper montane conifer forest at Lassen Volcanic National Park, California: American Midland Naturalist, v. 143, p. 126–140.

Lee, Y. I., 1999, Stable isotopic composition of calcic paleosols of the Early Cretaceous Hasandong Formation, southeastern Korea: Palaeogeography, Palaeoclimatology, Palaeoecology: v. 150 123-133.

Lee, Y. I., Hisada, K., 1999, Stable isotopic composition of pedogenic carbonates of the Early Cretaceous Shimonoseki Subgroup, western Honshu, Japan: Palaeogeography, Palaeoclimatology, Palaeoecology: v. 153, 127-138.

Leier, A., Quade, J., DeCelles, P., and Kapp, P., 2009, Stable isotopic results from paleosol carbonate in South Asia: Paleoenvironmental reconstructions and selective alteration: Earth and Planetary Science Letters, v. 279, p. 242-254.

Lohmann, K.C., 1987, Geochemical patterns of meteoric diagenetic systems and their application to studies of paleokarst, *in* James N.P., and Choquette P.W., eds., Paleokarst: Society for Sedimentary Geology Special Publication v. 125, p. 58-80.

Machette, M.N., 1985, Calcic soils of the southwestern United States, *in* Weide, D.L., ed., Soils and Quaternary geology of the southwestern United States: Geological Society of America, Special Paper, v. 203, p. 10-21.

McCarthy, P.J., Plint, G.A., 1998, Recognition of interfluve sequence boundaries: Integrating paleopedology and sequence stratigraphy, Geology, v. 26, p. 387-390.

McCave, I.N., 1969, Correlation of marine and nonmarine strata with examples from Devonian of New York State: American Association of Petroleum Geologists Bulletin, v. 53, p.155-162.

Meyer-Berthaud, B., and Decombeix, A., 2007, A tree without leaves: Nature, v. 446, p. 861–862.

Miller, W.L., and Bragg, A.L., 2007, Soil characterization and hydrological monitoring project, Brazoria County, Texas, bottomland hardwood Vertisols: United States Department of Agriculture, Natural Resources Conservation Service, 333 p.

Miller, D.L., Mora, C.I., and Driese, S.G., 2007, Isotopically concentric growth in large carbonate nodules in Vertisols: implications for climate and ecosystem assessments: Geoderma, v. 142, p. 104-111.

Mintz, J.S., Stinchcomb, G.E., Laudadio, C., Oliver, P., Erney, A., Gobbi, K., Kirsch, A., Mitchell, N., Jannett, P., and Terry, D.O. Jr., 2006, Paleopedology of the East Windham roadcut, East Windham, New York: Geological Society of America, Abstracts with Programs, Northeastern Section Meeting, v. 38, n. 2, p. 30.

Mintz, J.S., Driese, S.G., and White, J.D., 2010, Environmental and ecological variability of Middle Devonian (Givetian) forests in Appalachian basin paleosols, New York, United States: Palaios, v. 25, p. 85-96.

Mintz, J.S., Driese, S.G., Breecker, D.O. and Ludvigson, G.A., in press, Influence of changing hydrology on pedogenic calcite precipitation in Vertisols, Dance Bayou, Brazoria County, TX: Implications for estimating paleoatmospheric pCO_2: Journal of Sedimentary Research.

Mintz, J.S., Harlow, R.H., Driese, S.G., Atchley, S.C. and Wright, T.C., in review, Middle Devonian Landscapes, climates and the correlation of continental strata in the northern Appalachian basin, Geological Society of America Bulletin.

Mitchum, R.M., 1977, Seismic stratigraphy and global changes of sea level, Part 1: Glossary of terms used in seismic stratigraphy, *in*, Payton, C.E., (ed.), Seismic stratigraphy—Applications to hydrocarbonexploration: AAPG Memoir 26, p. 63-62.

Montañez, I.P., Tabor, N.J., Niemeier, D., DiMichele, W.A., Frank, T.D., Fielding, C.R.,vand Isbell, J.L., 2007, CO_2-forced climate and vegetation instability during late Paleozoic deglaciation, Science, v. 315, p. 87–91.

Mora, C.L., Driese, S.G., and Seager, P.A., 1991, Carbon dioxide in the Paleozoic atmosphere: evidence from carbon isotope compositions of pedogenic carbonate: Geology, v. 19, p. 1017–1020.

Mora, C.I., and Driese, S.G., 1993, A steep, mid- to late Paleozoic decline in atmospheric CO_2: evidence from the soil carbonate CO_2 paleobarometer: Chemical Geology, v. 107, p. 217-219.

Mora, C.I., Driese, S.G., and Colarusso, L.A., 1996, Middle to Late Paleozoic atmospheric CO_2 from soil carbonate and organic matter: Science, v. 271, p. 1105–1107.

Mora, C.I, Sheldon, B.T, Elliot, W.C., Driese, S.G., 1998, An oxygen isotope study of illite and calcite in three Appalachian Paleozoic vertic paleosols: Journal of Sedimentary Research, v. 68, p. 456-464.

Nordt, L.C., Atchley, S.C., and Dworkin, S.I., 2002, Paleosol barometer indicates extremefluctuations in atmospheric CO_2 across the Cretaceous-Tertiary boundary: Geology, v. 30, p. 703–706.

Nordt, L.C., Atchley, S.C., and Dworkin, S.I., 2003, Terrestrial evidence for two greenhouse events in the latest Cretaceous: Geological Society of America Today, v. 13, no. 12, p. 4–9.

Nordt, L.C., and Driese, S.G., 2009, Hydropedological model of Vertisol formation along the Gulf Coast Prairie land resource area of Texas: Hydrology and Earth System Sciences, v. 13, p. 2039-2053.

Nordt , L.C. and Driese, S.D., 2010, New weathering index improves paleorainfall estimates from Vertisols: Geology, v. 38, p. 407-410.

Nordt, L., Orosz, M., Driese, S., and Tubbs, J., 2006, Vertisol carbonate properties in relation to mean annual precipitation: Implications for paleoprecipitation estimates: Journal of Geology, v. 114, p. 501-510.

O'Leary, M.H., 1984, Measurement of the isotope fractionation associated with diffusion of carbon dioxide in aqueous solution: Journal of Physical Chemistry, v. 88, p. 823-825.

Passey, B.H., Cerling, T.E., Perkins, M.E., Voorhies, M.R., Harris, J.M., and Tucker, S.T., 2002, Environmetal change in the Great Plains: An isotopic record from fossil horses: The Journal of Geology, v. 110. P. 123-140.

Purdy, E.G., Pusey, W.C, and Wantland, K.F., 1975, Continental shelf of Belize: Regional shelf attributes, *in*, Wantland, K.F., and Pusey, W.C. (eds.), Belize shelf: Carbonates, clastics and ecology, American Association of Petroleum Geologists, studies in geology, v.2, p. 1-39.

Quast, A., Hoefs, J., and Paul, J., 2006, Pedogenic carbonates as a proxy for palaeo- CO_2 in the Palaeozoic atmosphere: Palaeogeography, Palaeoclimatology, Palaeoecology, v. 242, p. 110-125.

Retallack, G.J., 1988, Field recognition of paleosols, *in* Reinhardt, J., and Sigleo, W.R. (eds.), Paleosols and Weathering Through Geologic Time: Techniques and Applications, Geological Society of America, Special Paper 216, p. 1–20.

Retallack, G.J., 1997, Early forest soils and their role in Devonian global change: Science, v. 276, p. 583–585.

Retallack, G.J., 1994, The Environmental Factor Approach to the Interpretation of Paleosols, *in* Amundson, R., Harden, J. and Singer, M. (eds.), Factors of Soil Formation: A Fiftieth Anniversary Retrospective: Soil Science Society of America Special Publication no. 33, p. 31-64.

Retallack, G.J., 2001, Soils of the past, Second edition: Oxford, U.K., Blackwell Science, 404 p.

Retallack, G.J., 2005, Pedogenic carbonate proxies for amount and seasonality of precipitation in paleosols: Geology, v. 33, p. 333–336.

Retallack, G.J. and Huang, C., in press, Ecology and evolution of Devonian trees in New York, USA: Palaeogeography, Palaeoclimatology, Palaeoecology.

Rickard, L.V., 1975, Correlation of the Devonian rocks in New York State: New York Museum and Science Service, Map and Chart series, n. 24.

Robinson, S.A., Andrews, J.E., Hesselbo, S.P., Radley, J.D., Dennis, P.F., Harding, I.C., and Allen, P., 2002, Atmospheric pCO_2 and depositional environment from stable-isotope geochemistry of calcrete nodules (Barremian, Lower Cretaceous, Wealden Beds, England): Journal of the Geological Society, London, v. 159, p. 215-224.

Romanek, C.S., Grossman, E.L., and Morse, J.W., 1992, Carbon isotopic fractionation in synthetic aragonite and calcite; effects of temperature and precipitation rate: Geochimica et Cosmochimica Acta, v. 56, p. 419-430.

Royer, D.L., 1999, Depth to pedogenic carbonate horizon as a paleoprecipitation indicator?: Geology, v. 27, p. 1123–1126.

Royer, D.L., 2006, CO_2-forced climate thresholds during the Phanerozoic: Geochimica et Cosmochimica Acta, v. 70, p. 5665-5675.

Sevon, W.D., and Woodrow, D.L., 1985, Middle and Upper Devonian stratigraphy within the Appalachian Basin, *in* Woodrow, D.L., and Sevon, W.D., eds., The Catskill Delta: Geological Society of America Special Paper 201, p. 1–7.

Sevon, W.D., 1985, Nonmarine facies of the Middle and Late Devonian Catskill coastal alluvial plain, *in* Woodrow, D.L., and Sevon, W.D. (eds.), The Catskill Delta: Geological Society of America, Special Paper 201, p. 79-90.

Scheckler, S.E. 1986, Floras of the Devonian–Mississippian transition, *in* Broadhead, T.W., ed., Land Plants: Notes for a Short Course: University of Tennessee, Department of Geological Sciences, Studies in Geology 15, p. 81–96.

Schoeneberger, P.J., Wysocki, D.A., Benham, E.C., and Broderson, W.D., eds., 2002, Field Book for Describing and Sampling Soils, Version 2.0.: U.S. Department of Agriculture, Natural Resources Conservation Service, National Soil Survey Center, Lincoln, Nebraska, ~228 p., 1.6 MB, checked October 30, 2009, ftp://ftp-fc.sc.egov.usda.gov/NSSC/Field_Book/FieldBookVer2.pdf.

Scotese, C.R. Bambach, R.K., Barton, C., van der Voo, R., and Ziegler, A.M., 1979, Paleozoic base maps: Journal of Geology, v. 87, p. 217–268.

Sheldon, N.D. and Retallack, G.J., 2001, Equation for compaction of paleosols due to burial: Geology, v. 29, p. 247-250.

Sheldon, N.D., Retallack, G. J., Tanaka, S., 2002, Geochemical Climofunctions from North American Soils and Application to Paleosols across the Eocene-Oligocene Boundary in Oregon: Geology, v. 110, p. 687-696.

Sheldon, N.D., and Tabor, N.J., 2009, Quantitative paleoenvironmental and paleoclimatic reconstruction using paleosols: Earth-Science Reviews, v. 95, p. 1-52.

Soil Survey Staff, 1990, Keys to Soil Taxonomy, Fourth Edition: Soil Management Support Services Technical Monograph 19, Virginia Polytechnic Institute and State University, Blacksburg, 420 p.

Soil Survey Staff, 1999, Soil taxonomy: A basic system of soil classification for making and interpreting soil surveys, 2nd eds.: U.S. Department of Argriculture, 871 p.

Soil Survey Staff, 2010, Keys to Soil Taxonomy, 11th ed. Soil Management Support Services Technical Monograph 19: Blacksburg, Virginia, Virginia Polytechnic Institute and State University.

Stein, W.E., Mannolini, F., Hernick, L. V., Landing, E., and Berry, C.M., 2007, Giant cladoxylopsid trees resolve the enigma of the Earth's earliest forest stumps at Gilboa, Nature, v. 446, p. 904–907.

Vepraskas, M.J., 2001, Morphological feature of seasonally reduced soils, *in* Richardon, J.L. and Vepraskas, M.J., eds., Wetland soils: Genesis , hydrology landscapes and classification: Boca Raton, Lewis Publishers, p. 163-182.

Ver Straeten, C.A., 2010, Lessons from the foreland basin: Northern Appalachian Basin perspectives on the Acadian orogeny, *in* Tollo, R.P., Bartholomew, M.J., Hibbard, J.P., Karabinos, P.M. (eds.) From Rodinia to Pangea: The lithotectonic record of the Appalachian region: The Geological Society of America Memoir 206, p. 251-273.

Whelan III, T., and Roberts, H.H., 1973, Carbon isotope composition of diagenetic carbonate nodules from freshwater swamp deposits: Journal of Sedimentary Petrology, v. 43, p. 54–58.

Wilding, L. P., and Puentes, R., editors, 1988, Vertisols: Their distribution, properties, classification and management: College Station, Texas A&M University Printing Center, 193 p.

Willis, B.J., and Bridge, J.S., 1988, Evolution of Catskill river systems, New York State, *in* McMillan N.J., Embry, A.F., and Glass, D.J., eds., Devonian of the World, Volume II: Canadian Society of Petroleum Geologists Memoir, v. 14, p. 85–106.

Woodrow, D.L., 1985, Paleogeography, paleoclimate, and sedimentary processes of the Late Devonian Catskill Delta, *in* Woodrow, D.L., and Sevon, W.D., eds., The Catskill Delta: Geological Society of America Special Paper 201, p. 39–51.

Woodrow, D.L., Fletcher, F.W., and Ahrnsbrak, W.F., 1973, Paleogeography and paleoclimate at the deposition sites of the Devonian Castskill and the Old Red Facies: Geological Society of America Bulletin, v. 84, p. 3051-3064.

Woodrow, D.L., and Sevon, W.D., eds., 1985, The Catskill Delta: Geological Society of America Special Paper 201, 246 p.

Wright, V.P., Marriott, S.B., 1993, The sequence stratigraphy of alluvial depositional systems: the role of floodplain sediment storage, Sedimentary Geology, v. 86 p. 240-252.

Wright, V.P., and Vanstone, S.D., 1991, Assessing the carbon dioxide content of ancient atmospheres using palaeo-calcretes: theoretical and empirical constraints: Journal of the Geological Society of London, v. 148, p. 945-947.

Zambito, J.J., Brett, C.E., Baird, G.C., in press, The Late Middle Devonian (Givetian) Global Taghanic Biocrisis in its type area (Northern Appalachian basin): Geologically rapid faunal transitions driven by global and local environmental change, *in* Talent, J. (ed.) Global biodiversity, extinction intervals and biogeographic perturbations through time, UNESCO.

Ziegler, A.M., Scotese, C.R., McKerrow, W.S., Johnson, M.E. and Bambach, R.K., 1979, Paleozoic paleogeography: Annual Reviews of Earth and Planetary Sciences, v. 7, p. 473–502.